AERO_TN_TailSizing_13-04-15

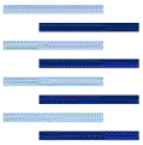

Hochschule für Angewandte Wissenschaften Hamburg

Hamburg University of Applied Sciences

Aircraft Design and Systems Group (AERO)
Department of Automotive and Aeronautical Engineering
Hamburg University of Applied Sciences
Berliner Tor 9
D - 20099 Hamburg

Empennage Statistics and Sizing Methods for Dorsal Fins

Priyanka Barua
Tahir Sousa
Dieter Scholz

2013-04-15

Technical Note

Dokumentationsblatt

<table>
<tr><td>1. Berichts-Nr.
AERO_TN_TailSizing</td><td>2. Auftragstitel
Airport2030
(Effizienter Flughafen 2030)</td><td>3. ISSN / ISBN
---</td></tr>
<tr><td colspan="2" rowspan="2">4. Sachtitel und Untertitel
Empennage Statistics and
Sizing Methods for Dorsal Fins</td><td>5. Abschlussdatum
2013-04-15</td></tr>
<tr><td>6. Ber. Nr. Auftragnehmer
AERO_TN_TailSizing</td></tr>
<tr><td colspan="2" rowspan="2">7. Autor(en) (Vorname, Name, E-Mail)
Priyanka Barua
Tahir Sousa
Dieter Scholz</td><td>8. Förderkennzeichen
03CL01G</td></tr>
<tr><td>9. Kassenzeichen
810302101951</td></tr>
<tr><td colspan="2" rowspan="3">10. Durchführende Institution (Name, Anschrift)
Aircraft Design and Systems Group (AERO)
Department Fahrzeugtechnik und Flugzeugbau
Fakultät Technik und Informatik
Hochschule für Angewandte Wissenschaften Hamburg (HAW)
Berliner Tor 9, D - 20099 Hamburg</td><td>11. Berichtsart
Technische Niederschrift</td></tr>
<tr><td>12. Berichtszeitraum
2012-10-15 – 2013-04-15</td></tr>
<tr><td>13. Seitenzahl
145</td></tr>
<tr><td colspan="2" rowspan="3">14. Auftraggeber (Name, Anschrift)
Bundesministerium für Bildung und Forschung (BMBF)
Heinemannstraße 2, D - 53175 Bonn - Bad Godesberg

Projektträger Jülich
Forschungszentrum Jülich GmbH
Wilhelm-Johnen-Straße, D - 52438 Jülich</td><td>15. Literaturangaben
81</td></tr>
<tr><td>16. Tabellen
48</td></tr>
<tr><td>17. Bilder
76</td></tr>
<tr><td colspan="3">18. Zusätzliche Angaben
Sprache: Englisch. URL: http://Reports_at_AERO.ProfScholz.de</td></tr>
<tr><td colspan="3">19. Kurzfassung
Dieser Bericht beschreibt verbesserte Methoden zur Abschätzung von Parametern des Höhen- und Seitenleitwerks. Weiterhin werden parameter der Rückenflossen aus den Parametern des Seitenleitwerks abgeleitet um den Vorentwurf zu unterstützen. Basis sind Statistiken aufbauend auf Daten, die aus Dreiseitenansichten gewonnen werden. Die betrachteten Parameter sind Leitwerksvolumenbeiwert, Streckung, Zuspitzung, Pfeilwinkel, relative Profildicke für Höhen- und Seitenleitwerk, sowie die Profiltiefe und Spannweite von Höhen- und Seitenruder. Der Bericht schlägt z.B. vor die relative Dicke des Höhenleitwerkes etwa als 81 % der relativen Dicke des Flügels anzusetzen. Die Methode zur Abschätzung der Parameter der Rückenflosse erreicht eine Genauigkeit von 18%.</td></tr>
<tr><td colspan="3">20. Deskriptoren / Schlagwörter
Leitwerk, Seitenleitwerk, Höhenleitwerk, Rückenflosse, Seitenruder, Höhenruder, Flugzeugentwurf</td></tr>
<tr><td colspan="3">21. Bezugsquelle
AERO, Department F+F, HAW Hamburg, Berliner Tor 9, D - 20099 Hamburg</td></tr>
<tr><td>22. Sicherheitsvermerk
keiner</td><td>23.</td><td>24. Preis</td></tr>
</table>

Dokumentationsblatt nach DIN 1422 Teil 4

Report Documentation Page

<table>
<tr><td>1. Report-Number
AERO_TN_TailSizing</td><td>2. Project Title
Airport2030
(Effizienter Flughafen 2030)</td><td>3. ISSN / ISBN
N/A</td></tr>
<tr><td colspan="2" rowspan="2">4. Title and Subtitle
Empennage Statistics and
Sizing Methods for Dorsal Fins</td><td>5. Report Date
2013-04-15</td></tr>
<tr><td>6. Performing Org. Rep. No
AERO_TN_TailSizing</td></tr>
<tr><td colspan="2" rowspan="2">7. Author(s) (First Name, Last Name)
Priyanka Barua
Tahir Sousa
Dieter Scholz</td><td>8. Contract Code
03CL01G</td></tr>
<tr><td>9. Payment Number
810302101951</td></tr>
<tr><td colspan="2" rowspan="3">10. Performing Agency (Name, Address)
Aircraft Design and Systems Group (AERO)
Department of Automotive and Aeronautical Engineering
Faculty of Engineering and Computer Science
Hamburg University of Applied Sciences (HAW)
Berliner Tor 9, D - 20099 Hamburg</td><td>11. Report Type
Technical Note</td></tr>
<tr><td>12. Time Period
2012-10-15 – 2013-04-15</td></tr>
<tr><td>13. Number of Pages
145</td></tr>
<tr><td colspan="2" rowspan="3">14. Sponsoring / Monitoring Agency (Name, Address)
Federal Ministry of Education and Research (BMBF)
Heinemannstraße 2, D - 53175 Bonn - Bad Godesberg

Projektträger Jülich
Forschungszentrum Jülich GmbH
Wilhelm-Johnen-Straße, D - 52438 Jülich</td><td>15. Number of References
81</td></tr>
<tr><td>16. Number of Tables
48</td></tr>
<tr><td>17. Number of Figures
76</td></tr>
<tr><td colspan="3">18. Supplementary Notes
Language: English; URL: http://Reports_at_AERO.ProfScholz.de</td></tr>
<tr><td colspan="3">19. Abstract
This report aims to suggest better estimations for tail parameter sizes and develop relations between the dorsal fin and vertical tail to aid in conceptual design. This is done mainly through statistical analyses based on measurements from 3-view drawings developing previously unexplored relationships. Parameter analyzed for horizontal and vertical tail are tail volume coefficient, aspect ratio, taper ratio, sweep angle and relative thickness of the airfoil, furthermore relative chord and span for elevator and rudder. This report proposes for example to take the relative thickness ratio of the horizontal tail as approximately 81% that of the wing. The final methods of dorsal fin sizing were found to achieve an average error of 18%.</td></tr>
<tr><td colspan="3">20. Subject Terms
empennage, tail, dorsal, fin, horizontal, vertical, rudder, elevator, aircraft, design, sizing, statistic</td></tr>
<tr><td colspan="3">21. Distribution
AERO, Department F+F, HAW Hamburg, Berliner Tor 9, D - 20099 Hamburg</td></tr>
<tr><td>22. Classification / Availability
unclassified - unlimited</td><td>23.</td><td>24. Price</td></tr>
</table>

Dokumentationsblatt nach DIN 1422 Teil 4

Abstract

In the tail sizing stage of conceptual design, it is aimed to estimate the different tail parameter sizes as accurately as possible. The first problem dealt with in this report is to suggest better estimations for tail parameter sizes. Data produced from measurements of aircraft 3-view diagrams and data of new aircraft are averaged with data published by previous authors to improve these estimates. Moreover, this report tries to develop previously unexplored relationships to aid in estimation. Parameters analyzed are volume coefficient, aspect ratio, taper ratio, quarter chord sweep angle, relative thickness of the airfoil and control surface chords and spans. This report proposes ranges of 3.38 to 5.34 and 0.27 to 0.51 for a horizontal tail aspect ratio and taper ratio respectively for jet transport aircraft. Also, it claims that the relative thickness ratio of the horizontal tail is approximately 81% that of the wing. The second problem dealt with is to develop relations between the dorsal fin and vertical tail to aid in conceptual design of the dorsal fin. A dorsal fin is an extension in front of the vertical tail stretching along the fuselage with a sweep angle higher than that of the vertical tail. A vertical tail needs to cope with high side slip angles in order to protect the aircraft. A dorsal fin can help to increase the stall angle of the isolated vertical tail. Vertical tails with low leading edge sweep benefit from an addition of a dorsal fin. The dorsal fin leading edge sweep is typically around 72˚ for jet and 75˚ for propeller aircraft. The proposed sizing method is based on statistics of regional jet and propeller airliners for the root chord of the dorsal fin as a function of the root chord of the tail. The final methods were found to achieve an average error of 18%. This report can therefore be useful to a designer attempting to estimate parameter sizes for the tail and dorsal fin of an aircraft during the conceptual design phase.

Table of Contents

List of Figures

List of Tables

List of Symbols

A	Aspect ratio
b	Span
c	Chord length
C	Coefficient
d	Diameter
E	Engine out ratio
$f( )$	Function
h	Height
l	Lever arm length
L	Length
m	Mass
M	Mach number
n	Number
R^2	Coefficient of determination
S	Area
t	Thickness
T	Thrust
t/c	Thickness chord ratio
w	Width
x	Position
y	Distance

Greek Symbols

α	Angle of attack
β	Sideslip angle
δ	Deflection angle
η	Efficiency
φ	Sweep angle
Δ	Difference
λ	Taper ratio

Indices

0	0% of the chord length or the leading edge
25	25% of the chord length
calc.	Calculated by author
cg	Centre of gravity
df	Dorsal fin
df+	Dorsal fin + common portion between vertical tail and dorsal fin

D	Dive
e	Engine
E	Elevator
f	Fuselage
flight	During flight
H	Horizontal tail
mto	Maximum Take Off
MO	Maximum Operating
MAC	Mean aerodynamic chord
MTOM	Maximum Take Off Mass
o	Out
P	Power
Pax	Maximum passengers
r	Root
R	Rudder
ref	Taken from reference material
t	Tip
T	Thrust total
TO	Take Off
v	Vertical Tail
v-df	Common portion between vertical tail and dorsal fin
vir	Virtual
wo/df	Without dorsal fin
W	Wing

List of Abbreviations

COM	Centre of Mass
GA	General Aviation
HT	Horizontal Tail
VT	Vertical Tail

Terms and Definitions

Airfoil
The shape of any flying surface, but principally a wing, as seen in side-view ("cross-section"). (**Aerofiles 2013**)

Angle of Incidence
Also called rigging angle of incidence, the angle between the chord line of an aircraft wing or tailplane and the aircraft's longitudinal axis is called the angle of incidence. Another common term for angle of incidence is Angle of attack. (**FreeDictionary 2013)**

Aspect Ratio
In aerodynamics, the Aspect ratio of a wing is essentially the ratio of its length (span) to its breadth (chord). A high aspect ratio indicates long, narrow wings, whereas a low aspect ratio indicates short, stubby wings. For most wings, the length of the chord is not a constant but varies along the wing, so the aspect ratio A is defined as the square of the wingspan b_w divided by the area S_w of the wing planform which is equal to the length-to-breadth ratio for a constant chord wing. (**Wikipedia 2013a**)

Center of Gravity (CG)
The longitudinal and lateral point in an aircraft where it is stable; the static balance point is called the Centre of Gravity. (**Aerofiles 2013**)

Coefficient of Determination
In statistics, the coefficient of determination, denoted R^2, is used in the context of statistical models whose main purpose is the prediction of future outcomes on the basis of other related information. R^2 is most often seen as a number between 0 and 1.0, used to describe how well a regression line fits a set of data. An R^2 near 1.0 indicates that a regression line fits the data well, while an R^2 closer to 0 indicates a regression line does not fit the data very well. (**Wikipedia 2013b**)

Coefficient of Tail Volume
The force due to tail lift is proportional to the tail area. Thus, the tail effectiveness is proportional to the tail area times the moment arm. This product has units of volume. Rendering this parameter non-dimensional requires dividing by some quantity with units of length. For a vertical tail, the wing yawing moments which must be countered are most directly related to the wing span, b_w. For a horizontal tail or canard meanwhile, the pitching moments which must be countered are most directly related to the wing mean chord. Thus, the tail volume coefficients for Vertical and Horizontal tails can be given by,

$$C_V = \frac{l_V S_V}{S_w b_w}$$

$$C_H = \frac{l_H S_H}{S_w c_{MAC}}$$

where, C is the Coefficient of Tail Volume, l is the Tail Lever arm length, S_w is the Wing area, c_{MAC} is the Wing mean chord and the sub-scripts $_v$ and $_H$ are used to denote "of Vertical Tail" and "of Horizontal tail" respectively. (**Torenbeek 1982**)

Conventional Gear
The aircraft landing gear having two main landing wheels at the front and a tailwheel or tail-skid at the rear as opposed to having a tricycle gear with three main wheels is called Conventional Gear. Such an aircraft is popularly called a Taildragger. (**Aerofiles 2013**)

Conventional Tail
An airplane tail design with the horizontal stabilizer mounted at the bottom of the vertical stabilizer. (**Crane 2012**)

Chord
The measurable distance between the leading and trailing edges of a wingform is called its chord. (**Aerofiles 2013**)

Dihedral Angle
Dihedral angle is the upward angle from horizontal of the wings or tailplane of a fixed-wing aircraft. "Anhedral angle" is the name given to negative dihedral angle, that is, when there is a *downward* angle from horizontal of the wings or tailplane of a fixed-wing aircraft. (**Roskam 1985**) **Torenbeek 1982** defines the Dihedral Angle as the angle between the projection of the quarter chord line on the Y-Z plane and the Y-axis (positive upwards).

Dorsal Fin
It is an extension of the vertical fin forward from its leading edge to a point along the fuselage length. (**MAD 1980**)

Dorsal Fin Extension
A thin line structure extending forward from either the fin or the dorsal fin along a significant length on the fuselage. See Figure 2.13 and 2.15. (Own definition)

Empennage
Empennage is the rear body of aircraft consists mainly of vertical stabilizer, horizontal stabilizer and its associated control surfaces rudder and elevator respectively. (**MAD 1980**)

Elevator
The horizontal, movable control surface in the tail section, or empennage, of an airplane. The elevator is hinged to the trailing edge of the fixed horizontal stabilizer. Moving the elevator

up or down, by fore-and-aft movement of the control yoke or stick, changes the aerodynamic force produced by the horizontal tail surface. (**Crane 2012**)

Gross or Design Wing Area
This is defined as the area enclosed by the wing outline, including wing flaps in the retracted position and ailerons, but excluding fillets or fairings, projected on the X-Y plane. The leading and trailing edge are assumed to be extended through the nacelles and fuselage to the X-Z plane in any reasonable manner. (**Torenbeek 1982**)

Half chord sweep Angle
This is the angle between the projection of the half chord line on the X-Y plane of the wing or tail and the Y-axis. (**Torenbeek 1982**)

Horizontal Tail, Stabilizer
The fixed horizontal surface on the tail of a conventional airplane. The horizontal stabilizer is usually adjustable in flight to vary the down-load produced by the tail. (**Crane 2012**)

Lateral Stability
Stability along the longitudinal axis (nose to tail) of an aircraft is known as lateral stability. An aircraft is laterally stable when it is able to correct any sideways disturbance like roll or yaw without any correction applied by the pilot. (**MAD 1980**)

Leading Edge
The leading edge is the part of the wing that first contacts the air. Alternatively it is the foremost edge of an airfoil section. The first is an aerodynamic definition, the second a structural one. As an example of the distinction, during a tailslide, from an aerodynamic point-of-view, the trailing edge becomes the leading edge and vice-versa but from a structural point of view the leading edge remains unchanged. In this report, the structural definition is used. (**Wikipedia 2013c**)

Leading edge sweep Angle
This is the angle between the projection of the leading edge line on the X-Y plane of the wing or tail and the Y-axis. (**Torenbeek 1982**)

Lift
The force exerted on the top of a moving airfoil as a low-pressure area that causes a wingform to rise. airfoils do not "float" on air, as is often assumed like a boat hull floats on water but are "pulled up" [lifted] by low air pressures trying to equalize. (**Aerofiles 2013**)

Mach Number
In fluid mechanics, Mach number (*M*) is a dimensionless quantity representing the ratio of speed of an object moving through a fluid and the local speed of sound.

$$M = \frac{v}{a}$$

where,

M is the Mach number,
v is the velocity of the source relative to the medium and
a is the speed of sound in the medium.

Mach number varies by the composition of the surrounding medium and also by local conditions, especially temperature and pressure. The Mach number can be used to determine if a flow can be treated as an incompressible flow. If M < 0.2–0.3 and the flow is (quasi) steady and isothermal, compressibility effects will be small and a simplified incompressible flow model can be used. (**Wikipedia 2013d**)

Mean Aerodynamic Chord
Mean aerodynamic chord (*MAC*) is defined as:

$$MAC = \frac{2}{S}\int_0^{\frac{b}{2}} c(y^2)dy$$

where, y is the coordinate along the wing span, c is the chord at the coordinate y, S_w is the wing area and b_w is the span of the wing.

Physically, *MAC* is the chord of a rectangular wing, which has the same area, aerodynamic force and position of the center of pressure at a given angle of attack as the given wing has. Simply stated, *MAC* is the width of an equivalent rectangular wing in given conditions. Therefore, not only the measure but also the position of *MAC* is often important. In particular, the position of center of mass (*CoM*) of an aircraft is usually measured relative to the *MAC*, as the percentage of the distance from the leading edge of *MAC* to *CoM* with respect to *MAC* itself. (**Wikipedia 2013e**)

NACA 4-digit series
The numbering system is based on the section geometry. The first integer indicates the maximum value of the mean line ordinate, y_c as a percentage of the chord. The second integer indicates the distance from the leading edge to the location of the maximum camber in tenths of the chord. The last two integers indicate the section thickness as a percentage of the chord. Hence, the NACA 2415 section has 2% camber at 0.4 of the chord from the leading edge and is 15% thick. (**Torenbeek 1982**)

Quarter chord line
This is the line through all points at 0.25*c* of the sections.

Quarter chord sweep Angle
This is the angle between the projection of the quarter chord line on the X-Y plane of the wing or tail and the Y-axis. Positive angle backwards (sweepback), negative forwards (sweep forward) (**Torenbeek 1982**)

Regression Analysis
Regression analysis is a statistical technique for estimating the relationships among variables. It includes many techniques for modeling and analyzing several variables, when the focus is on the relationship between a dependent variable and one or more independent variables. More specifically, regression analysis helps one understand how the typical value of the dependent variable changes when any one of the independent variables is varied. (**Wikipedia 2013f**)

Root Chord
The chord length of the wing or tail sections in the plane of symmetry is called the Root Chord. (**Torenbeek 1982**)

Round Edge Dorsal Fin
Rounded leading edge, filling the corner of the lower part of the fins leading edge blending into the upper surface of the fuselage. See Figure 2.16. (Own definition)

Rudder
The movable control surface mounted on the trailing edge of the vertical fin of an airplane. The rudder is moved by foot-operated pedals in the cockpit, and movement of the rudder rotates the airplane about its vertical axis. (**Crane 2012**)

Section Thickness
This is defined as the maximum distance between corresponding points on the upper and lower section surface. It is usually expressed as a thickness/ chord ratio (t/c). (**Torenbeek 1982**)

Sideslip
An aircraft is in a sideslip when its direction of motion (its velocity vector) does not lie on the plane passing vertically through the longitudinal axis. The angle between the velocity vector and vertical plane passing through the longitudinal axis is called sideslip angle, β. (**MAD 1980**)

Statistics
It is described as mathematical analysis and interpretation of numerical information from a set of data collected based on real world observation. The statistics collected for this report is mainly the parameters to size the empennage and dorsal fin, for different category of aircraft. (**MAD 1980**)

T-tail
The configuration of an aircraft empennage in which the horizontal surfaces are on top of the vertical surfaces, in the form of the letter T. (**Crane 2012**)

Taper Ratio
Taper ratio, λ is the ratio between the tip chord and the centreline root chord. Taper affects the distribution of lift along the span of the wing. (**Raymer 1992**)

Thrust
This is the driving force of a propeller in the line of its shaft or the forward force produced in reaction to the gases expelled rearward from a jet or rocket engine. Opposite of Drag. (**Aerofiles 2013**)

Tip Chord
The tip chord, c_t is the chord length of the wing or tail sections at the outer extremity of the wing or tail. (**Torenbeek 1982**)

Trailing Edge
The trailing edge of an aerodynamic surface such as a wing is its rear edge, where the airflow separated by the leading edge rejoins. Essential control surfaces are attached here to redirect the air flow and exert a controlling force by changing its momentum. (**Wikipedia 2013g**)

Trailing edge sweep Angle
This is the angle between the projection of the trailing edge line on the X-Y plane of the wing or tail and the Y-axis. (**Torenbeek 1982**)

Ventral Fin
A fixed vertical surface on an airplane that extends below the aft end of the fuselage. Ventral fins are used to increase the directional stability of an airplane. (**Crane 2012**)

Vertical Tail, Vertical Fin
The fixed vertical surface in the empennage of an airplane. The vertical fin acts as a weather vane to give the airplane directional stability. (**Crane 2012**)

Wing Span
The distance between the wing tips, measured perpendicular to the X-Z plane, navigation lights excluded. (**Torenbeek 1982**)

1 Introduction

1.1 Motivation

The goal of transport aircraft design is always the optimization of design, considering cost effectiveness, environmental factors and payload carrying capacity. The first necessity of a good design is an aircraft should be stable and balanced at all phases of flight. Conceptual design is the first step in aircraft design which uses the fundamental of flight mechanics, aerodynamics and statistics to size an aircraft. Tail design is therefore a part of conceptual design and hence determines how big or small, which shape and the need of a tail structure. The empennage of an aircraft is used to provide trim, stability and control for the aircraft. The empennage of an aircraft consists in general of vertical and horizontal stabilizers, control surfaces like rudder (vertical tail) and elevator (horizontal tail) and dorsal fin. In many references and sources generally available today there is currently no universally accepted method to size a dorsal fin, at least not to the general public. Dorsal fin is a variation in vertical stabilizer shape achieved to contribute in directional stability of an aircraft at high sideslip angle. It is mostly explained just as an addition of an extra area with vertical tail to correct directional stability of an aircraft. It is noticeable that designing a method to size a dorsal fin has never attracted enough attention amongst designers or it is kept private. Our finding in this report explains why dorsal fin is crucial in directional stability, explains its functions and advantages. And most importantly a sizing method for dorsal fin has been proposed based on statistics of jet and propeller transport aircraft. The idea of statistics in this project is to find the valuable relatedness and develop trends based on existing or previously designed aircraft. None of the references or sources available today offers any range values also to design dorsal fins. Therefore, the outcome of this report is truly beneficial since it offers a method and range values to design a dorsal fin.

Statistics has also been done on parameters, used in tail sizing equation, for different category of transport aircraft. Such statistics reveals the relation between the parameters and how the parameters are dependent on each other.

Findings of this report benefit a designer with a method to size dorsal fins and to decide the value of parameters to size tail of an aircraft. The statistics done for empennage covers all categories of aircraft and defines the range of values for each parameter, used for tail sizing. E.g. if a designer decides to design an empennage of a jet transport aircraft, the designer could fix the value from the given range and statistics based on jet transport aircraft. It is also aimed to present rational judgment for trends obtained for tail sizing. It benefits a designer to decide or understand better the properties of design factors.

1.2 Definitions

This report deals with "Empennage Statistics and Sizing Methods for Dorsal Fins". Short definitions of the terms in the report title are already given under "Terms and Definitions". This subsection will further clarify the task of this report.

Empennage
An empennage or tail unit is the combination of stabilizing and controlling surfaces situated at the rear of an aircraft (**MAD 1980**). It consists of vertical stabilizer, horizontal stabilizer and its associated control surfaces rudder and elevator respectively. Main functions of a tail in an aircraft are to stabilize an aircraft and provide adequate amount of control for trim and maneuver (**Raymer 1992**). Primarily, the moment generated by the wing is balanced by the lift generated by the horizontal stabilizer which is acting through a tail moment arm about the centre of gravity of the aircraft. In case of the vertical stabilizer, generation of a trim force is not required since the aircraft is symmetric and does not generate any unbalanced moments in normal operation. Tail sizing is also influenced by the control power of the control surfaces which are the rudder and elevator. Control by the tail depends upon the size and type of control surfaces as well as the total tail size and shape.

Statistics
It is defined as a quantity calculated from a sample of observations usually as an estimate of some population parameter such as mean or standard deviation (**MAD 1980**). Interpretation of standard deviation or mean provides numerical information about the sample collected. The statistics collected for this report is mainly in two parts. The first part contains data based on tail sizing parameters like volume coefficient, horizontal tail sweep, thickness ratio, etc. for different category of aircraft. Such statistics displays the relatedness between parameters and results obtained are used to size the tail. The second part is statistics on parameters of the vertical stabilizer to develop a method to size dorsal fins for jet and propeller transport aircraft containing dorsal fins. Parameters considered for dorsal fin sizing are vertical tail sweep, vertical tail area, dorsal fin sweep, etc. Statistics on collected data are done in Microsoft Office Excel for this project.

Sizing Method
Sizing in terms of aircraft design is defined as the operations performed to produce specified dimensions and tolerances (**MAD 1980**). Therefore, a sizing method is to form a method which could be applied to produce dimension of a section in an aircraft. The sizing method developed in this project is based on the results from statistics of the tail and the dorsal fin of aircraft.

Dorsal Fin
A dorsal fin in most aircraft is mainly used to provide directional stability at higher sideslip angle (**Crawford 2009**). It could be described as an extension of the vertical tail, outward

along the fuselage length from its leading edge. Figure 1.1 shows a conventional vertical tail with a dorsal fin and Figure 1.2 shows a cut away section to give a clear idea of dorsal fin structure. It can be observed from Figure 1.2 that the dorsal fin is mainly not an extension of the airfoil section of the leading edge of the vertical tail. It is more like a projected area, for extension, from the leading edge which is converged along the fuselage length. According to **Crawford 2009** the effectiveness of the vertical tail increases with the addition of a dorsal fin, without adding much weight or drag. As per investigation done for this paper, dorsal fin is very common in combat aircraft and homebuilt aircraft. But it is also implemented on commercial aircraft.

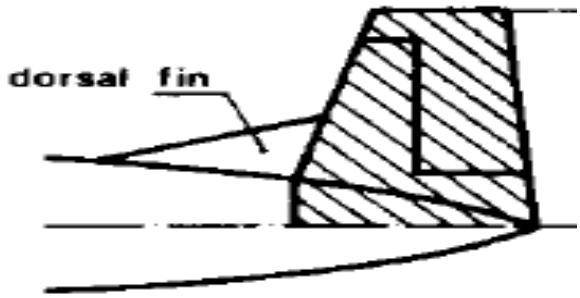

Figure 1.1 Conventional vertical tail with dorsal fin (**Torenbeek 1982**)

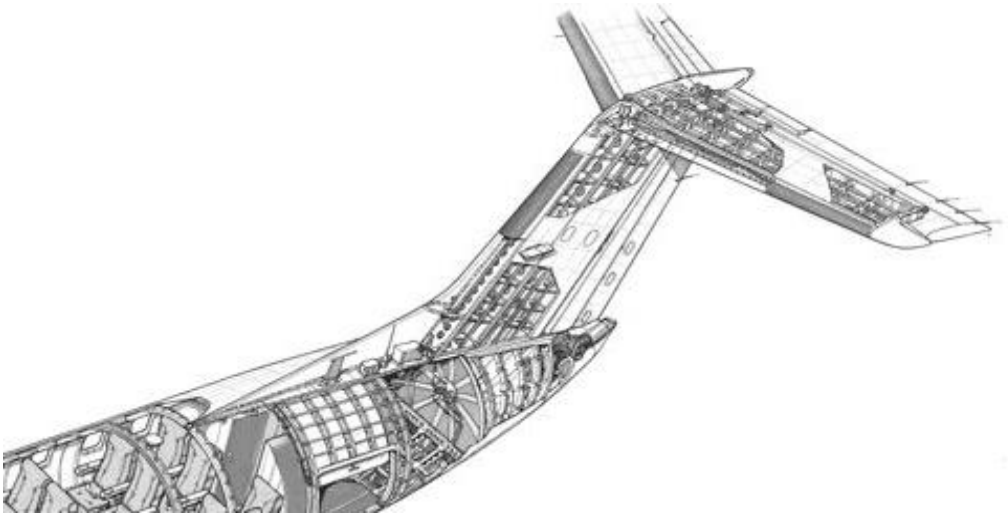

Figure 1.2 Cut away section of vertical tail with dorsal fin of Embraer 120 (**FlightGlobal 2013**)

This report is hence about statistics for empennage sizing and about statistics and a sizing methodology for dorsal fins in commercial aircraft.

1.3 Objectives

This report aims at giving users more refined starting values for different parameters of the tailplane and dorsal fin. After analyzing results from literature prior to this report, it was de-

cided to improve these results and to produce values closer to real aircraft. These values may then be used for the different design parameters. This is to be achieved through statistical methods. The tail sizing is to be achieved through several statistics conducted on various parameters of the tail. The list of parameters on which statistics were conducted is given under List of Symbols. Some parameters of the wing and some general aircraft parameters are also included in this list as these have been used in comparison with parameters of the tail with the aim to develop correlations between already established parameter values and tail parameter values.

On the other hand, the dorsal fin sizing methods have to be developed from statistics of jet and propeller aircraft. Surveys have to be conducted to find out the different types of dorsal fins in practice. Classification of dorsal fins has to be discussed. Then parameters which size dorsal fins have to be defined and with the help of 3 views parameters have to be measured. All possible relationships have to be checked to find the correlation between the parameters. These correlations then combine to form the final sizing methods.
The methodology used in this report is described in more detail in Chapter 1.4.

1.4 Methodology

Collecting Numerical Data
The main focus area of this report is the study of transport aircraft, though empennage statistics are review of other aircraft categories too. **Jane's 2008-09** and **Roux 2007** were examined and only aircraft with dorsal fin and round edge dorsal fin were shortlisted and data was collected for further studies. Aircraft data was then categorized under:

- jet transport with dorsal fin,
- propeller transport with dorsal fin,
- jet transport with round edge.

Collecting Data from 3-View-Drawings
3-view drawings were collected of all selected aircraft from **Blueprint 2013** and in airport planning manuals:

- Airbus: **A300 2002, A300-600 2002**, **A300-F4/600 2002**, **A310 2002**, **A318 2005**, **A319 2005**, **A320 2005**, **A321 2005**, **A330 2005**, **A340-200/300 2005**, **A340-500/600 2005**, **A350-900 2005**, **A380 2005**.
- Boeing: **B707 2011**, **B717 2011**, **B720 2011**, **B727 2011**, **B737 2011**, **B747-8 2012**, **B757 2011**, **B767 2011**, **B777 2011**, **B787 2011**.
- Embraer: **EMB120 2000**, **EMB170 2003**, **EMB175 2012**, **EMB190 2012**, **EMB195 2012**, **ERJ135 2008**, **ERJ140 2005**, **ERJ145 2007**.

Required parameters were measured from 3-views given in these manuals. Parameter measured were e.g. the height of the vertical tail or the tail chord length. For better precision and

accuracy of measurements, CorelDRAW, a vector graphic software, was used for the measurement of parameters. In order to use CorelDRAW, it was necessary to convert all the 3-views obtained as pixel graphic into a format that can be used by CorelDRAW. This format is Encapsulated Postscript known also as EPS format. Measured parameters were then listed and converted to aircraft scale using Excel.

Plotting and Evaluating Data for Synthesizing a Design Methodology
Plots were produced in Excel using the parameters that could possibly support the development of a sizing method. Regression analysis of the plots was done in order to measure the relatedness between the parameters. The relatedness was expressed with Excel in form of the coefficient of determination, R^2. The parameters were also considered in their aerodynamic context. Selected parameters were finally put together to for synthesizing a design methodology. Observations were then compiled to produce this report.

Comparison with Design Rules and Methods from Text Books
A new method had to be synthesized for dorsal fin sizing. For general tail parameters reference values and sizing methods are already available in aircraft design text books. These books were consulted and design rules and methods challenged by checking them with collected aircraft data. Parameters collected for tail sizing method came from 3-views and aircraft design books available. Again, CorelDRAW and Microsoft Office Excel were used to measure and plot the parameters. As per the outcome logical conclusions are drawn and design ranges for the parameters are set.

1.5 Literature

The understanding of dorsal fin mainly started from **Patent US 2356139**. Dorsal fin was patented in the year 1944 and the report explains the aerodynamic behavior of the vertical tail with various type of dorsal fin. Advantages are significant according to the experimental data presented in **Patent US 2356139**. This patent report is the starting point to understand and study the dorsal fin for this paper.

Literature for this report could be categorized into two parts: numerical data and literature references. Numerical data for parameters were collected mostly from **Blueprints 2013** and airport planning manuals mentioned in chapter 1.1. Snapshots showing types of dorsal fins were compiled from an Internet image search. This leads to different sources on the Internet quoted each time an image is presented in this report.

To understand the aerodynamic characteristics of dorsal fins, **Obert 2009** was used as reference. **Obert 2009** provides experimental data to consolidate its theoretical knowledge about the dorsal fin in an aircraft. It covers a major part of this report and helps the reader under-

stand dorsal fins better with real investigated data displayed. Other aircraft design books taken under consideration for this report do not contain as much detailed information about dorsal fin as **Obert 2009**. To understand the dorsal fin, it is also important to learn and discuss the vertical tail in aircraft. It is mainly the directional stability which is associated with the vertical tail and dorsal fin in an aircraft. Cumulative knowledge from **Whitford 1987, Raymer 1992 and Crawford 2013** has been used to explain general characteristics of the vertical tail and a dorsal fin influencing directional stability in an aircraft. It helps the reader to understand how the vertical tail and vertical tail with dorsal fin behave at high sideslip angle.

Aerodynamic characteristics of wings at high angle of attack were investigated using a method given in **DATCOM 1978.** Such investigations show how aerodynamic properties like maximum lift coefficient and the stall angle of a wing are affected by factors like aspect ratio, sweep angle, Mach number, etc. **DATCOM 1978** provides important results which show similarity up to a certain extent with the concepts gathered from other sources about vertical tails and dorsal fins.

1.6 Structure of the Report

This report aims at giving users more refined starting values for different parameters of the tailplane and dorsal fin. After analyzing work done in this direction prior to this report, it is attempted to improve on earlier results and produce values that are closer to the final values an aircraft designer may use for the different parameters discussed.

Chapter 2 gives an introduction to an aircraft's tail with emphasis to the vertical tail and work done in tail sizing by various other authors so far. It starts off by describing some of the general characteristics of vertical tails, dorsal and ventral fins. The aerodynamic characteristics of vertical tails and in particular dorsal fins are then analysed. After discussing different types of dorsal fins currently in use, this chapter ends with a section dealing with tail sizing and work done on it prior to this report.

Chapter 3 deals with sizing of the horizontal and vertical tails and their control surfaces. It starts off with a detailed analysis of the tail volume coefficients, moving a step ahead in choosing good initial estimates for the same. The tail geometry is then considered and each parameter discussed in Chapter 2 is analyzed further and results to arrive at better preliminary values for the conceptual design phase are suggested.

Chapter 4 goes into the in-depth analysis of an aircraft's dorsal fin geometry. In this the dorsal fin and the round edge dorsal fin are considered and methods to size the two are suggested after statistical analysis of various relationships between unknown dorsal fin parameters and known vertical tail parameters.

2 State of the Art

2.1 General Characteristics of Vertical Tails, Dorsal and Ventral Fins

The vertical tail as a whole is responsible to provide the aircraft lateral/directional stability.

> *Some form of vertical stabiliser is needed to give directional stability (also called weathercock stability). If a stable aircraft is disturbed in yaw – by a gust, say, as shown in* [See *Figure 2.1*] *– it will tend to return to its original equilibrium state. The forward fuselage ahead of the aircraft's centre of gravity produces a side force which tends to make the nose swing away from the relative wind and thereby increases the angle. This is an unstable tendency, and if it is unchecked the nose will diverge further away from the direction in which it was originally pointing. Thus a force to counteract this diverging tendency is required: the wings contribute little, and though the rear fuselage does counter the motion to a degree, a vertical stabiliser or fin is needed for acceptable directional stability ... No mention has yet been made of the pilot's reaction to the disturbance in yaw; indeed, in this analysis the pilot is assumed not to be touching the controls ... Fin size and shape, position and number all contribute to directional stability. The minimum permissible fin area can be fixed by the requirement for inherent static weathercock stability. If this requirement was the sole criterion, aircraft would have smaller vertical stabilisers than they do. In practice fin size is however influenced by a host of other constraints, such as how quickly the disturbance is to be eliminated, spin prevention / recovery, asymmetric flight, and the intended speed /manoeuvre envelope of the aircraft. In the past, aircraft have "grown" dorsal fin extensions during their development to combat the risk of fin stalling. The fin extension does not improve effectiveness very much at small sideslip angles but it has powerful anti-stall and stabilising properties at large angles.* (**Whitford 1987**)

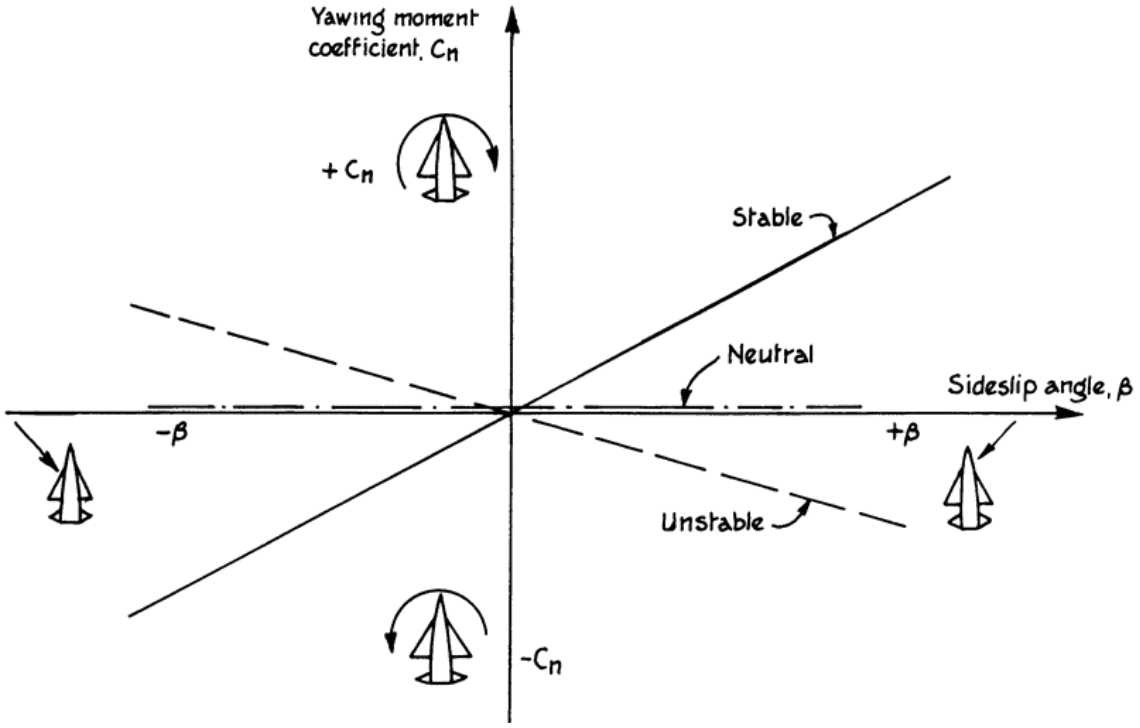

Figure 2.1 Directional stability (**Whitford 1987**)

> *The dorsal fin improves tail effectiveness at high angles of sideslip by creating a vortex that attaches to the vertical tail. This tends to prevent the high angles of sideslip seen in spins, and augments rudder control in the spin.* (**Raymer 1992**)

A dorsal fin is advantageous since it increases the vertical tail area without significant increase of weight and drag as mentioned in Chapter 1.1. It could be observed from Figure 1.2 that the dorsal fin section is hollow which could possibly explain why a dorsal fin is not as heavy compared to a vertical tail of the same area.

Figure 2.2 demonstrates the contribution of different components of the aircraft towards directional stability.

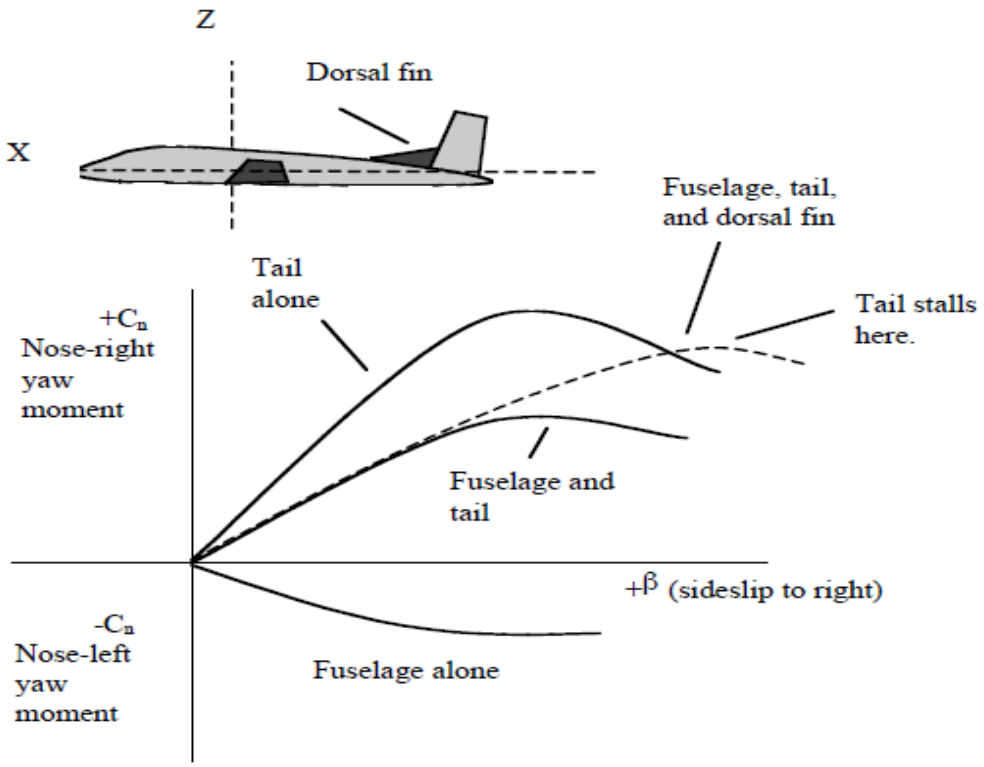

Figure 2.2 Contributions to directional stability (**Crawford 2009**)

It can be observed from Figure 2.2 that the addition of a dorsal fin increases the yawing moment at high angles of sideslip. A fuselage alone generates a negative yaw moment. A tail is required in an aircraft to counteract this negative yaw moment to maintain equilibrium in all flight conditions.

> *Rudder deflections, wind gusts, asymmetric thrust, adverse yaw, yaw due to roll, and bank angles in which the effective lift is less than aircraft weight can all cause sideslips.* (**Crawford 2009**)

> *Of course, the vertical tail contributes most to directional stability. The yaw moment produced by the tail depends on the force its surface generates and on the moment arm between the tail's center of lift and the aircraft's center of gravity. (Therefore, a smaller tail needs a longer arm to produce a yaw moment equivalent to a bigger tail on a shorter arm. That being said, changing the c.g. location for a given aircraft, within the envelope for longitudinal stability, has little effect on its directional stability.) The rate of the increase in force generated by the tail as β increases depends on the tail's lift curve slope (just as the rate of increase in C_L with angle of attack depends on the*

> *slope of the lift curve of a wing). Lift curve slope is itself a function of aspect ratio. Higher aspect ratios produce steeper slopes.* [See *Figure 2.2*] *The $C_{n\beta}$ directional stability curve for the fuselage and tail together reaches its peak when the tail stalls ... adding a dorsal fin increases the tail's effectiveness (and without adding much weight or drag). Because of its higher aspect ratio and steeper lift curve, the vertical tail proper produces strong and rapidly increasing yaw moments at lower sideslip angles, but soon stalls. But the dorsal fin, with its low aspect ratio and more gradual lift curve, goes to a higher angle of attack before stalling, and so helps the aircraft retain directional stability at higher sideslip angles. The dorsal fin can also generate a vortex that delays the vertical tail's stall.* (**Crawford 2009**)

An alternative for a dorsal fin in an aircraft can be either a highly swept tail or a ventral fin. Ventral fin is defined as a fixed vertical surface on an airplane that extends below the aft end of the fuselage (**Crane 2013**). Figure 2.3 shows an image of a ventral fin in an aircraft.

> *The ventral tail also tends to prevent high sideslip, and has the extra advantage of being where it cannot be blanketed by the wing wake. Ventral tails are also used to avoid lateral instability in high-speed flight.* (**Raymer 1992**)

On passenger jets ventral fins seldom used because they are in the way when the aircraft rotates on the runway for take-off or in the landing flare. In order to avoid such problem it would be necessary to introduce a longer landing gear so that the aircraft is positioned higher with respect to the ground. The longer than normal landing gear would lead to an increase in weight and space. Also, an isolated ventral fin has not the same aerodynamic effect as a dorsal fin in combination with the fin.

> *Instead of a lightly-swept leading edge in combination with a dorsal fin also a fully-swept-back leading edge on a vertical tail surface may produce favourable sideslip characteristics."* (**Obert 2009**)

This phenomenon is explained in details in Chapter 2.2.

Figure 2.3 Ventral fin (marked with a red circle) (**Audries 2013**)

2.2 Aerodynamic Characteristics of Vertical Tails

Chapter 2.1 explains the characteristics of the vertical tail, dorsal fin and ventral fin. In this chapter, the aerodynamic characteristics of the vertical tail (as discussed in Chapter 2.1) will be investigated. **Truckenbrodt 2001** and **Datcom 1978** provide methods and theories to understand the aerodynamic characteristics of the vertical tail. Results obtained from the investigation give an insight to understand how the geometrical parameters of the vertical tail affect the lift force and stall at high sideslip angle of the vertical tail. Geometric parameters that are considered are: sweep, aspect ratio, taper ratio, relative thickness of the airfoil and Mach number. Factors like Reynold's number, altitude, etc are kept constant.

Figure 2.4 presents a plot that shows the variation of lift curve gradient with aspect ratio of the vertical tail.

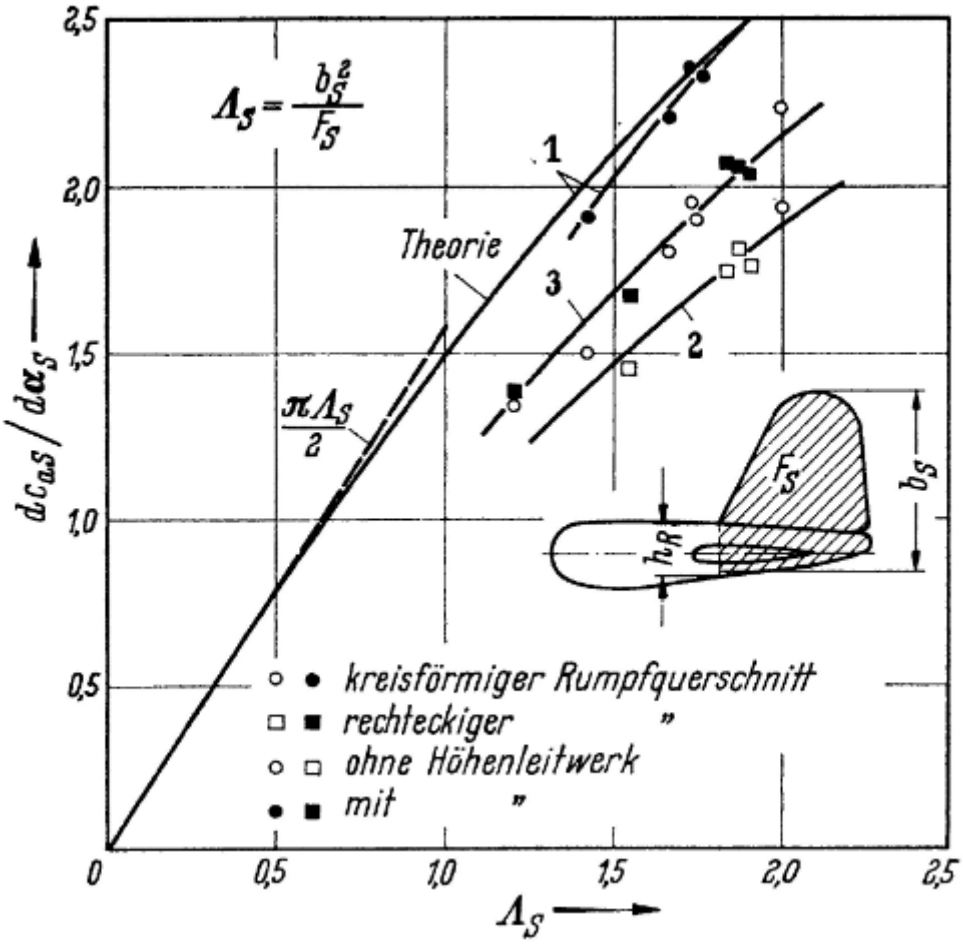

Figure 2.4 Variation of lift curve gradient with aspect ratio of the vertical tail (**Truckenbrodt 2001**)

As observed from the figure, a vertical tail at the right side corner indicates the area and tail span considered for the investigation in **Truckenbrodt 2001** method. The aspect ratio is defined as

$$A = \frac{b_v^{\,2}}{S_v} \tag{2.1}$$

where,

A Aspect ratio of the vertical tail

b_v span of the vertical tail

S_v Vertical tail area

Obert 2009 states

> *According to lifting surface theory the gradient of the lift coefficient vs. angle-of-attack curve is linear with aspect ratio for airfoils with low aspect ratio (up to about A = 1.5) and practically independent of planform…For A < 1.5, the lift gradient equals* $C_{L_\alpha} = \frac{\pi A}{2}$ *(rad⁻¹)*

$C_{L\alpha}$ (as defined in **Obert 2009**) is the lift gradient for the vertical tail and similar to $\frac{dc_{\alpha s}}{d\alpha_s}$ (as defined in **Truckenbrodt 2001**). The dotted line beside the theory line (Figure 2.4) indicates the linear behavior as learned from **Obert 2009**. In Figure 2.4, the linear lift gradient is drawn only up to aspect ratio 1.0.

However, the theory line represents the lift gradient of the vertical tail and experimental data for a vertical tail close to this theory line is considered to be a measure of the accuracy of aerodynamic properties. Vertical tail lift gradient, $\frac{dc_{\alpha s}}{d\alpha_s}$ is defined as

$$\frac{dc_{\alpha s}}{d\alpha_s} = \frac{2\pi A_s}{\sqrt{A_s^2 + 4} + 2} \tag{2.2}$$

Lines 1, 2 and 3 represent the lift gradient from the experimental data. In Figure 2.4 the circular and rectangular symbol (at the bottom) indicates as follows:

○ ●	Circular fuselage cross section
□ ■	Rectangular fuselage cross section
○ □	Without horizontal tail
● ■	With horizontal tail

Therefore, line 1 indicates the experimental data of a vertical tail is obtained when the vertical tail is attached with round fuselage cross section and horizontal tail. Similarly, line 2 signifies the experimental data of a vertical tail with rectangular fuselage cross section and without horizontal tail. Thus, circular and rectangular figures explained could be implied to understand the result of line 3.

It could be noticed from Figure 2.4 that line 1, i.e, lift gradient of the vertical tail with circular fuselage cross section and horizontal tail is closest to the theory line than other line.

To further understand the aerodynamic characteristics of a vertical tail it is assumed that the vertical tail, also being a lift surface, should exhibit similar behavior like low aspect ratio wing. To test this hypothesis, the lift gradient for low aspect ratio vertical tails is investigated. **Datcom 1978** provides a method to calculate the lift slope for low aspect ratio wing. Aspect ratio, taper ratio and quarter chord sweep angle measured from the vertical tail in Figure 2.4 are applied to the method applicable to low aspect ratio wings as given in **Datcom 1978**. Mach number is considered to be 0.2 throughout for simplicity of **Datcom 1978** method as explained in **Scholz 2009**.

Figure 2.5 demonstrates the plot of lift slope obtained from **Datcom 1978** method and **Truckenbrodt 2001** method.

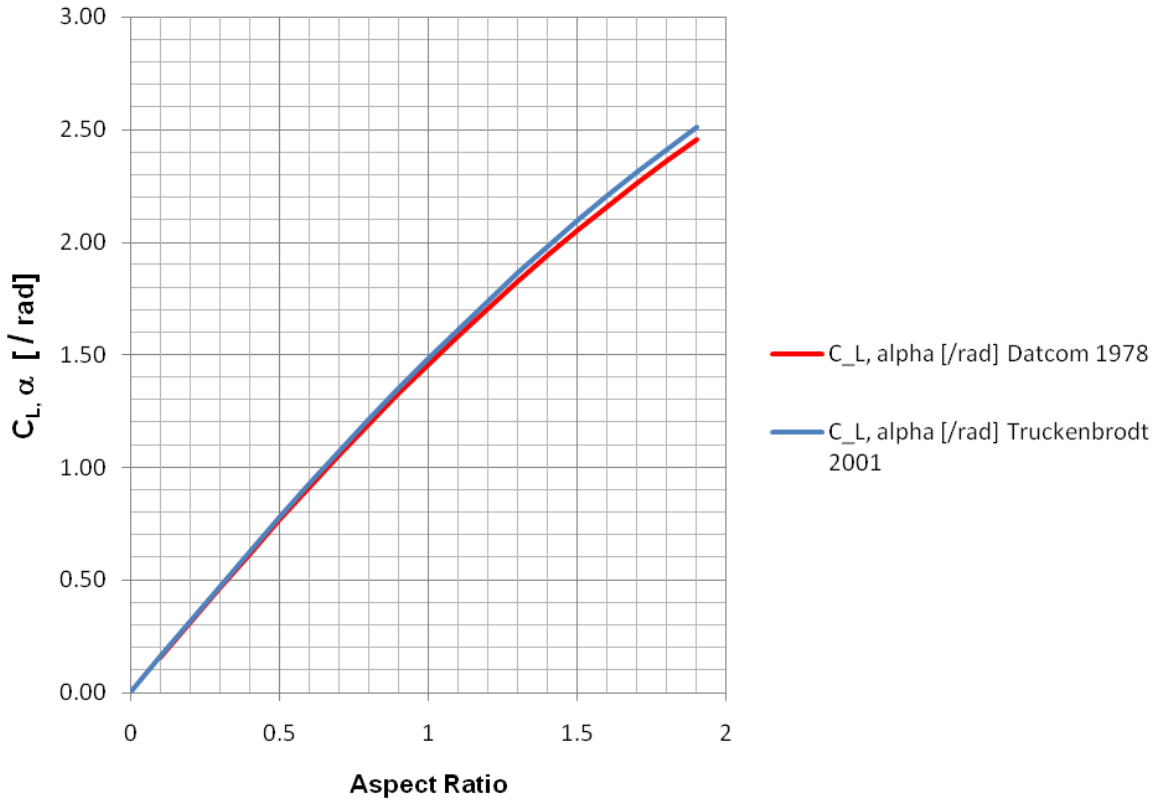

Figure 2.5 Comparison of lift slope for low aspect ratio lift surface obtained from **Truckenbrodt 2001** and **Datcom 1978**

Lift slope equation for low aspect ratio wing from **Datcom 1978** is

$$C_{L_\alpha} = \frac{2\pi A}{2 + \sqrt{A^2 (1 + \tan\varphi_{50}) - M^2 + 4}} \tag{2.3}$$

where,

A Aspect Ratio

$\tan\varphi_{50}$ half chord sweep angle
M Mach number

The lift slope curve obtained from **Datcom 1978** equation shows a similar trend when plotted with the lift slope curve from **Truckenbrodt 2001** equation (Figure 2.5). Moreover, both the curves tend to be quite close to each other. Lift slope curve of **Datcom 1978** (red line in Figure 2.5) being below, near and similar to the theory line (blue line in Figure 2.5) of **Truckenbrodt 2001** validates that **Datcom 1978** method for low aspect ratio wing could be used to investigate aerodynamic characteristics of the vertical tail. **Datcom 1978** method is used to understand the behavior of the vertical tail when subjected to variation of different parameters.

2.2.1 Application of Datcom Method to understand the aerodynamic behavior of the vertical tail

Datcom 1978 presents two methods to calculate the maximum lift and angle at maximum lift of the lift surface. According to **Datcom 1978**, Method 1 is applicable if the user has an accurate wing spanwise- loading computer program. If no such computer programming is available user may apply Method 2 and 3 to calculate the maximum lift and angle at maximum lift.

Since the input parameters considered for this report are the average values from Chapter 3 and no such computer programming is available, Methods 2 and 3 are used to continue with the investigation. In this chapter only the result from Methods 2 and 3 of **Datcom 1978** are discussed and the complete methods are not presented. To know more about the methods **Datcom 1978** could be referred.

Method 2, according to **Datcom 1978**, is mainly applicable for high aspect ratio lift surfaces and Method 3 is applicable for low aspect ratio lift surfaces. For an aspect ratio in between the low and high aspect ratio values that do not satisfy the conditions to determine and follow Method 2 or 3, it is allowed to choose any of the two methods (**Datcom 1978**). It is examined however, that for aspect ratios where either method is supposed to be valid, the methods do not result in similar or approximate values. So, it is conceived to average the results from both the methods in order to obtain a better result. Figure 2.6 represents the variation of the lift slope, maximum lift and angle at maximum lift with aspect ratio. It also shows the borderline to indicate the range of aspect ratio that validates Methods 2, 3 and interpolation.

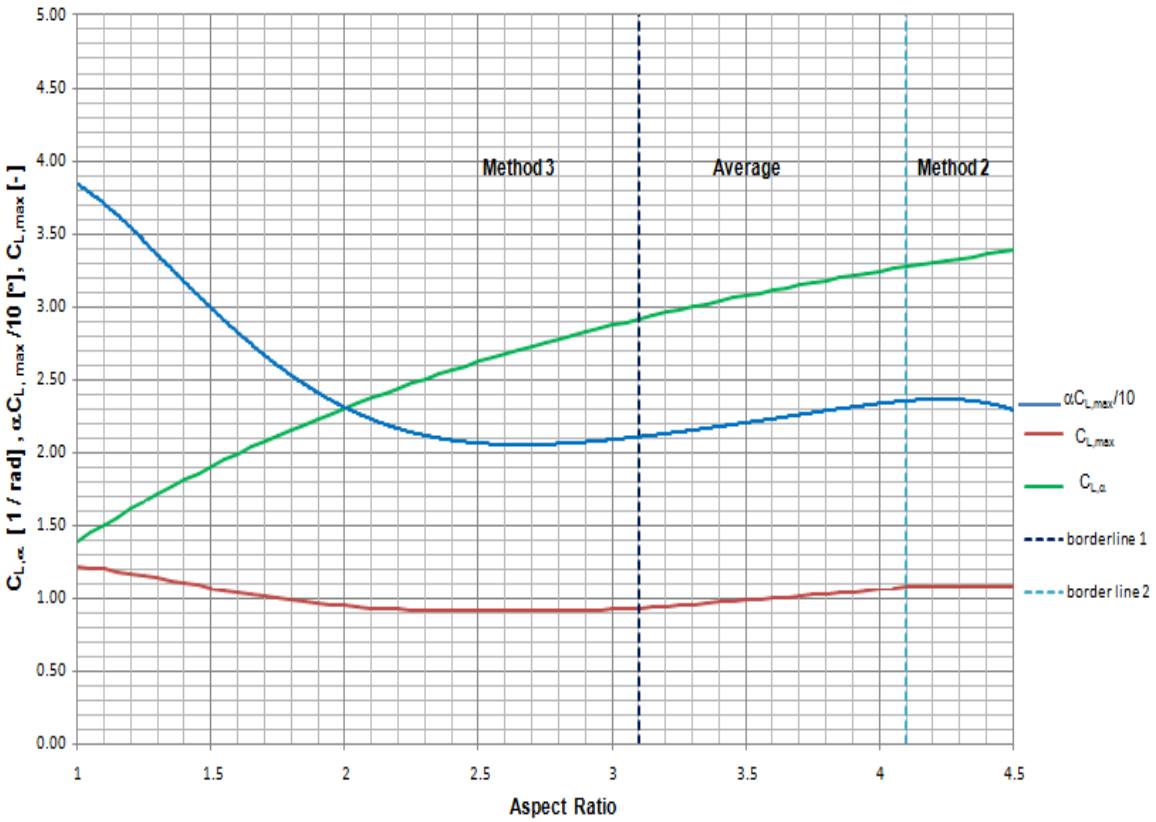

Figure 2.6 Variation of lift slope, maximum lift and angle at maximum lift for a vertical tail with aspect ratio using methods from **Datcom 1978**.

In Figure 2.6, x- axis is the aspect ratio and y- axis represents the lift gradient ($C_{L,\alpha}$), angle at maximum lift ($\alpha C_{L,\,max}$) and maximum lift ($C_{L,\,max}$) with their units (1/rad), (°) and (-), respectively. (-) signifies no unit for $C_{L,\,max}$, since it is a coefficient. $C_{L,\,max}$ also indicates maximum lift generated over the lift surface. Higher the value of $C_{L,\,max,}$ higher is the value of maximum lift.

Chapter 3 lists the average values of quarter chord sweep angle, taper ratio, thickness to chord ratio, etc that could be considered for the preliminary design of the vertical tail of jet transport. Listed average values from Chapter 3 are used to calculate the lift slope, maximum lift and stall angle at maximum lift with **Datcom 1978** methods. Average values of the parameters for the vertical tail considered are:

Aspect Ratio, A	1.45
Quarter chord sweep angle, $\varphi_{0,25}$	40.1
Taper ratio, λ	0.48
Relative thickness, t/c_{max}	10.5%
Maximum thickness at chord, $x_{t/c}$	30%

Figure 2.6 indicates that for aspect ratios lying in the range of 1.0 to 3.1, Method 3 is valid, for aspect ratios more than 4.1 Method 2 is valid and for aspect ratios in the range of 3.1 to 4.1, averages between Method 2 and Method 3 are calculated.

The average aspect ratio for the vertical tail of jet transport is 1.45 (Chapter 3). The focus of this report is to study the vertical tail and dorsal fin of commercial aircraft, and mainly jet liners. Therefore, for aspect ratio 1.45, Method 3 is valid (Figure 2.6) to investigate the aerodynamic behaviors of the vertical tail. For the vertical tail of aspect ratio 1.45 and with average values from Chapter 3, effect of different parameters like sweep angle, taper ratio, relative thickness and Mach number over maximum lift, stall angle and lift slope is investigated with Method 3 of **Datcom 1978**.

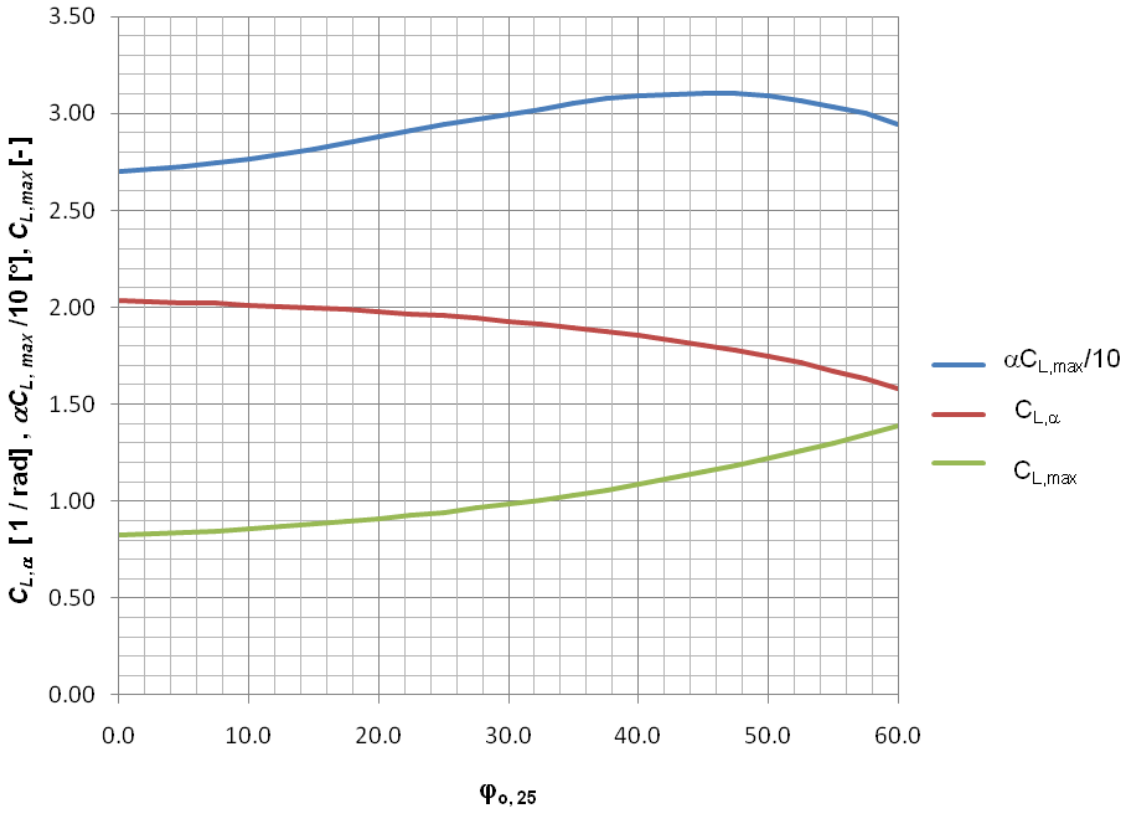

Figure 2.7 Effect of quarter chord sweep on lift slope, maximum lift and angle at maximum lift of the vertical tail with the application of **Datcom 1978** Method 3.

It should be noticed that angle at maximum lift, $\alpha C_{L,\,max}$, in Figure 2.7 is calculated as $\alpha C_{L,\,max}$/ 10. Therefore, the values noted from Figure 2.7 have to be multiplied by 10 to get the correct value of angle at maximum lift. Similar should be followed for other plots (Figure 2.8, Figure 2.9 and Figure 2.10). As quarter chord sweep angle, $\varphi_{0,\,25}$ of the vertical tail increases from 0° to 60°, angle at maximum lift ($\alpha C_{L,\,max}$ [°] in Figure 2.7) also increases from 27° (at $\varphi_{0,\,25}$ = 0°) to maximum 31° at 45° quarter chord sweep angle and again decreases till 29.5° (at $\varphi_{0,25}$ = 60°). However, maximum lift ($C_{L,\,max}$ in Figure 2.7) increases significantly from 0.8 to 1.40 with the increase of φ_{25}. The lift slope ($C_{L,\alpha}$ [1/rad] in Figure 2.7) deceases gradually from 2.1 (at $\varphi_{0,\,25}$ = 0°) to 1.59 (at $\varphi_{0,25}$ = 60°). With the increase of sweep angle in a vertical tail lift, maximum lift increases significantly at the given relative thickness of 10.5%. Angle at maximum lift also increases but for maximum lift, angle at maximum lift is not the maximum.

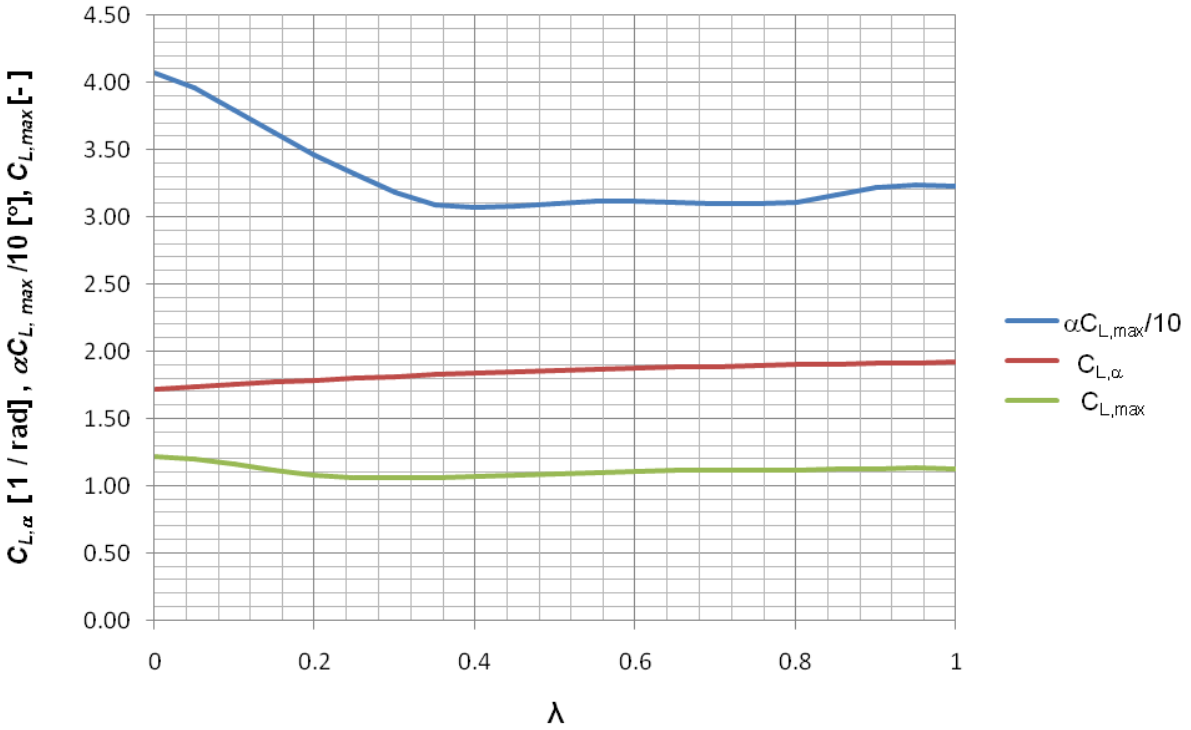

Figure 2.8 Effect of taper ratio on lift slope, maximum lift and stall angle of the vertical tail with the application of **Datcom 1978** Method 3.

As taper ratio λ, increases from 0 to 0.4, angle at maximum lift ($\alpha C_{L,max}$ [°] in Figure 2.8) decreases significantly from 41° to 31°. From a taper ratio of 0.4, the angle at maximum lift of the vertical tail is almost constant. Similar trend is observed for maximum lift ($C_{L,max}$ in Figure 2.8). Maximum lift decreases from 1.2 (at $\lambda = 0$ in Figure 2.8) to 1.0 (at $\lambda = 0.2$ in Figure 2.8) and then remains almost constant. Lift gradient ($C_{L,\alpha}$ [1/rad] in Figure 2.8) remains approximately constant with the increase of taper ratio. Therefore, it can be concluded that lower taper ratio planform results in a high angle at maximum lift. Maximum lift generated is not much affected by taper ratio. Lift slope is constant and results in no change with the variation of taper ratio.

Relative thickness of the airfoil shows no effect in maximum lift, lift slope and angle at maximum lift of the vertical tail (see Figure 2.9). Angle at maximum lift is constant at 31°, maximum lift is constant at 1.1 and lift slope is constant at 2.0 with the increase of relative thickness from 7% to 12%.

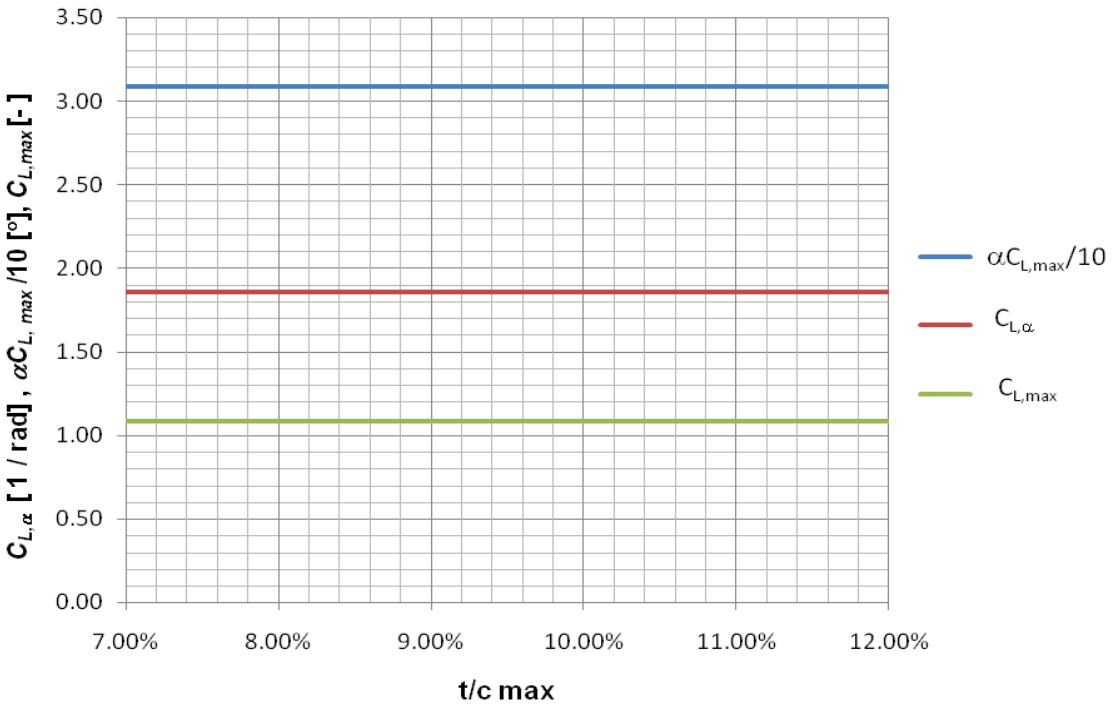

Figure 2.9 Effect of relative thickness on lift slope, maximum lift and angle at maximum lift of the vertical tail with the application of **Datcom 1978** Method 3.

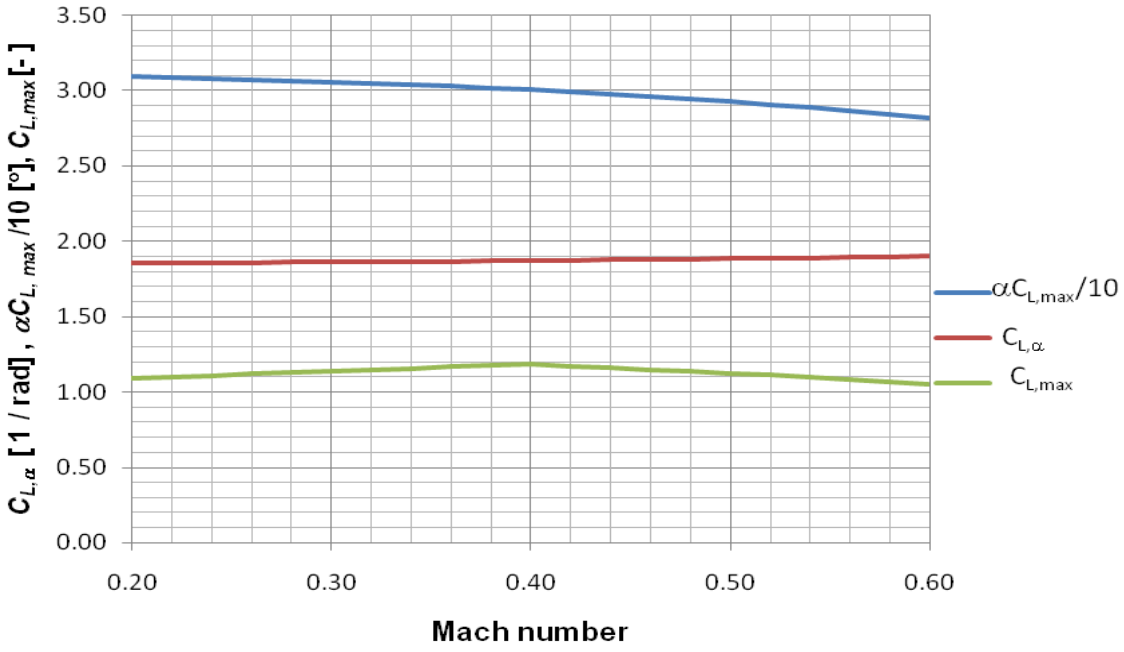

Figure 2.10 Effect of Mach number on lift slope, maximum lift and angle at maximum lift of the vertical tail with the application of **Datcom 1978** Method 3.

Mach number has no effect in the lift slope ($C_{L,\alpha}$ [1/rad] Figure 2.10). Angle at maximum lift (($\alpha C_{L,max}$ [°] in Figure 2.10) decreases from 31° to 28° as Mach number, M increases from 0.2 to 0.6. Maximum lift ($C_{L,max}$ in Figure 2.10) increases gradually from 1.1 (at 0.2 M in Figure 2.10) to the peak 1.2 (at 0.4 M in Figure 2.10). From maximum lift of 1.2 it decreases gradually till 1.07 (at 0.6 M in Figure 2.10).

After studying the trends with the application of **Datcom 1978** method, it can be observed that sweep angle and taper ratio (up to an extent) has a significant effect on the maximum lift and angle at maximum lift of the vertical tail. Maximum lift measured from **Datcom 1978** signifies the lift force for the yawing moment of the vertical tail when subjected to sideslip. Angle at maximum lift signifies the maximum sideslip angle the vertical tail can cope with.

2.3 Aerodynamic Characteristics of Dorsal Fins

Obert 2009 investigates various dorsal fins in the development of Fokker F-27. Figure 2.11 shows different dorsal fins which were investigated.

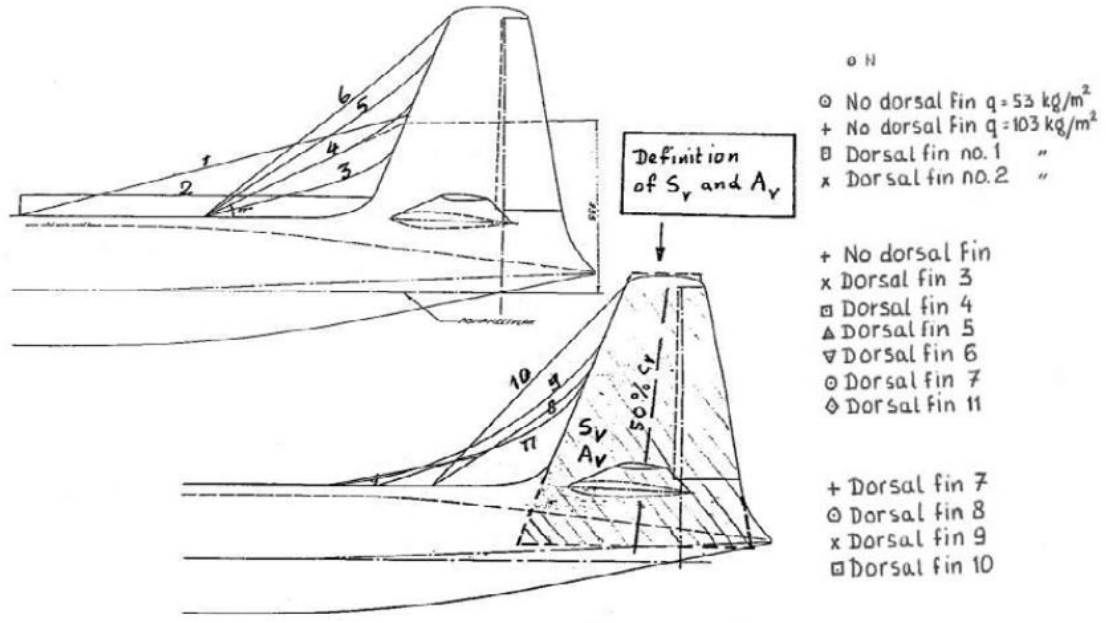

Figure 2.11 Different dorsal fins investigated for a Fokker F-27 (**Obert 2009**)

The effects of different dorsal fins on the aircraft yawing moment are presented in Figure 2.12 and Figure 2.13.

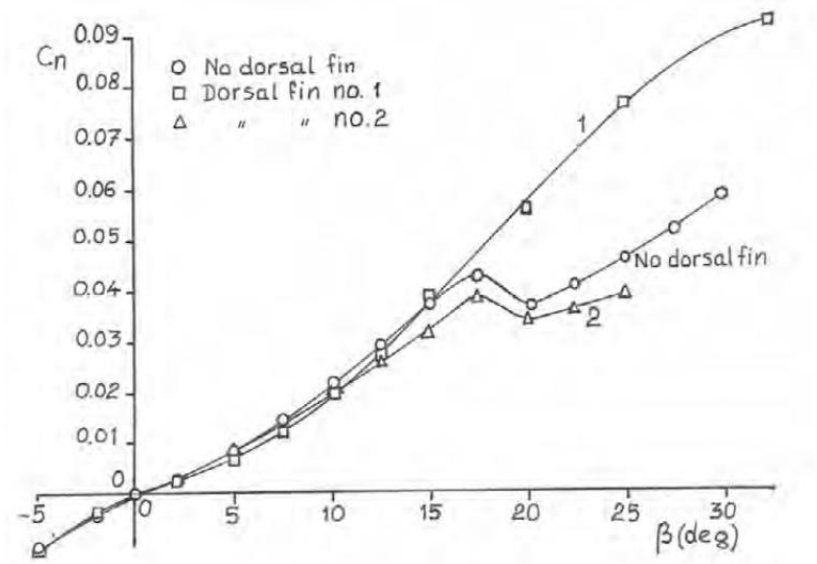

Figure 2.12 Effect of a dorsal fin on the yawing moment coefficient (**Obert 2009**)

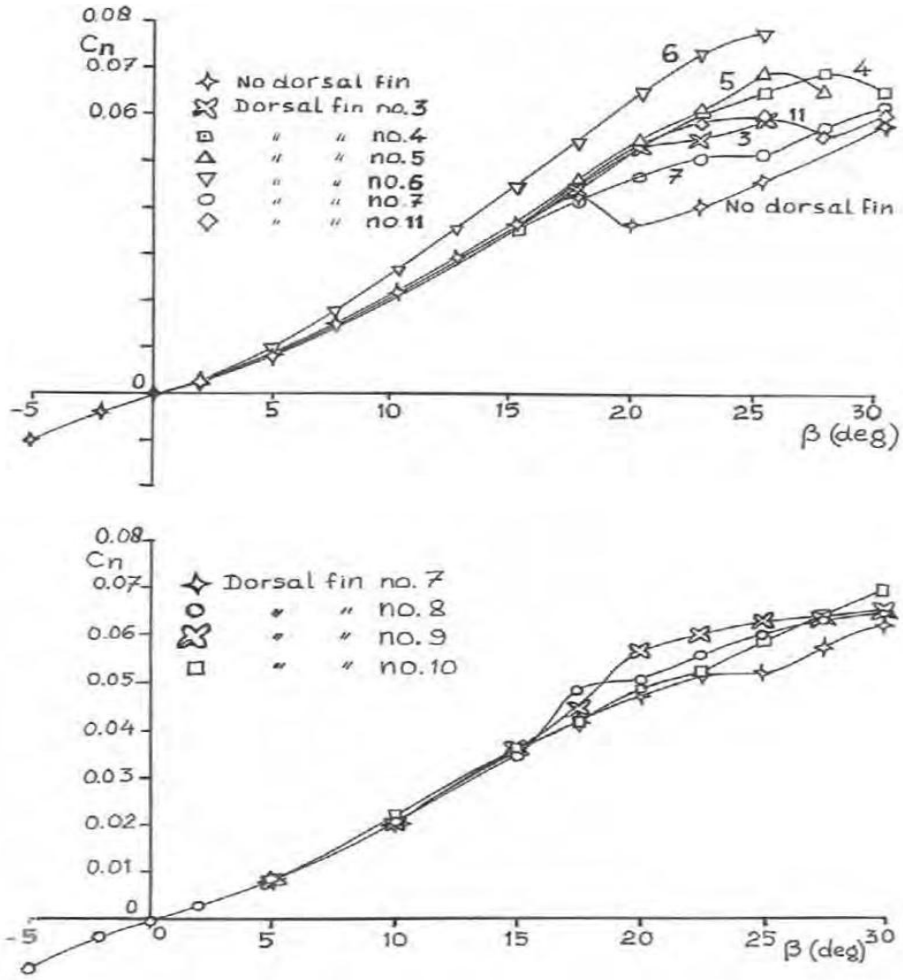

Figure 2.13 Effect of a dorsal fin on the yawing moment coefficient (**Obert 2009**)

Up to 15 deg angle-of-sideslip, the dorsal fin does not affect the lift curve. From 15 deg on, whereas without dorsal fin the maximum lift is almost reached, the dorsal fin modifies the flow over the vertical tail due to the vortex springing from its leading edge. This is controlled local flow

separation which stabilises the flow further outboard postponing complete flow separation to a higher angle of-sideslip. Thus a higher maximum lift and a higher stall angle are achieved. On the full-scale F-27 dorsal fin no.1 was selected. The reason is evident although fin no.6 could also have been a candidate. Instead of a lightly-swept leading edge in combination with a dorsal fin also a fully-swept-back leading edge on a vertical tail surface may produce favourable sideslip characteristics. This was already demonstrated by fin no.6. (**Obert 2009**)

Figure 2.14 shows the vortex generation by a dorsal fin at high sideslip angles.

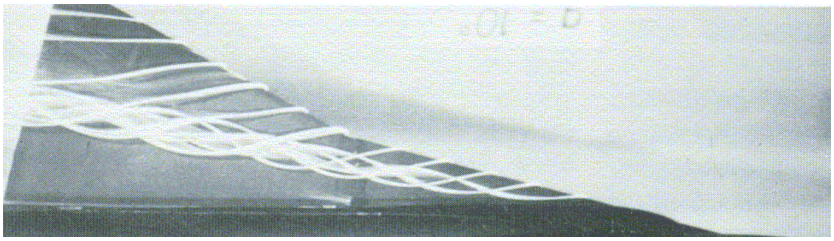

Figure 2.14 Vortex formations by a dorsal fin (**Huenecke 1987**)

Figure 2.15 shows side views of vertical tail surfaces and a dorsal fin chosen to further investigate if all of them exhibit same characteristics.

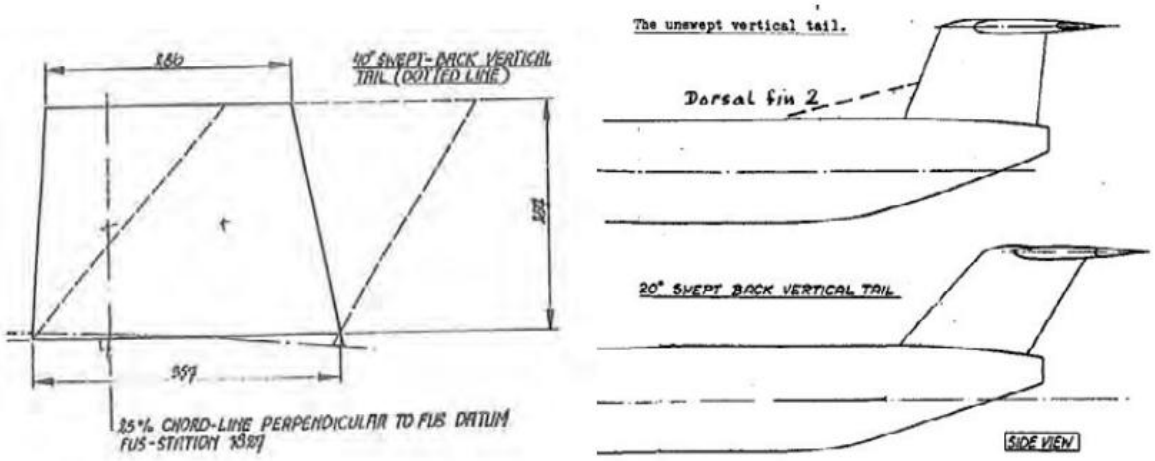

Figure 2.15 Side view of three vertical tail surfaces and a dorsal fin investigated during the development of the Fokker F-28 (**Obert 2009**)

Further, Figure 2.16 to 2.19 show test results of the investigation on these three tail configurations with these differences in leading edge geometry, performed during the development of the Fokker F-28. Figure 2.16 and Figure 2.10 presents yawing moment vs. sideslip angle for two aircraft angles-of-attack for the three configurations investigated.

For the linear regime, the three curves practically coincide. At higher side-slip angles above β = 15 deg, it appears that for zero angle-of-attack applying fin sweep or adding a dorsal fin has nearly the same favourable effect on the yawing moment curve. But, when the aircraft angle-of-attack is increased to 8 deg, the lightly-swept tailplane with a dorsal fin performs better than the fully-swept-back vertical tail surface, although also the latter performs better than the basic tail surface without dorsal fin. (**Obert 2009**)

In Figures 2.18 and 2.19

> *The tail contribution to the yawing moment has been converted to a vertical tail lift curve both with and without horizontal tail surface. Again it is clear that a dorsal fin or a high leading-edge sweep angle improves the sideslip characteristics of tail surfaces. The above shows that also on low-speed aircraft sweep on the fin may be beneficial.* (**Obert 2009**)

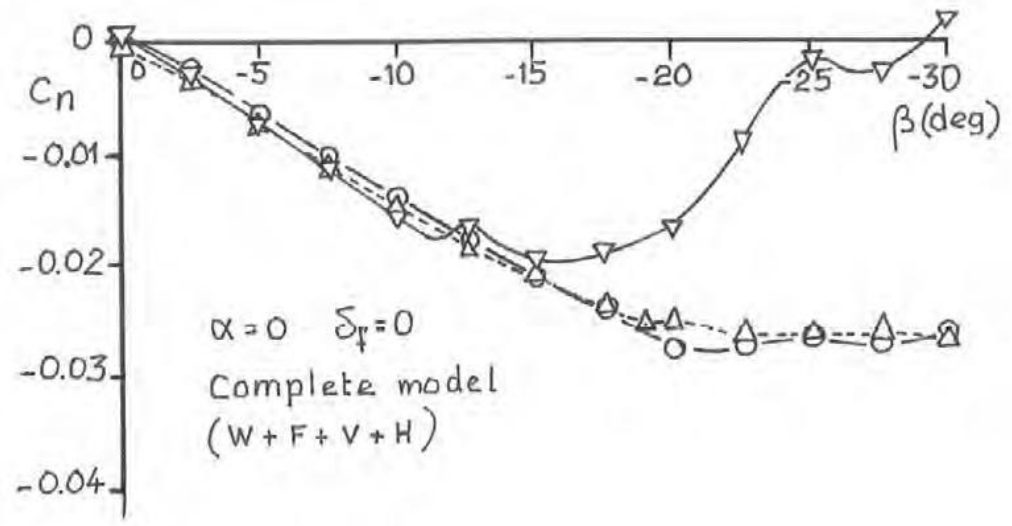

Figure 2.16 Effect of sweep angle on vertical tailplane lift curve. Angle of attack 0°. (**Obert 2009**)

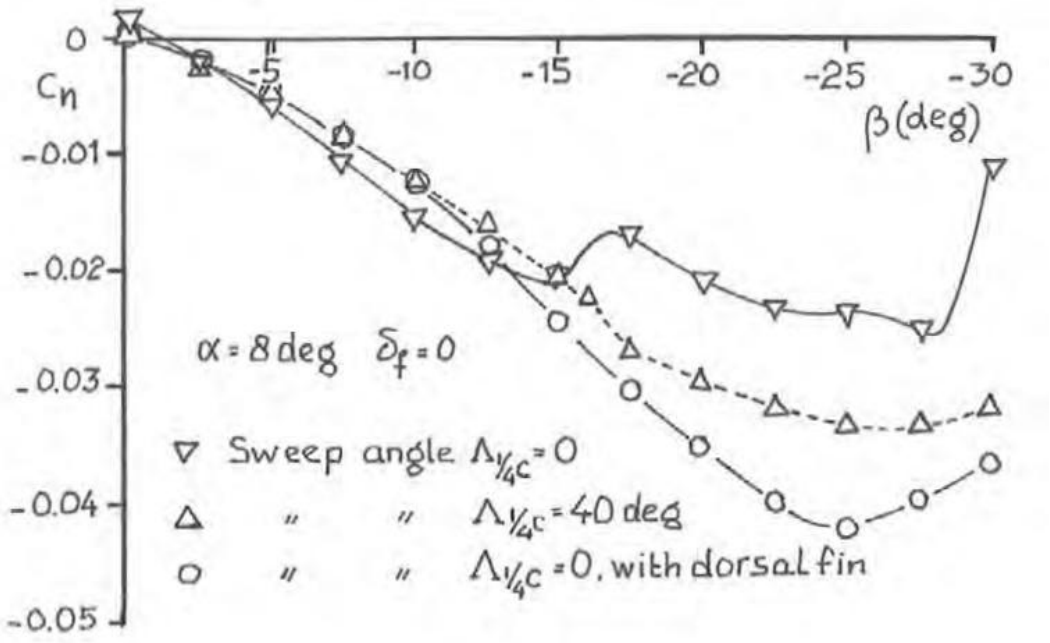

Figure 2.17 Effect of sweep angle on vertical tailplane lift curve. Angle of attack 8°. (**Obert 2009**)

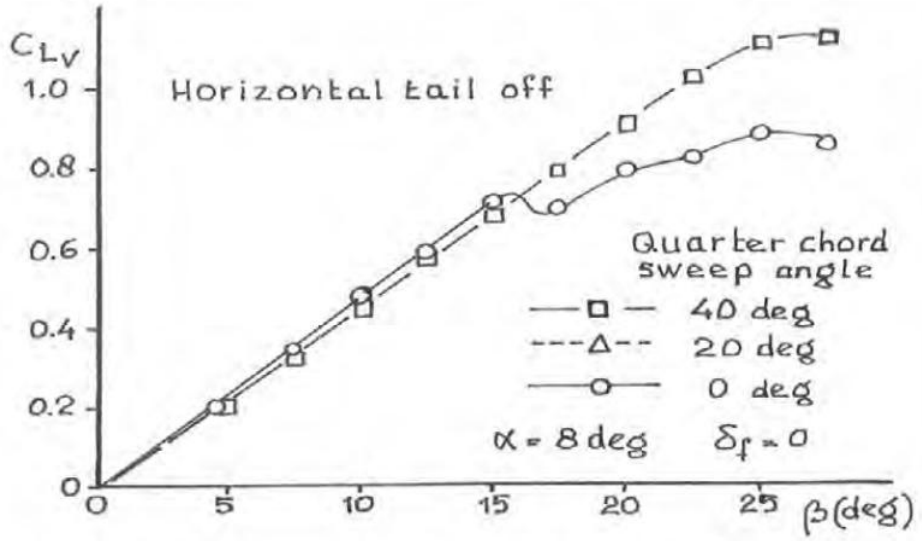

Figure 2.18 Effect of the sweep angle and of the horizontal tail plane on the lift (side force) of the vertical tailplane in sideslip (**Obert 2009**)

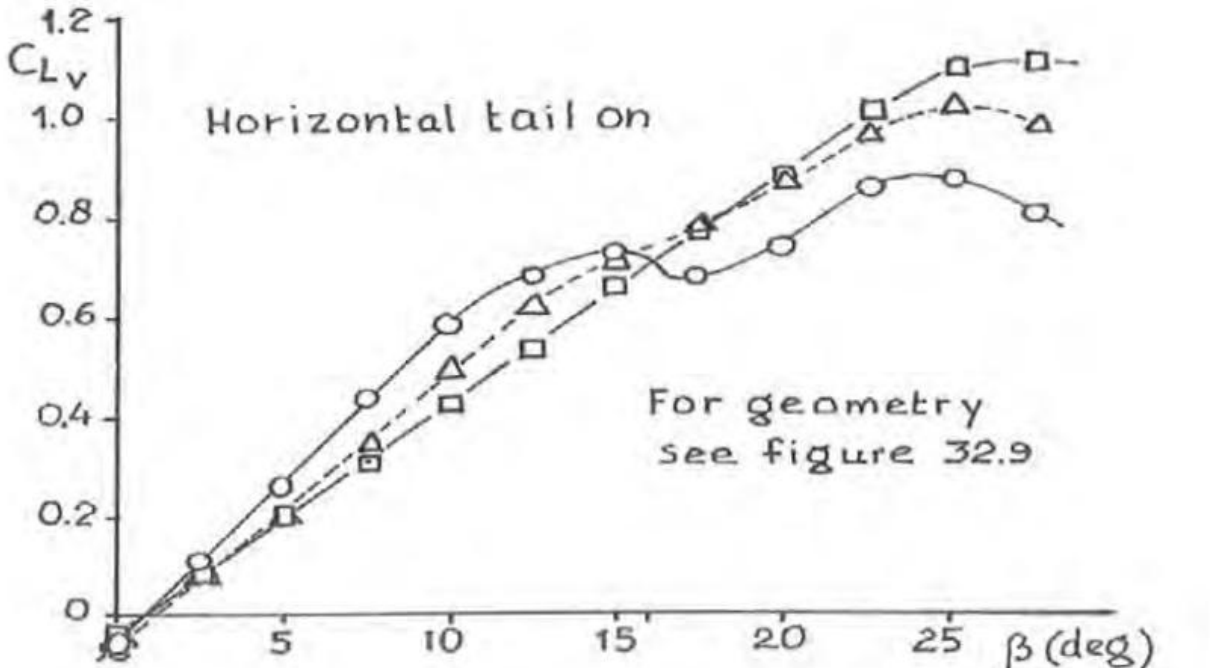

Figure 2.19 Effect of the sweep angle and of the horizontal tail plane on the lift (side force) of the vertical tailplane in sideslip (**Obert 2009**)

2.4 Types of Dorsal Fins

For the purpose of this report several aircraft have been examined. Aircraft have different types of dorsal fins. Figures 2.20 to 2.25 show the different types of dorsal fins that have been found. The survey is performed mainly on commercial aircraft.

Figure 2.20 shows an aircraft with a conventional tail with no dorsal fin or any extension of vertical tail. It has a straight leading edge from tip of the vertical tail to the root, where it joins with the fuselage. This sharp blend between leading edge and fuselage may be called here "sharp leading edge". Generally, it is the design of this is conventional tail which is given in aircraft design books. Figure 2.21 presents an aircraft with a dorsal fin added to the conventional vertical tail. Figure 2.22 present an aircraft with a round edge dorsal fin. Synthesis of new sizing methods for this report is done only for aircraft having a regular dorsal fin (as shown in Figure 2.21) or a round edge (Figure 2.22). Figure 2.23 shows a dorsal fin with an integrated air intake ram. This is done probably to save space and provide better support to the component. Figures 2.24 and 2.25 show aircraft with dorsal fin extensions. In Figure 2.24 the vertical tail, dorsal fin and dorsal fin extension can be distinguished as separate entities joined together. However, in Figure 2.25 it can be observed that the dorsal fin and dorsal fin extension merge gradually with the vertical tail.

Figures are compiled from an internet image search. The rear segment of the aircraft in each picture was cropped to present an orthogonal view of the tail section.

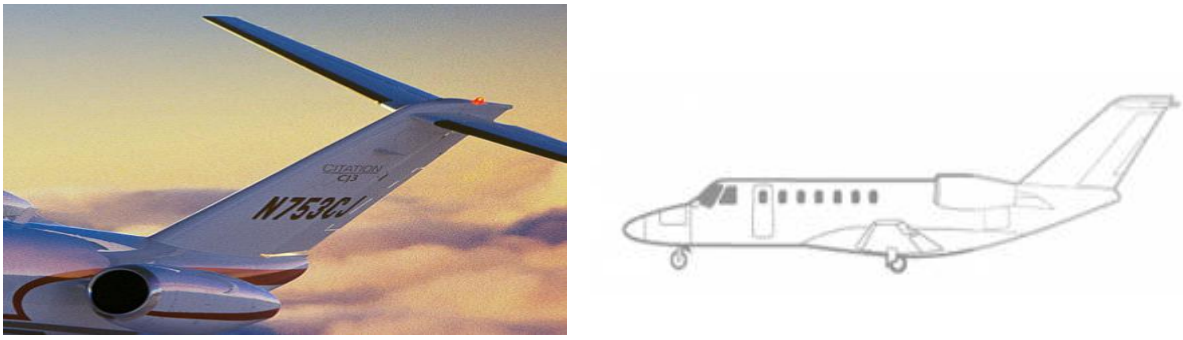

Figure 2.20 3D view and side view of a conventional tail (with a sharp leading edge) of a Cessna Citation CJ3 (**Automobile 2013** and **Blueprints 2013**)

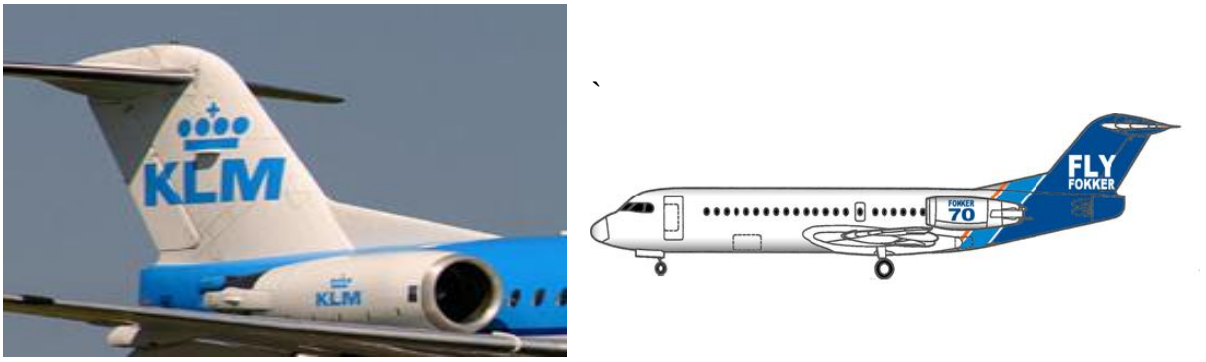

Figure 2.21 3D view and side view of a dorsal fin of a Fokker F-70 (**Aero 2013** and **Fly Fokker 2013**)

Figure 2.22 Side views of a round edge dorsal fin of an A 320 (**Prendrel 2013** and **Aerospaceweb 2013**)

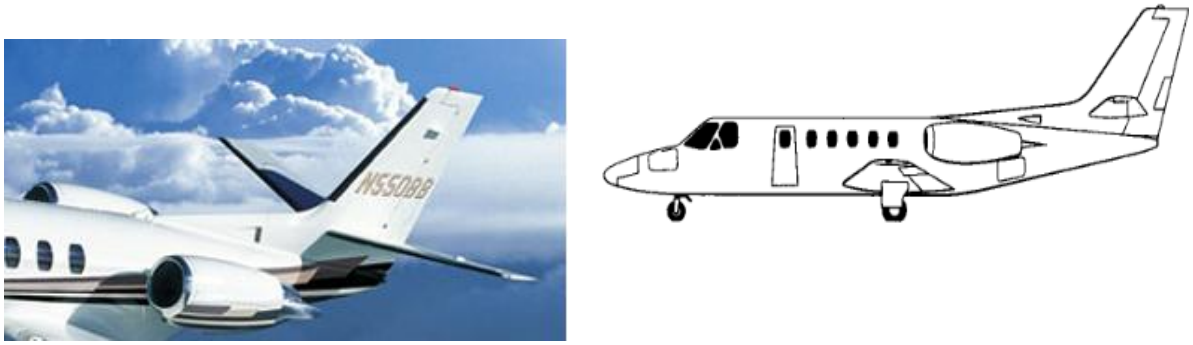

Figure 2.23 3D view and side view of a dorsal fin with air intake ram of a Cessna Citation Bravo (**Stajets 2013** and **Aviastar 2013b**)

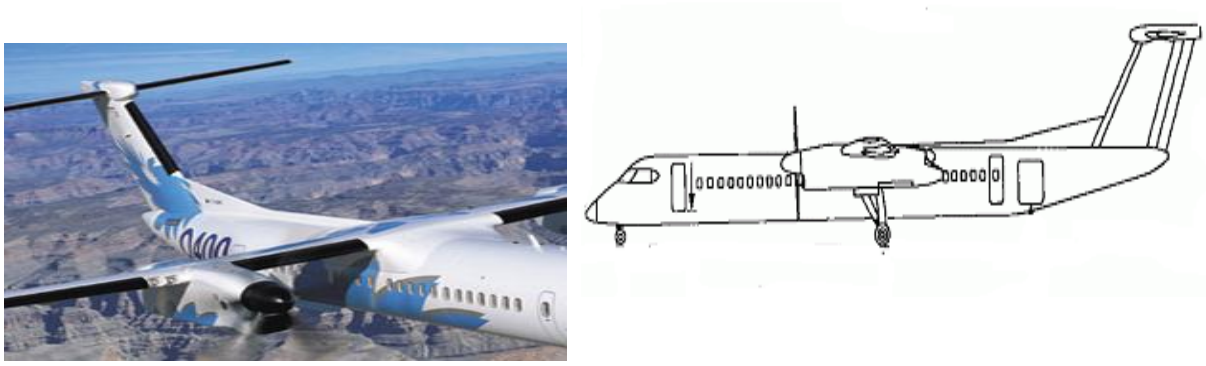

Figure 2.24 3D view and side view of combined dorsal fin with dorsal fin extention of a Q- 400 dash 8 (**Aerospace 2013** and **Aviastar 2013c**)

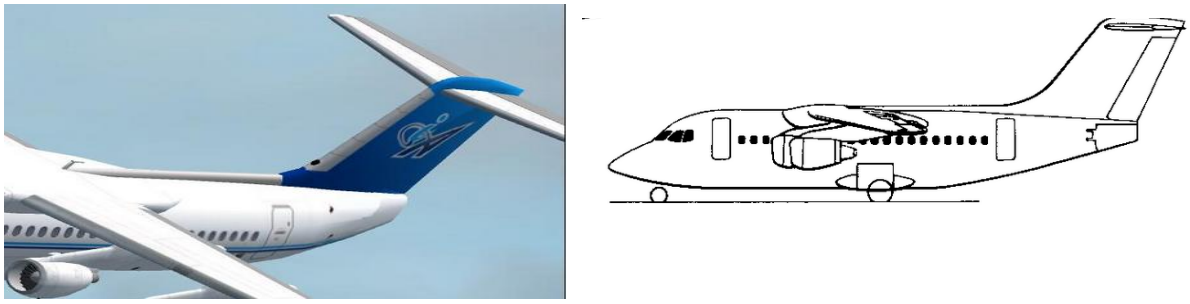

Figure 2.25 3D view and side view of a combined dorsal fin with dorsal fin extension blending into one another on a BAe 146 – an aircraft with a dorsal fin extension (**Tutavia 2013** and **Aviastar 2013a)**

2.5 Tail Sizing

For the purposes of early conceptual design it is useful to estimate the required size of tail surfaces very simply. Through the statistical method, this can be done on the basis of comparison with other aircraft (**Kroo 2013**). This report deals mainly with statistical methods to establish correlations between the desired tail sizes and aircraft sizes that are determined in previous phases of design. This sub-chapter is further divided based on the parameters analyzed in this study.

2.5.1 Tail Area and Tail Span

The tail size can be estimated from the tail volume coefficients if the tail lever arms l_H and l_v are known (see Equations 2.4 and 2.5). The lever arms are not, however, fixed until the position of the wing has been established. However, this only takes place after the "mass and Centre of Gravity" design phase. For this reason, the tail lever arms can only be estimated from the length of the fuselage. (**Scholz 2009**)

$$S_H = \frac{C_H S_W c_{MAC}}{l_H} \tag{2.4}$$

$$S_v = \frac{C_v S_W b_W}{l_v} \tag{2.5}$$

l_H the lever arm of the horizontal tailplane is the distance between the aerodynamic centers of wing and horizontal tailplane,
l_v the lever arm of the vertical tailplane is the distance between the aerodynamic centers of wing and vertical tailplane.
C_H horizontal tail volume coefficient
C_v vertical tail volume coefficient
S_W wing reference area
b_W wing span
c_{MAC} wing mean aerodynamic chord (MAC).

Thus, the vertical tail areas, S_H and S_v, can be determined from Equations 2.4 and 2.5. Estimation of the tail volume coefficients is described in detail later in this Chapter and in Chapter 3. For an initial estimation of the tail lever arms, Table 2.1 can be used.

Table 2.1 Conventional tail lever arms of horizontal and vertical tails (**Raymer 1992**)

Aircraft configuration	Average l_H *and* l_v
Propeller in front of fuselage	0.60 L_F
Engines on the wing	0.50 L_F … *0.55* L_F
Engines on the tail	0.45 L_F … *0.50* L_F
Control canard	0.30 L_F … *0.50* L_F
Sailplane	0.65 L_F

L_F stands for length of fuselage

Apart from **Raymer 1992**, hints for good initial estimations are prescribed by many other authors. However, this is not within the scope of this report and so shall not be discussed further.

Vertical Tail

Figure 2.26 defines the parameters of the vertical tail. The vertical tail is special as the side view is not symmetrical with respect to the line of symmetry of the (cylindrical) fuselage. Different definitions exist for the vertical tail span b_v and vertical tail area S_v. According to **Sadrey 2012** (see Figure 2.26) and **Roskam 1985** (see Figure 2.27) the tail area is the exposed area. **Raymer 1992** (see Figure 2.28) shows a vertical tail area almost identical to the exposed area in Figure 2.27. Note that the small dorsal fin (or rounded edge) is <u>not</u> considered in the tail area! **Obert 2009** draws a line of symmetry only in the tail cone. A point is marked where the 50%-line crosses the line of symmetry of the tail cone. The root of the vertical tail goes through this point, but parallel to the fuselage base line (upper or lower side of the cylindrical fuselage). See Figures 2.29 and 2.30 for further details. Meanwhile, Figure 2.31 defines the vertical tail area as the area encompassing the area of fuselage under the line of symmetry too in addition to the area defined by **Obert 2009**.
In this report the vertical tail area has been taken as the exposed area (Figure 2.26) and the vertical tail span is defined accordingly. Considering the fact that almost each author has his

own definition of the tail area and span, it does not come as a surprise that measured data from three-view-drawings does never exactly match given numbers.

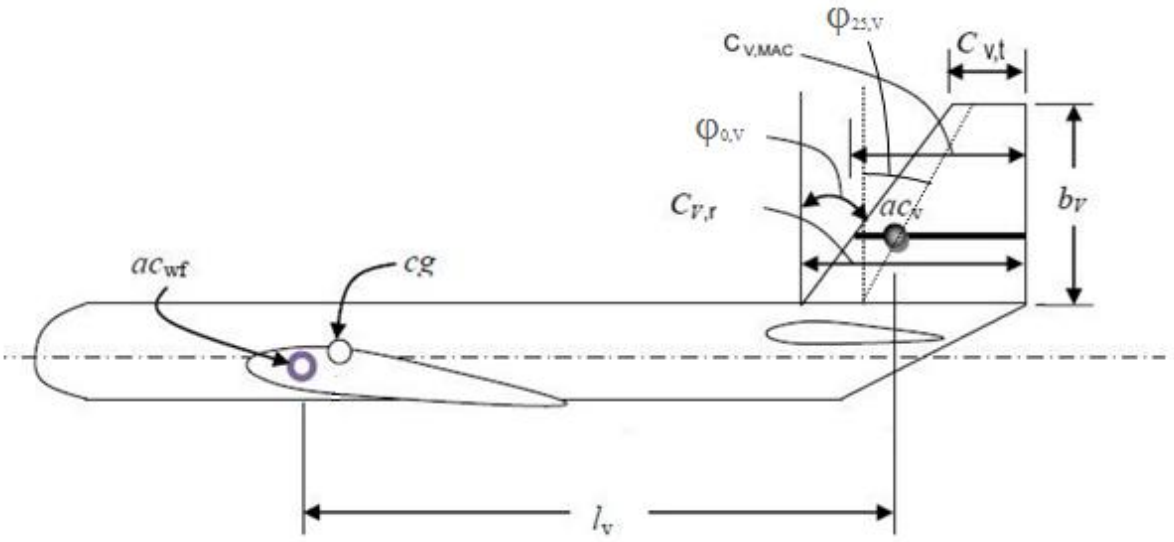

Figure 2.26 Definition of vertical tail parameters (adapted from **Sadraey 2012**)

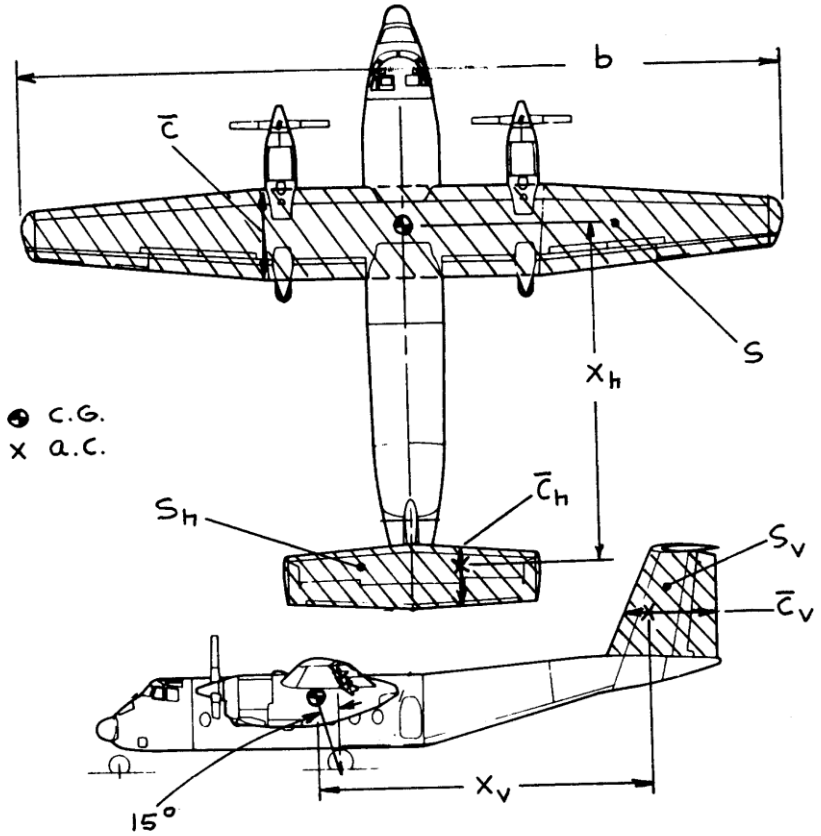

Figure 2.27 Definition of volume coefficient quantities (**Roskam 1985**)

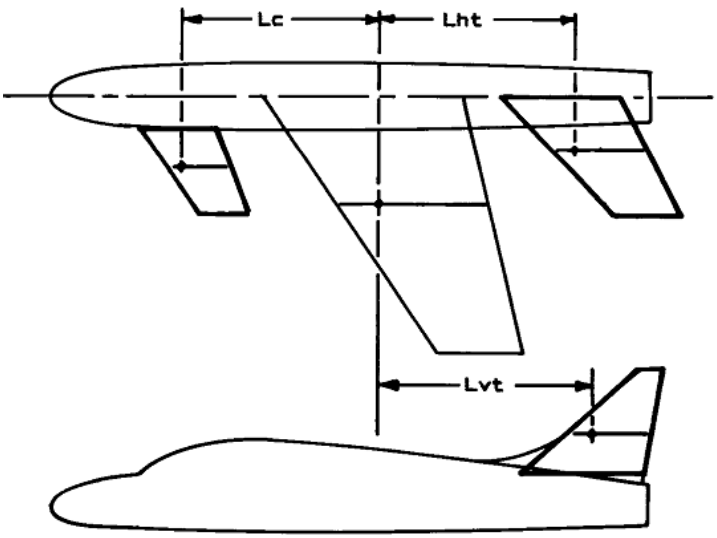

Figure 2.28 Definition of vertical tail area and moment arm (**Raymer 1992**)

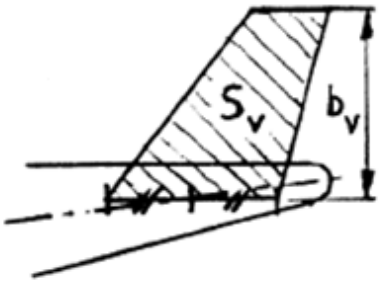

Figure 2.29 Definition of vertical tail area (**Obert 2009**)

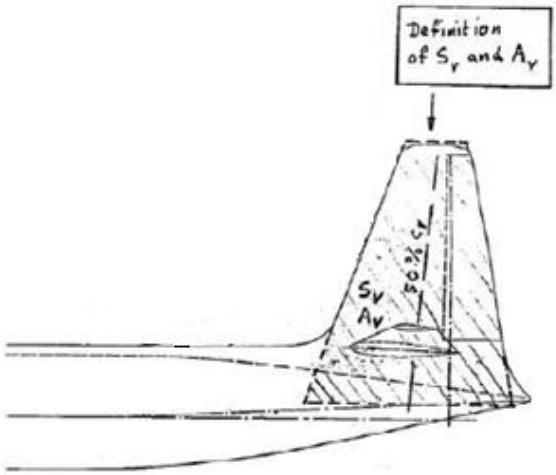

Figure 2.30 Definition of vertical tail area and aspect ratio (adapted from **Obert 2009**)

Figure 2.30 is used again in this report to describe the different types of dorsal fins as seen in the Fokker F-27 (see Figure 2.11).

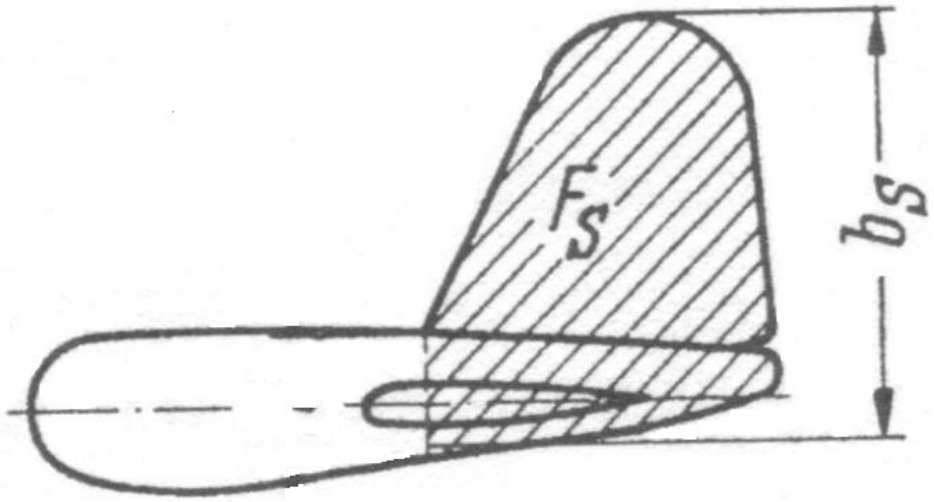

Figure 2.31 Definition of vertical tail area and span (adapted from **Truckenbrodt 2001**)

In Figure 2.31, the area defined as F_S refers to the vertical tail area. In this report, we have used the notation S_v to denote this area. The vertical tail span is referred to as b_S (in this report, b_v).

Horizontal Tail

Figure 2.32 defines the parameters of the horizontal tail. Parameter definitions of the horizontal tail are in principle the same as for the wing.

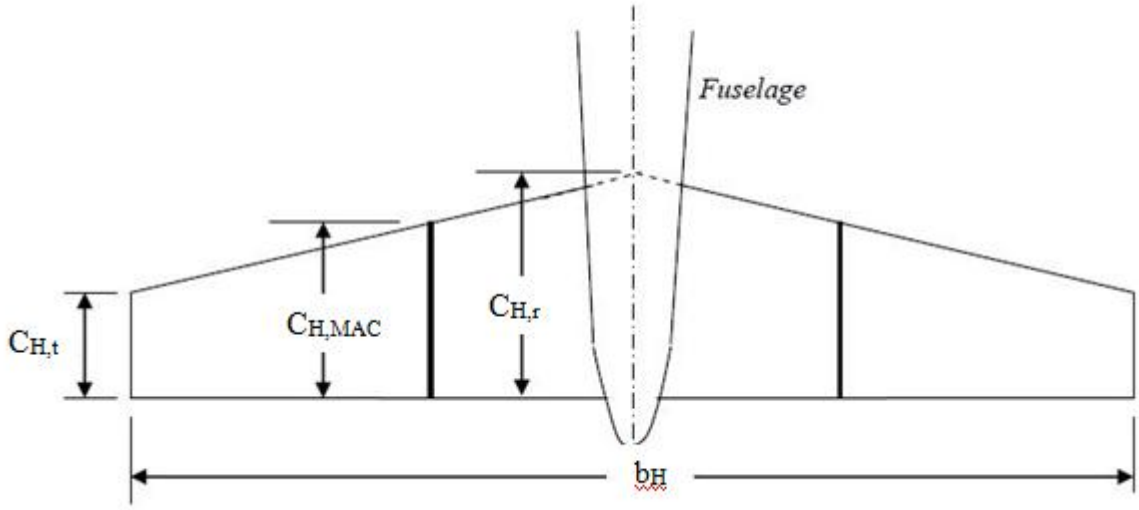

Figure 2.32 Definition of horizontal tail parameters (**Sadraey 2012**)

Please note that Figure 2.26 to Figure 2.32 contain parameters that are represented by different symbols than those used in this text. This is because these figures have been adapted directly or with minor changes from other publications.

2.5.2 Tail Volume Coefficients

The area of the horizontal tailplane, S_H or the vertical tailplane, S_v multiplied by the lever arm, l_H or l_v respectively is called the tail volume. The tail volume coefficient is defined for the horizontal tailplane as

$$C_v = \frac{S_v \, l_v}{S_W \, b_W} \tag{2.6}$$

and for the vertical tailplane as

$$C_H = \frac{S_H \, l_H}{S_W \, c_{MAC}} \tag{2.7}$$

l_H the lever arm of the horizontal
l_v the lever arm of the vertical
S_W wing reference area
b_W wing span
c_{MAC} wing mean aerodynamic chord (MAC).

> *Typical values for the volume coefficient vary widely between different aircraft types. ... For initial project design purposes, it is necessary to evaluate the volume coefficients for aircraft with similar layout, operation and weight to the proposed design and then use this value for estimation of tail areas.* (**Jenkinson 1999***)*

As it is known that aircraft from the same category generally show similarity in values of its parameters, we too have categorized all aircraft on the basis of maximum number of passengers, certification and engine type (jet or propeller). Table 2.2 shows this basis on which categorization of aircraft was done for this report. Statistics have been carried out only on these categories of aircraft. Data provided on all other categories mentioned in this report is obtained purely from reference material available till this time and has not been measured from 3-view diagrams. Each of these categories is therefore dependent on the definitions in use by the authors of the respective reference material.

Table 2.2 Basis of categorization of aircraft

Aircraft type	Certification (US)	Certification (Europe)	Type	m_{MTO}	n_{Pax}
Sailplane		CS-22			
Personal	FAR Part 23	CS-23	Normal, Utility, Aerobatic	≤ 5700 kg	≤ 9
Commuter	FAR Part 23	CS-23	Commuter	≤ 8600 kg	≤ 19
Regional Turboprop	FAR Part 25	CS-25		no limit	
Business Jet	FAR Part 23/ 25	CS-23 or 25			
Jet Transport	FAR Part 25	CS-25		no limit	
Military Transport	None	None			
Military Fighter	None	None			

m_{MTO} stands for maximum take-off mass
n_{Pax} stands for maximum number of passengers

Most commonly, authors have divided all aircraft into different categories and presented an average or range of values for C_H and C_v. In some cases, authors have tried to find good correlations between the tail volume coefficients and known parameters of the aircraft.

Table 2.3 Suggestions for tail volume coefficient of horizontal tail by various authors (**Raymer 1992**, **Jenkinson 1999**, **Roskam 1985**, **Torenbeek 1982**, **Nicolai 1975**, **Schaufele 2007**)

Aircraft Type	Raymer	Roskam	Torenbeek	Howe	Schaufele	Jenkinson	Nicolai
Sailplane	0.500			0.500			
Civil props							
Homebuilts	0.500	0.467					
Personal					0.48-0.92		
GA[a]- Single engine	0.700	0.667		0.650			
GA[a]- Twin engine	0.800	0.786		0.850			
Commuter					0.46-1.07		
Regional Turboprop	0.900	1.075	1.006	1.000	0.83-1.47		
Jet							
Business Jets		0.721	0.691	0.700	0.51-0.99		
Jet transport	1.000	1.010	0.904	1.200	0.54-1.48	0.875	
Supersonic Cruise Airplanes		0.535					
Military							
Jet Trainer	0.700	0.639		0.650			
Jet Fighter	0.400	0.362			0.20-0.75		0.307
Military Transport	1.000	0.891	0.850	0.650			
Special Purpose							
Agricultural	0.500	0.526					
Flying Boat	0.700	0.641					

[a] GA stands for General Aviation

In Tables 2.3 and 2.4, the suggestions of the various authors (as listed in the top row) for the tail volume coefficients are given. These have been listed on the basis of type of aircraft. In case of the first five authors, the average values of C_H and C_v are given. Only **Schaufele 2007** gives a range for the values of C_H and C_v.

Table 2.4 Suggestions for tail volume coefficient of vertical tail by various authors (**Raymer 1992**, **Jenkinson 1999**, **Roskam 1985**, **Torenbeek 1982**, **Nicolai 1975**, **Schaufele 2007**)

Aircraft Type	Raymer	Roskam	Howe	Toren. [a]	Schaufele	Jenk. [b]	Nicolai
Sailplane	0.020		0.018				
Civil props							
Homebuilts	0.040	0.036					
Personal					0.024 … 0.086		
GA- single engine	0.040	0.043	0.050				
GA- twin engine	0.070	0.062	0.065				
Commuter					0.041 … 0.097		
Regional Turboprop	0.080	0.083	0.080	0.077	0.065 … 0.121		
Jet							
Business Jets		0.073	0.065	0.069	0.061 … 0.093		
Jet transport	0.090	0.079	0.090	0.074	0.038 … 0.120	0.076	
Supersonic Cruise Airplanes		0.062	0.065				
Military							
Military Trainer	0.060	0.061	0.065				
Military Fighter	0.070	0.077			0.041 … 0.130		0.064
Military Transport	0.080	0.073	0.065				
Special Purpose							
Agricultural	0.040	0.032					
Flying Boat	0.060	0.050					

[a] Toren. stands for the author Torenbeek
[b] Jenk. stands for the author Jenkinson

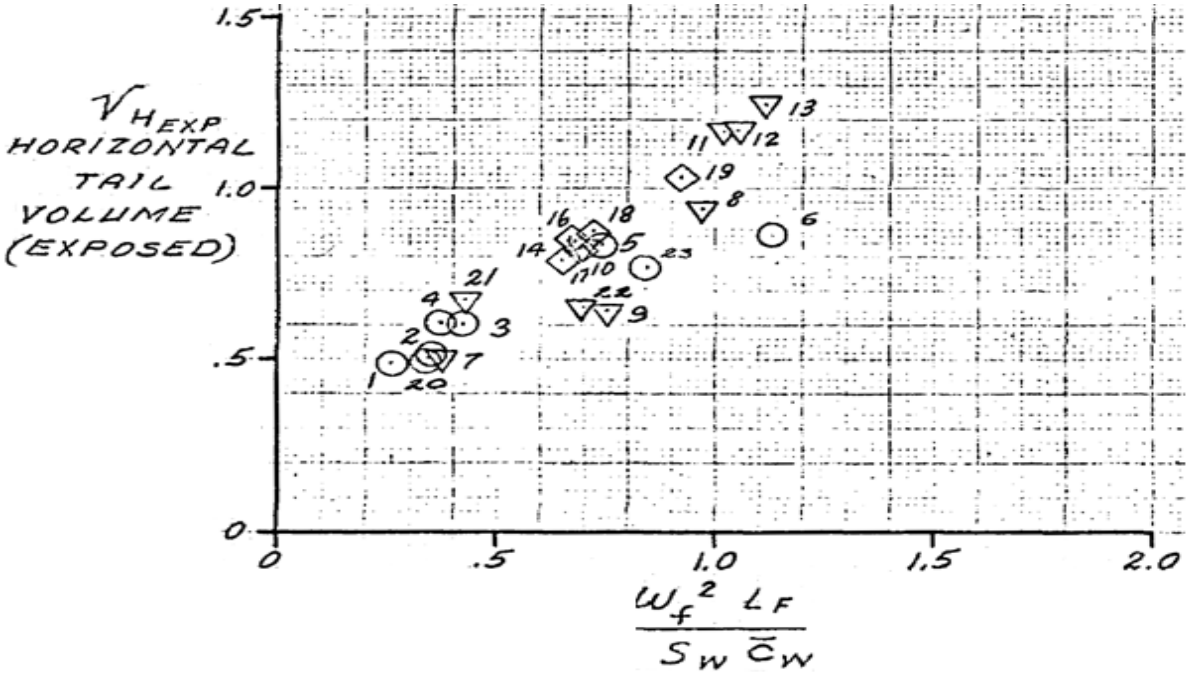

Figure 2.33 Plot of tail volume coefficient for horizontal tail (C_H) (**Kroo 2013**)

Schaufele 2007 presents a similar approach as seen in Figure 2.33. This is further explored in Chapter 3 (see Figure 3.1 and Figure 3.2).

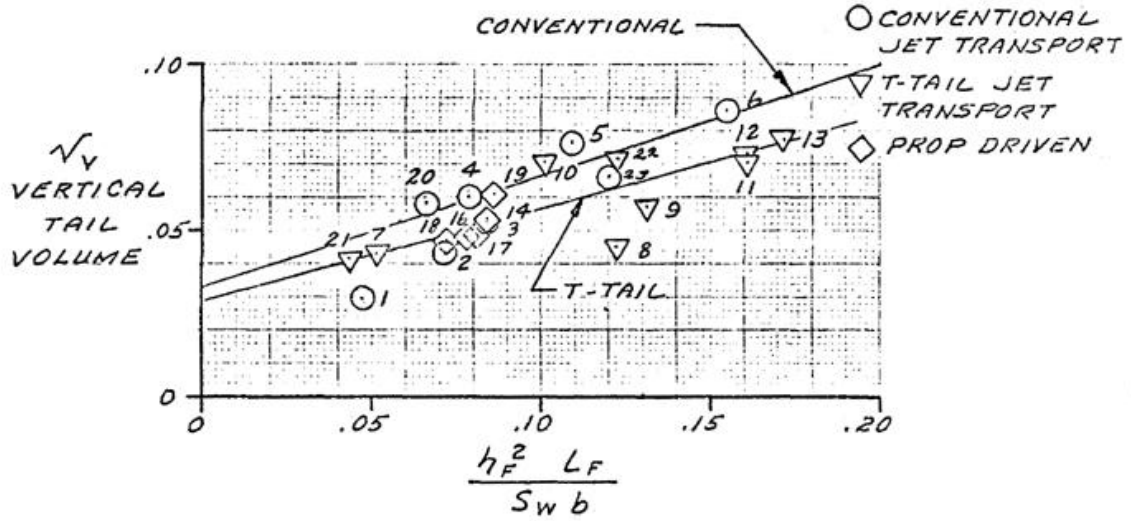

Figure 2.34 Plot of tail volume coefficient for vertical tail (C_v) (**Kroo 2013**)

In Figure 2.33 and Figure 2.34, the author has tried to establish correlations between the tail volume coefficients and parameters determined during previous design phases of the aircraft like during wing sizing and fuselage sizing. As it can be seen, C_H shows a good linear correlation with the ratio,

$$\frac{w_F^2 \ L_F}{S_W \ \overline{c_w}} \tag{2.8}$$

w_F width of the aircraft fuselage

L_F length of the aircraft fuselage

$\overline{c_W}$ wing mean aerodynamic chord (MAC), c_{MAC}

Similarly, C_v is observed to show a good linear correlation with the ratio,

$$\frac{h_F^2 \ L_F}{S_W \ b} \tag{2.9}$$

h_F height of the aircraft fuselage

b wing span, b_W

Some authors suggest modifications to the tail volume coefficients on the basis of their tail configuration.

> *For an all moving tail, the volume coefficient can be reduced by about 10-15%. For a "T-tail," the vertical tail volume coefficient can be reduced by approximately 5% due to the end plate effect, and the horizontal tail volume coefficient can be reduced by about 5% due to the clean air seen by the horizontal. Similarly, the horizontal tail volume coefficient for an "H-tail" can be reduced by about 5%.* (**Raymer 1992**)

Sadraey 2012 presents the same values of C_H and C_v as in **Roskam 1985**.

2.5.3 Aspect Ratio

Aspect ratio, *A* is defined as the ratio of span squared over the area. This is also true in case of the vertical tail for which span is only the distance from the fuselage to the tip of the vertical tail (in contrast to the wing and horizontal tail where span is measured from left to right tip) (**Truckenbrodt 2001**) (Figure 2.31). Thus,

$$A_v = \frac{b_v^2}{S_v} \tag{2.10}$$

Figure 2.32 shows the span, b_H in case of horizontal tail. Thus,

$$A_H = \frac{b_H^2}{S_H} \tag{2.11}$$

Most authors suggest a range of values for aspect ratio depending on the aircraft category it falls into. An aircraft designer then uses a value lying in the suggested range of values in the preliminary designing phase. This value is refined in the later stages of design for optimum performance.

> *A high aspect ratio tailplane [A_v] is effective at small angles of sideslip, but it has a small stalling angle of attack. A low A_v is required with a high mounted horizontal tailplane to provide adequate rigidity of the fin without an excessive weight penalty.* (**Torenbeek 1982**)

> *Some general aviation aircraft use untapered horizontal tails to reduce manufacturing costs.* (**Raymer 1992**)

> *A lower aspect ratio [A_H] is desirable for tail, compared with that of the wing. The reason is that the deflection of the elevator creates a large bending moment at the tail root. Hence, the lower the aspect ratio results in a smaller bending moment.* (**Sadraey 2012**)

> *In a single engine prop-driven aircraft, it is recommended to have an aspect ratio such that the tail span (b_H) is longer than the propeller diameter (d_p). This provision insures that the tail flow field is fresh and clean of wake and out of propwash area. Therefore, the efficiency of the tail (η_H) will be increased. … An initial value for the tail aspect ratio may be determined [from $A_H = 2/3\ A_W$]. A typical value for the horizontal aspect ratio is about 3 to 5. … As a starting point, a value between 1 and 2 is recommended for the vertical tail aspect ratio.* (**Sadraey 2012**)

> *The vertical tail aspect ratio is lower on T-tail aircraft because the effectiveness of the vertical tail increases due to the horizontal tailplane functioning as an endplate.* (**Obert 2009**)

Tables 2.5 and 2.6 show a summary of such suggested values for aspect ratio by various authors.

Table 2.5 Suggestions for aspect ratio of horizontal tail by various authors (**Raymer 1992**, **Roskam 1985**, **Schaufele 2007**, **Torenbeek 1982**, **Obert 2009**)

Aircraft type	Schaufele	Raymer	Roskam	Torenbeek	Obert
Sail Plane		6.0 ... 10.0			
Civil props					
Homebuilts			1.8 … 4.5		
Personal	3.5 ... 5.0				5.0 … 7.4
GA - single engine			4.0 ... 6.3		
GA- Twin Engine			3.7 ... 7.7		
Commuters	3.5 ... 5.0				3.7 … 6.2
Regional Turboprop	3.5 ... 5.0		3.4 ... 7.7		3.9 … 6.3
Jet					
Business jets	3.5 ... 5.0		3.2 ... 6.3		3.9 … 6.5
Jet Transports	3.5 ... 5.0		3.4 ... 6.1	3.4 … 4.9	2.7 … 5.3
Supersonic Cruise airplanes			1.8 ... 2.6		
Military					
Military Trainers			3.0 ... 5.1		
Military Fighter	3.0 ... 4.0	3.0 ... 4.0	2.3 ... 5.8		
Military transport (Propeller)					4.2 … 6.6
Military transport			1.3 ... 6.9		
Special Purpose					
Agricultural			2.7 ... 5.4		
Flying Boats, Amphibian And Float Airplanes			2.2 ... 5.1		

Morichon 2006a (see Figure 2.35) plots the aspect ratio of the horizontal tail against that of the wing. This statistic achieves quite a high regression value and therefore proves that there exists a good relationship between the two parameters in consideration. It must be noted however that this statistic was conducted using only jet transport aircraft data and thus the relationship may not hold true for aircraft belonging to other categories. Equation 2.12 can therefore be used to calculate the aspect ratio of the horizontal tail of jet transport aircraft when the aspect ratio of the wing is known.

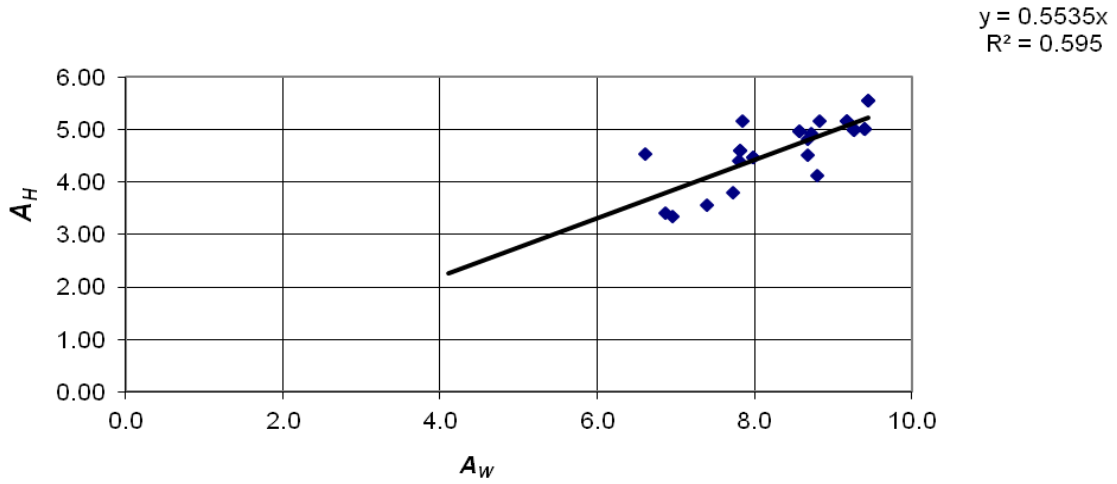

Figure 2.35 Aspect ratio of the horizontal tail versus aspect ratio of the wing (**Morichon 2006a**)

$$A_H = 0.5535 A_W \tag{2.12}$$

Table 2.6 Suggestions for aspect ratio of vertical tail by various authors (**Raymer 1992**, **Roskam 1985**, **Schaufele 2007**, **Torenbeek 1982**, **Obert 2009**)

Aircraft type	Schaufele	Raymer	Roskam	Torenbeek	Obert
Sail Plane		1.5 ... 2.0			
Civil props					
Homebuilts			0.4 ... 1.4		
Personal	1.2 ... 1.8				1.1 … 1.8
GA - single engine			0.9 ... 2.2		
GA - twin engine			0.7 ... 1.8		
Commuters	1.2 ... 1.8				1.2 … 1.9
Regional Turboprop	1.4 ... 1.8		0.8 ... 1.7		1.3 … 2.2
Jet					
Business jets	0.8 ... 1.6		0.8 ... 1.6		0.9 … 1.8
Jet Transports	0.8 ... 1.8		0.7 ... 2.0	0.8 … 2.0	0.9 … 2.2
Supersonic Cruise airplanes			1.2 ... 2.4		
Military					
Military Trainers			1.0 ... 2.9		
Military Fighter	1.2 ... 1.6	0.6 ... 1.4	0.4 ... 2.0		
Military transport (Propeller)					1.3 … 1.9
Military transport			0.9 ... 1.9		
Special Purpose					
Agricultural			0.6 ... 1.4		
Flying Boats, Amphibian and Float Airplanes			0.4 ... 2.0		

In addition, the aspect ratio also varies based on the tail type. **Howe 2000** and **Raymer 1992** gives a range of values for different types of tails as can be seen in Tables 2.7 and 2.8.

Table 2.7 Suggestions for aspect ratio of transport aircraft based on tail type (**Raymer 1992**)

Tail Type	*A*v
Conventional Tail	1.3 … 2.0
T-tail	0.7 … 1.2

Table 2.8 Suggestions for aspect ratio on the basis of tail type (**Howe 2000**)

Tail Type	*A*
Horizontal Tail	(0.5 - 0.6)A_w
Canard	(1.0 - 1.3)A_w
Vertical Tail	0.9 - 3.0[$]

[$] If aircraft has a single engine, A = 0.9, else A > 1.2. For transport aircraft, A > 3.0.

A_W Aspect ratio of the wing

2.5.4 Taper Ratio

Taper ratio, λ is the ratio between the tip chord and the centreline root chord (**Raymer 1992**). Equations 2.13 and 2.14 below show how taper ratio is defined for vertical and horizontal tails.

$$\lambda_H = \frac{c_{H,t}}{c_{H,r}} \tag{2.13}$$

$$\lambda_v = \frac{c_{v,t}}{c_{v,r}} \tag{2.14}$$

The tip and root chord lengths, $c_{H,t}$, $c_{H,r}$, $c_{v,t}$ *and* $c_{v,r}$ are as defined in Figure 2.26 and Figure 2.32.

> *A moderate taper [on the horizontal tailplane] is usually chosen to save structural weight. ... Little taper [on the vertical tailplane] is possible on T-tails. (**Torenbeek 1982**)*

> *The [horizontal] tail taper ratio is typically smaller than the wing taper ratio. The tail taper ratio is typically between 0.7 and 1 for GA [General Aviation] aircraft and between 0.4 and 0.7 for transport aircraft. (**Sadraey 2012**)*

> *The vertical tail surfaces on T-tails have less taper, so that a sufficiently large tip chord provides space and stiffness to carry the horizontal tail. (**Obert 2009**)*

In case of taper ratio too, most authors assign a range of values depending on the aircraft category. An aircraft designer then uses a value lying in the suggested range of values in the preliminary designing phase. This value is refined in the later stages of design for optimum performance. Tables 2.9 and 2.10 show a summary of such suggested values for taper ratio by various authors.

Morichon 2006a plots the taper ratio of the horizontal tail against that of the wing (see Figure 2.36). The low regression value shown at the top right of the figure indicates a bad relationship being shown between the two parameters in consideration. It is to be noted that data of only jet transport aircraft were used for this statistic and hence, the relationship being shown in Figure 2.36 may vary for aircraft of other categories.

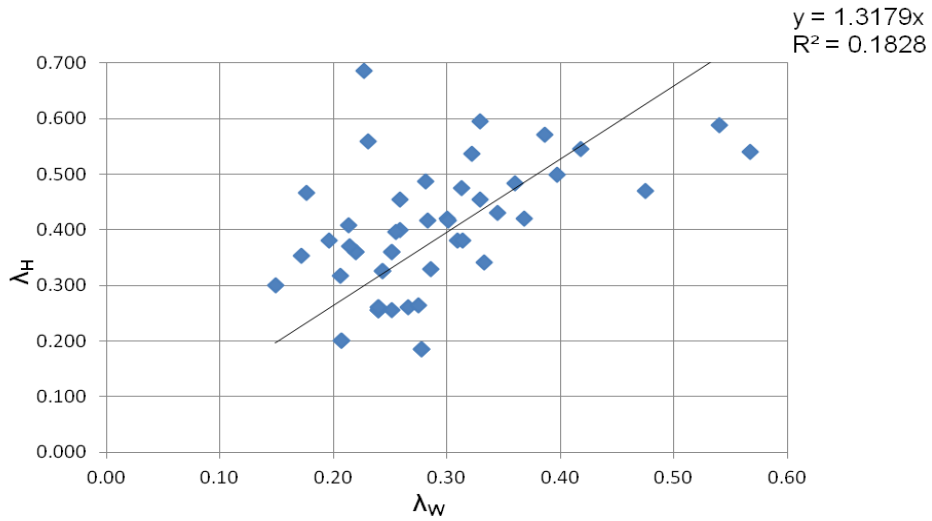

Figure 2.36 Taper ratio of the horizontal tail versus taper ratio of the wing (**Morichon 2006a**)

Table 2.9 Suggestions for taper ratio of horizontal tail by various authors (**Raymer 1992, Roskam 1985, Schaufele 2007, Torenbeek 1982**, **Obert 2009**)

Aircraft type	Schaufele	Raymer	Roskam	Torenbeek	Obert
Sail Plane		0.30 ... 0.50			
Civil props					
Homebuilts			0.29 … 1.00		
Personal	0.50 ... 1.00				0.39 … 1.00
GA - Single Engine			0.45 ... 1.00		
GA- Twin Engine			0.48 ... 1.00		
Commuters	0.50 ... 1.00				0.29 … 1.00
Regional Turboprop	0.50 ... 0.80		0.39 ... 1.00		0.30 … 1.00
Jet					
Business jets	0.35 ... 0.50		0.32 ... 0.57		0.31 … 0.64
Jet Transports	0.25 ... 0.45		0.27 ... 0.62	0.26 … 0.60	0.26 … 0.60
Supersonic Cruise airplanes			0.14 ... 0.39		
Military					
Military Trainers			0.36 ... 1.00		
Military Fighter	0.25 ... 0.40	0.20 ... 0.40	0.16 ... 1.00		
Military transport (Prop)					0.28 … 0.78
Military transport			0.31 ... 0.80		
Special Purpose					
Agricultural			0.59 ... 1.00		
Flying Boats, Amphibian and Float Airplanes			0.33 ... 1.00		

Table 2.10 Suggestions for taper ratio of vertical tail by various authors (**Raymer 1992, Roskam 1985, Schaufele 2007, Torenbeek 1982**, **Obert 2009**)

Aircraft type	Schaufele	Raymer	Roskam	Obert
Sail Plane		0.40 ... 0.60		
Civil props				
Homebuilts			0.26 ... 0.71	
Personal	0.30 ... 0.50			0.27 … 0.55
GA- Single Engine			0.32 ... 0.58	
GA- Twin Engine			0.33 ... 0.74	
Commuters	0.30 ... 0.80			0.23 … 0.60
Regional Turboprop	0.30 ... 0.70		0.32 ... 1.00	0.26 … 0.60
Jet				
Business jets	0.30 ... 0.80		0.30 ... 0.74	0.25 … 0.72
Jet Transports	0.30 ... 0.80		0.26 ... 0.73	0.25 … 0.71
Supersonic Cruise airplanes			0.37 ... 1.00	
Military				
Military Trainers			0.32 ... 0.74	
Military Fighter	0.25 ... 0.40	0.20 ... 0.40	0.19 ... 0.57	
Military transport (Prop)				0.23 … 0.58
Military transport			0.28 ... 1.0	
Special Purpose				
Agricultural			0.43 ... 0.74	
Flying Boats, Amphibian and Float Airplanes			0.19 ... 0.57	

In addition, the taper ratio also varies based on the tail type. **Howe 2000** and **Raymer 1992** gives a range of values for different types of tails as can be seen in Tables 2.11 and 2.12.

Table 2.11 Suggestions for taper ratio of transport aircraft based on tail type (**Raymer 1992**)

Tail Type	λv
Conventional Tail	0.3 … 0.6
T-tail	0.6 … 1.0

Table 2.12 Suggestions for taper ratio on the basis of tail type (**Howe 2000**)

Tail Type	λ
Horizontal Tail	$1.2*\lambda_w$
Canard	$1.3*\lambda_w$
Vertical Tail	$0.5*\lambda_w$

λ_W taper ratio of the wing

2.5.5 Quarter Chord Sweep Angle

This is the angle between the projection of the quarter chord line on the X-Y plane of the tail and the Y-axis (**Torenbeek 1982**).

Quarter chord angles for vertical and horizontal tails are marked as $\varphi_{25,v}$ and $\varphi_{25,H}$ respectively in Figure 2.26 and Figure 2.32.

> *In the case of high speed aircraft the tailplane angle of sweep, in combination with its thickness ratio, is chosen so that at the design driving Mach number strong shocks are not jet formed. The same procedure as applied to the wing will then result in a thinner section and / or larger [φ_H] as compared with the wing. Positive sweepback is occasionally used on low –speed aircraft to increase the tailplane moment arm and the stalling angle of attack, although the result is a decrease in the lift-curve slope. Up to about 25 degrees of sweepback there is still an advantage. (**Torenbeek 1982**)*

The sweep angle of the vertical tailplane is 35° ... 55° for aircraft with "high airspeeds" (flight with compressibility effects). This is used primarily to ensure that the tail's Critical Mach Number is higher than the wing's. The sweep angle of the vertical tailplane for aircraft with low airspeeds (flight without compressibility effects) should be less than 20°. (**Raymer 1992**)

> *The leading edge sweep of the horizontal tailplane is usually set to about 5 degrees more than the wing sweep. This tends to make the tail stall after the wing, and also provides the tail with a higher critical mach number than the wing, which avoids loss of elevator effectiveness due to shock formation. (**Raymer 1992**)*

> *As an initial selection in preliminary design phase, select the value of [φ_H] to be the same as the wing sweep angle [φ_W]. ... It is suggested to initially adopt [φ_v] similar to the sweep angle of the wing. (**Sadraey 2012**)*

> *The sweep angle of the majority of the tailplanes on the jet aircraft is 5 to 10 degrees larger than on the wing, particularly on aircraft with reversible control systems, to prevent control problems between M_{MO} and M_D. ... On aircraft with irreversible control systems (and usually high M_{MO} and M_D), ... transonic flow on the tailplane is accepted and the sweep angle is identical to the wing sweep angle. (**Obert 2009**)*

Given one sweep angle (e.g. the leading edge sweep), another sweep angle (e.g. the quarter chord sweep) can be calculated from

$$\tan\varphi_m = \tan\varphi_n - \frac{4}{A}\frac{(m-n)}{100}\frac{(1-\lambda)}{(1+\lambda)} \tag{2.15}$$

φ_m unknown sweep angle (in this case m = 25)
φ_n known sweep angle (in this case n = 0)
A aspect ratio
λ taper ratio

Some authors give a range of values for quarter chord sweep based on aircraft category as shown in Tables 2.13 and 2.14.

Table 2.13 Suggestions for quarter chord sweep angle of horizontal tail by various authors (**Roskam 1985**, **Torenbeek 1982**, **Obert 2009**)

Aircraft type	Roskam	Torenbeek	Obert
	°	°	°
Civil props			
Homebuilts	0 ... 20		
GA- Single Engine	0 ... 10		
GA- Twin Engine	0 ... 17		
Commuters			
Regional Turboprop	0 ... 33		
Jet			
Business jets	0 ... 35		20 … 34
Jet Transports	18 ... 37	12 … 35	21 … 37
Supersonic Cruise airplanes	32 ... 60		
Military			
Military Trainers	0 ... 30		
Military Fighter	0 ... 55		
Military transport	5 … 35		
Special Purpose			
Agricultural	0 ... 10		
Flying Boats, Amphibian And Float Airplanes	0 ... 17		

Table 2.14 Suggestions for quarter chord sweep angle of vertical tail by various authors (**Roskam 1985**, **Torenbeek 1982**, **Obert 2009**)

Aircraft type	Roskam	Torenbeek	Obert
	°	°	°
Civil props			
Homebuilts	0 ... 47		
Personal			24 … 31
GA - single engine	12 ... 42		
GA - single engine	18 ... 45		
Commuters			22 … 36
Regional Turboprop	0 ... 45		17 … 28
Jet			
Business jets	28 ... 55		34 … 55
Jet Transports	33 ... 53	31 … 55	33 … 45
Supersonic Cruise airplanes	37 ... 65		
Military			
Military Trainers	0 ... 45		
Military Fighters	9 ... 60		
Military transport (Propeller)			10 … 23
Military transport	0 ... 37		
Special Purpose			
Agricultural	0 ... 32		
Flying Boats, Amphibian And Float Airplanes	0 ... 32		

In addition, some authors propose the sweep angle values as a function of the wing sweep angle. (see Table 2.15)

Table 2.15 Suggestions for quarter chord sweep on the basis of tail type (**Howe 2000**)

Tail Type	φ
Horizontal Tail	φ_W
Canard	$(0.80–1.15)*\varphi_W$
Vertical Tail	$^{\&}\varphi_W$

$^{\&}$ Usually not less than 20˚ on quarter chord
φ_W Quarter chord sweep angle of the wing.

Morichon 2006b has an interesting statistic as shown in Figure 2.37. This shows a particular trend being followed by the ratio of vertical to horizontal tail sweep angles on one hand with the wing sweep angle on the other hand. It can be observed that vertical tail sweep tends to be higher than horizontal tail sweep. This is especially true for slow flying aircraft which have no or only little wing sweep. This finding can be expressed with the relationship given in Equation 2.16. It should be noted however that this statistic is calculated only for jet transport aircraft.

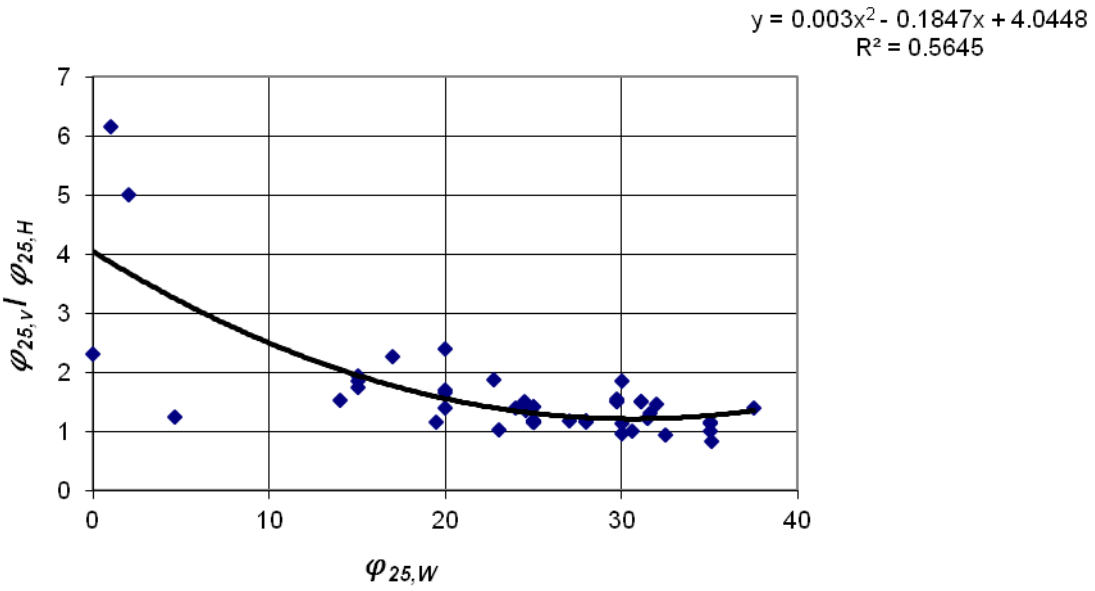

Figure 2.37 Plot of $\varphi_{25,V}$ / $\varphi_{25,H}$ against $\varphi_{25,W}$ (**Morichon 2006b**)

$$\frac{\varphi_{25,V}}{\varphi_{25,H}} = 0.003\varphi_{25,W}^2 - 0.1847\varphi_{25,W} + 4.0448 \tag{2.16}$$

2.5.6 Relative Thickness Ratio

The measurable distance between the leading and trailing edges of a wingform is called its chord, *c* (**Aerofiles 2013**). Section thickness, *t* is defined as the maximum distance between

corresponding points on the upper and lower section surface. It is usually expressed as a thickness to chord ratio *t/c* called relative thickness ratio (**Torenbeek 1982**).

Below suggestions are given by various authors to determine a value for relative thickness ratio of the tail.

> *Tail thickness ratio is usually similar to the wing thickness ratio. ... For a high speed aircraft, the horizontal tail is usually about 10% thinner than the wing to ensure that the tail has a higher critical mach number. (**Raymer 1992**)*

> *[Particularly on aircraft with reversible control systems, $(t/c)_H$] is 1 to 2% thinner than the airfoil section on the outer wing [to prevent control problems between M_{MO} and M_D]. (**Obert 2009**)*

Table 2.16 Suggestions for relative thickness ratio of horizontal tail (**Schaufele 2007, Torenbeek 1982**)

Aircraft type	Schaufele	Torenbeek
Civil props		
Personal	0.06 … 0.09	
Commuters	0.06 … 0.09	
Regional Turboprop	0.06 … 0.09	
Jet		
Business jets	0.06 … 0.09	
Jet Transports	0.06 … 0.09	0.08 … 0.12
Military		
Military Fighter	0.03 … 0.04	

Table 2.17 Suggestions for relative thickness ratio of vertical tail (**Schaufele 2007**, **Torenbeek 1982**)

Aircraft type	Schaufele	Torenbeek
Civil props		
Personal	0.06 … 0.09	
Commuters	0.06 … 0.09	
Regional Turboprop	0.06 … 0.09	
Jet		
Business jets	0.06 … 0.09	
Jet Transports	0.08 … 0.10	0.09 … 0.13
Military		
Military Fighter	0.03 … 0.09	

2.5.7 Control Surface Parameters

The above sections, Sections 2.5.1 - 2.5.6 define various parameters of the horizontal and vertical tails respectively and provide statistical analyses to aid in sizing them. This section deals with some geometrical parameters of the horizontal and vertical tail control surfaces namely the elevator and the rudder respectively. Figures 2.38 and 2.39 show the definitions for the various parameters that are studied in this section. The control surfaces are marked red in the

figures, the 25% chord-lines yellow and the horizontal and vertical tails blue. In addition, the location of the Mean Aerodynamic Chord (MAC) on the horizontal and vertical tails is marked with a red dot.

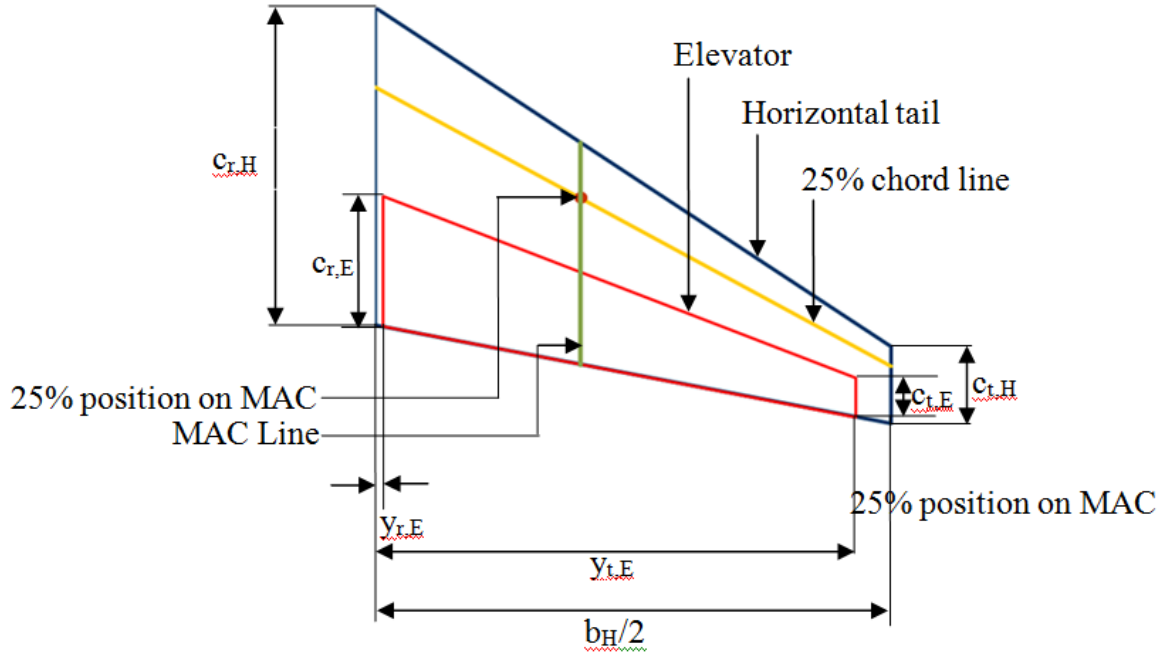

Figure 2.38 Definition of horizontal tail control surface parameters

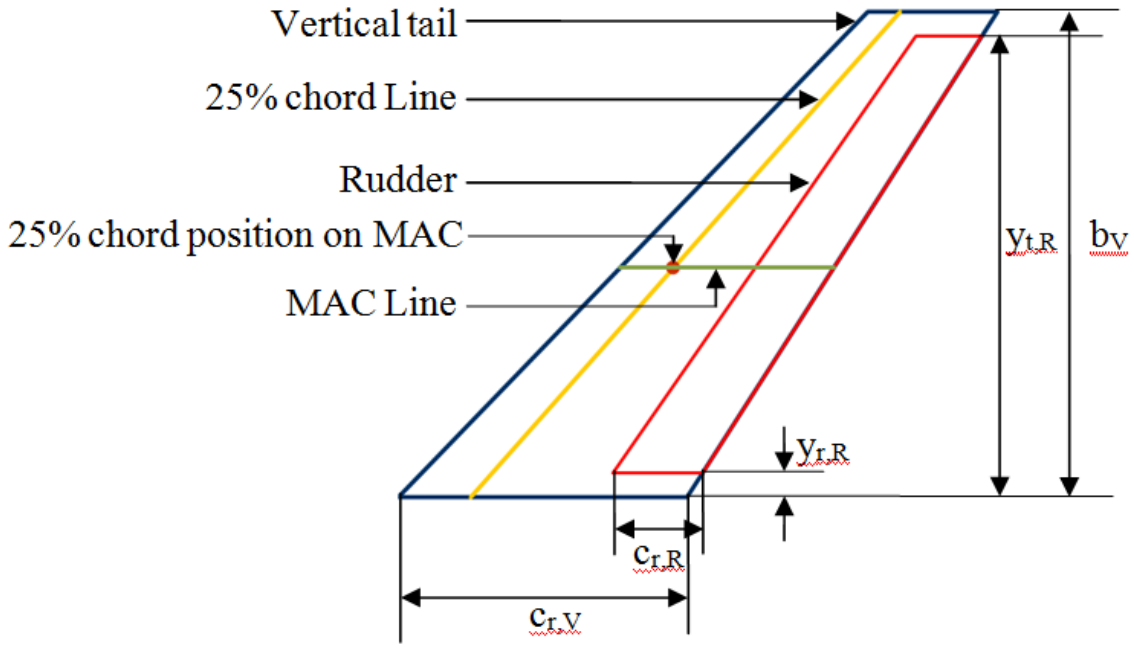

Figure 2.39 Definition of vertical tail control surface parameters

Two parameters of the horizontal and vertical tails namely, $b_H/2$ (half span of horizontal tail) and b_v (span of vertical tail) are also shown in the figures. These are used later to develop useful relationships to determine good initial values for the control surface parameters.

This section deals with estimations for the various control surface parameters given by various authors. Below is a block quotation, quoting **Raymer 1992**. The text can be easily translated into suggested ranges for the different parameters given in Figures 2.38 (horizontal tail) and 2.39 (vertical tail).

> *Elevators and rudders generally begin at the side of the fuselage and extend to the tip of the tail or to about 90% of the tail span. High speed aircraft sometimes use rudders of large chord which only extend to about 50% of the span. This avoids a rudder effectiveness problem similar to aileron reversal. … Rudders and elevators are typically about 25-50% of the tail chord. … The hinge axis should be no farther aft than about 20% of the average chord of the control surface. (**Raymer 1992**)*

Tables 2.18 and 2.19 are the results of a compilation of suggestions on the ratios, c_E/c_H and c_R/c_v from various authors. In this case, c_E or c_R refer to the chord of the elevator or rudder respectively at a given section and c_H or c_V refer to the corresponding chord of horizontal or vertical tail respectively calculated at the same section. As before, in this study too, the aircraft are divided into the various categories to check whether the deviations get smaller.

Table 2.18 Suggestions for c_E/c_H as given by various authors (**Roskam 1985, Schaufele 2007, Torenbeek 1982**, **Sadraey 2013**)

Aircraft Type	Roskam	Schaufele	Torenbeek	Sadraey	Av.	Range
Civil Props						
Homebuilt	0.34 … 0.56				0.45	0.34 … 0.56
Personal		0.35 … 0.45			0.40	0.35 … 0.45
GA- Single Engine	0.39 … 0.46				0.43	0.39 … 0.46
GA- Twin Engine	0.37 … 0.43				0.40	0.37 … 0.43
Commuters		0.35 … 0.45			0.40	0.35 … 0.45
Regional Turboprop	0.37 … 0.49	0.30 … 0.45			0.40	0.33 … 0.47
Jet						
Business Jets	0.28 … 0.40	0.30 … 0.40			0.35	0.29 … 0.40
Jet Transport	0.27 … 0.38	0.30 … 0.35	0.23 … 0.30	0.24 … 0.32	0.30	0.26 … 0.34
Military						
Jet trainers	0.35 … 0.50				0.42	0.35 … 0.50
Jet Fighters		0.30 … 1.00			0.65	0.30 … 1.00
Military transport	0.29 … 0.40				0.34	0.29 … 0.40
Special Purpose						
Agricultural	0.40 … 0.51				0.46	0.40 … 0.51
Flying Boat	0.33 … 0.50				0.41	0.33 … 0.50

Av. Average value of category

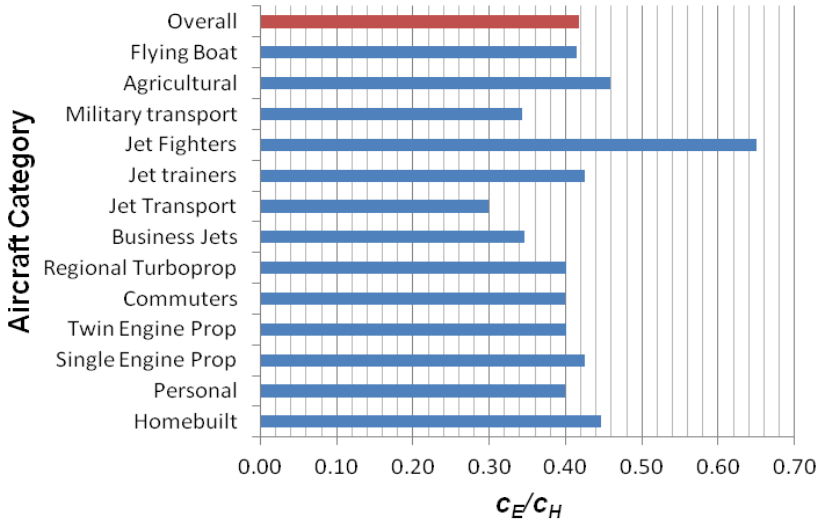

Figure 2.40 Comparison of c_E/c_H values for different aircraft categories

Table 2.19 Suggestions for c_R/c_v as given by various authors (**Roskam 1985, Schaufele 2007, Torenbeek 1982**, **Sadraey 2013**)

Aircraft Type	Roskam	Schaufele	Torenbeek	Sadraey	Av.	Range
Civil props						
Homebuilt	0.32 … 0.61				0.47	0.32 … 0.61
Personal		0.25 … 0.45			0.35	0.25 … 0.45
GA-Single Engine	0.37 … 0.44				0.41	0.37 … 0.44
GA- Twin Engine	0.36 … 0.44				0.40	0.36 … 0.44
Commuters		0.35 … 0.45			0.40	0.35 … 0.45
Regional Turboprop	0.32 … 0.44	0.25 … 0.45			0.36	0.28 … 0.44
Jet						
Business Jets	0.26 … 0.37	0.25 … 0.35			0.31	0.26 … 0.36
Jet Transport	0.28 … 0.40	0.25 … 0.40	0.23 … 0.36	0.25 … 0.35	0.32	0.25 … 0.38
Supersonic Cruise Airplanes	0.25 … 0.36				0.30	0.25 … 0.36
Military						
Jet trainers	0.34 … 0.48				0.41	0.34 ... 0.48
Jet Fighters	0.24 … 0.35	0.20 … 0.35			0.29	0.22 … 0.35
Military transport	0.31 … 0.46				0.39	0.31 … 0.46
Special Purpose						
Agricultural	0.36 … 0.56				0.46	0.36 … 0.56
Flying Boat	0.33 … 0.53				0.43	0.33 … 0.53

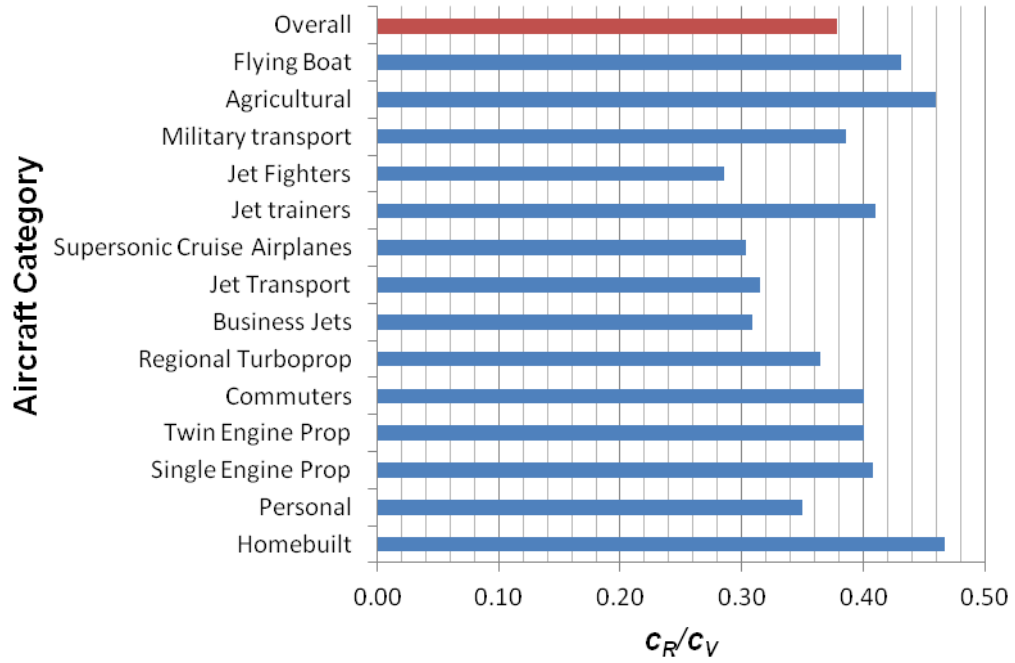

Figure 2.41 Comparison of c_R/c_v values for different aircraft categories

Figures 2.40 and 2.41 compare the average values of c_E/c_H and c_R/c_v for different categories. The overall averages are also displayed and are marked in red. It can be seen in Figures 2.40 and 2.41 that there is not much deviation from one aircraft category to another. Only, in case of military fighter (see Figure 2.41) a huge deviation is seen. This can be because the average and range are calculated based entirely on the suggestion given by 1 author i.e. **Schaufele 2007**. This is the only author to have suggested ranges for the different categories. The calculation style for calculating these ranges is unclear in this case. It is possible that the author could have taken the maximum and minimum observed values amongst military aircraft and calculated the range with these values. All the other authors referred to in the above 3 tables, list various aircraft along with their corresponding c_E/c_H and c_R/c_v values. To compile the above tables all the aircraft were divided into the various categories and then average and range values were calculated. The range values are calculated as the range within which most aircraft that are listed by the corresponding authors fall. This means, all values that lie within 1 standard deviation on either side of the average constitute the range.

Overall average and range values are calculated and presented in Table 2.21.

Table 2.20 Overall average and range values for c_E/c_H and c_R/c_v

Parameter	Average	Range
c_E/c_H	0.42	0.34 … 0.50
c_R/c_v	0.38	0.30 … 0.45

A more in-depth analysis of results from one of the authors, namely **Torenbeek 1982** shall be discussed here. **Torenbeek 1982** gives the hinge position as a percentage of c_H. Dividing this by 100 and subtracting from 1 gives the ratio, c_E/c_H**.** A comparison of many aircraft with respect to this ratio is done in Figure 2.42. The average and standard deviation are then calculated and given as results.

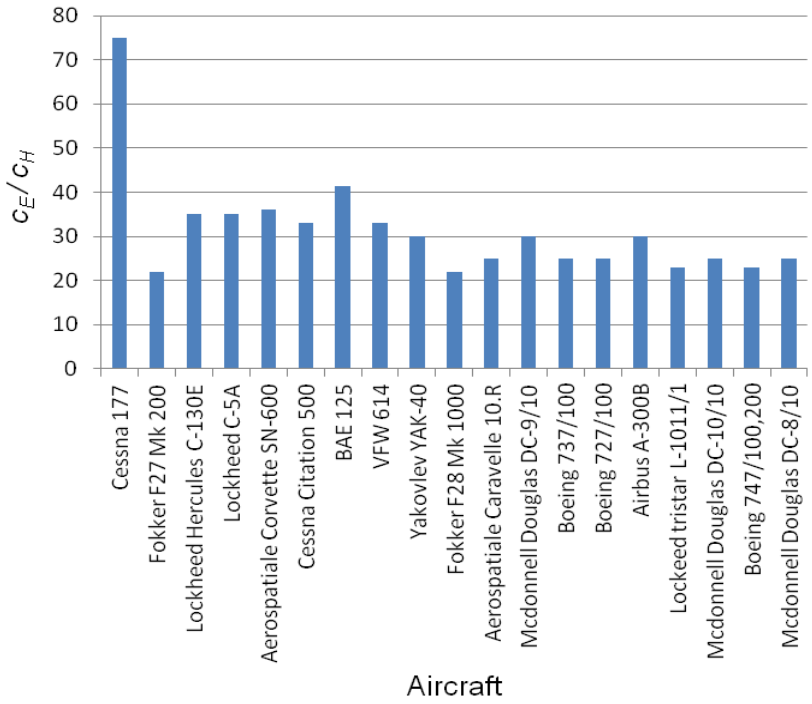

Figure 2.42 Statistics of c_E/c_H for different aircraft (adapted from **Torenbeek 1982**)

It can be seen from Figure 2.42 that most of the aircraft lie in a fairly close range with the exception of Cessna 177. This maybe because this statistic contains mainly aircraft of the jet transport category and Cessna 177 is the only aircraft in this statistic to belong to the Personal category. Due to unavailability of sufficient data of different categories, an individual statistic of only the jet transport category can be done. The results of these statistics are given in Tables 2.21 and 2.22.

Table 2.21 Average and standard deviation values for c_E/c_H

Average	0.31
Standard Deviation	0.12

Table 2.22 Average and standard deviation values for c_E/c_H (only jet transport aircraft considered)

Average	0.26
Standard Deviation	0.03

It can be observed that there is a fairly constant value of the ratio, c_E/c_H. As the standard deviation is very low when only jet transport aircraft are considered, it leads to the conclusion that the average value given in Table 2.22 may be a fairly good initial estimate for c_E/c_H in case of jet transports. It should be noted here that other categories have not been analysed from **Torenbeek 1982** as it contains insufficient data for other categories to obtain a good average.

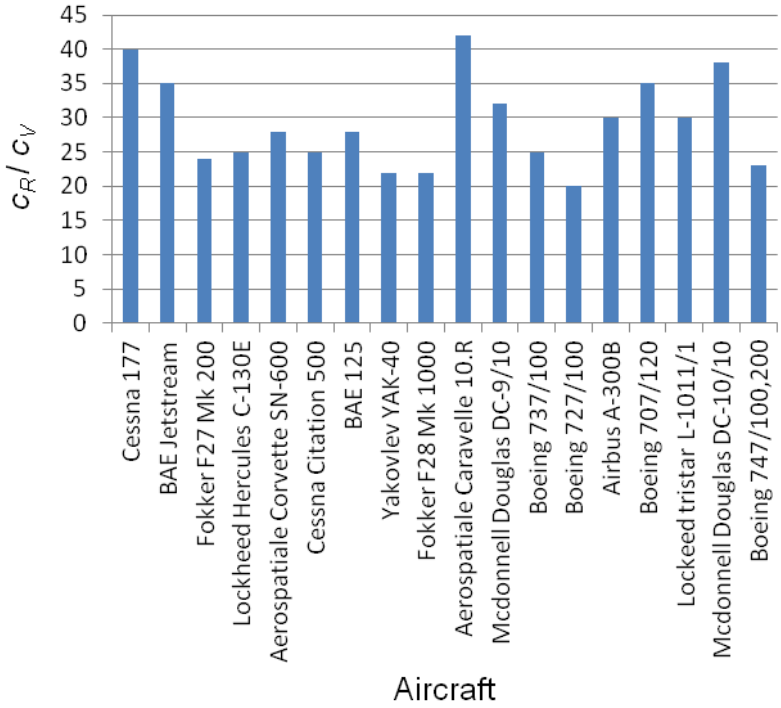

Figure 2.43 c_R/c_v statistics for various aircraft (adapted from **Torenbeek 1982**)

Figure 2.43 shows statistics undertaken for the ratio of c_R/c_v. Unlike in the case of the horizontal tail, these statistics do not improve on categorization on the basis of aircraft type and so results applicable to aircraft in general are given. Table 2.23 gives the average and standard deviation values of this ratio.

Table 2.23 Average and standard deviation values for c_R/c_v

Average	0.29
Standard Deviation	0.06

As the standard deviation is already quite small, the average value of c_R/c_v can be used for initial estimation during the conceptual design phase.

3 Tail Sizing

This chapter describes various relationships considered for aiding in the process of tail sizing.

3.1 Tail Volume Coefficient

In Chapter 2, suggestions by various authors are presented in the form of tables and figures. In this Chapter, the objective is to establish previously unexplored relationships between the various unknown tail parameter sizes on one hand and known parameter values on the other. These known parameters come as output from previous design phases like wing design. Also, averaging of the various authors' values give us better averages and results that can be used for the purpose of tail sizing. As it is known that aircraft from the same category generally show similarity in values of its parameters, we too have categorized all aircraft on the basis of maximum number of passengers, certification and engine type (jet or propeller). Table 2.2 shows this basis on which categorization of aircraft was done for this report.

Tail sizing usually starts with the estimation of the tail volume coefficient. As was described earlier, in Chapter 2, the tail volume coefficients refer to two non-dimensional parameters that can be defined by Equations 2.6 or 2.7 depending on whether the horizontal or vertical tail is in consideration.

3.1.1 Horizontal Tail Volume Coefficient

Table **3.1** contains three columns. All aircraft are divided on the basis of the aircraft category they fall into. This is listed in the first column. The middle column, "Aero, Ref." includes the statistics carried out by our research group (Aero). "Ref." denotes that the data comes from collecting the value of C_H from different reference sources and not measuring them ourselves. "Aero, Ref." has the same meaning throughout the remainder of this report. As statistics have been done on only the most common aircraft categories, many blank spaces can be seen in this column. Also, as the group is based in a university, the emphasis lies on non-military aircraft.

The last column has been formed from averaging the suggestions given by various authors (see Table 2.3) with "Aero, Ref.". This column is suggested to readers for choosing an initial value for horizontal tail volume coefficient, C_H.

Table 3.1 Suggested values for tail volume coefficient of horizontal tail (C_H)

Aircraft Type	Aero, Ref.	Average
Sailplane		0.500
Civil Props		
Homebuilt		0.484
Personal	0.593	0.593
GA- single engine		0.672
GA - twin engine		0.812
Commuter	0.930	0.930
Regional Turboprop	1.039	1.004
Jet		
Business Jets	0.664	0.694
Jet transport	0.954	0.991
Supersonic Cruise Airplanes		0.535
Military		
Jet Trainer		0.663
Jet Fighter		0.356
Military Transport	0.903	0.859
Special purpose		
Flying Boat		0.671
Agricultural		0.513

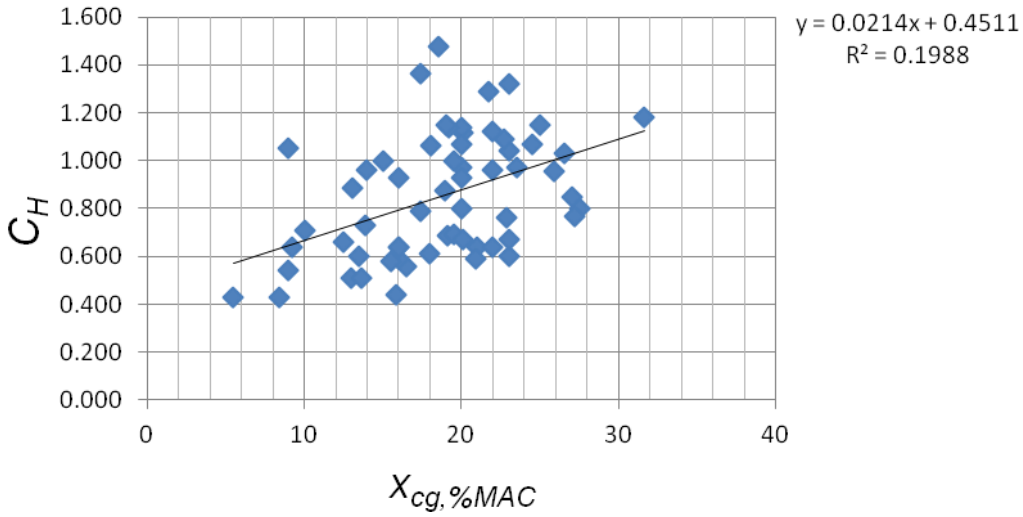

Figure 3.1 Graph of C_H vs $x_{cg,\%MAC}$

Figure **3.1** shows the plot of C_H vs $x_{cg,\%MAC}$ without sorting of aircraft into different categories. It was attempted to examine how the horizontal tail volume coefficient varies with change in the factor, $x_{cg,\%MAC}$. This factor is defined as in Equation 3.1.

$$x_{cg,\%MAC} = \frac{x_{r,MTOM,flight} - x_{f,MTOM,flight}}{c_{MAC}}\% \tag{3.1}$$

$x_{r,MTOM,flight}$ rear limit of the Maximum Take Off Mass (MTOM) C.G. position during flight
$x_{f,MTOM,flight}$ forward limit of the Maximum Take Off Mass C.G. position during flight
c_{MAC} wing Mean Aerodynamic Chord (MAC)

Inspiration for finding a relationship between these two parameters was derived from **Schaufele 2007** where the author produced a graph displaying the correlation between "Horizontal tail volume per unit of cg range/ %MAC" and "longitudinal fuselage volume parameter". The low regression value of 0.1988 in Figure 3.1 proves that there is no clear trend being followed. Thus, it was decided to classify the aircraft and then re-analyze the results for any improvement.

Figure 3.2 shows the same relationship being considered for only the Personal aircraft category. It can be seen from the scatter plot between C_H and $x_{cg,\%MAC}$ that to a certain extent, C_H is dependent on $x_{cg,\%MAC}$. The relationship between these two parameters can be given by,

$$C_H = 0.0115 x_{cg,\%MAC} + 0.4101 \tag{3.2}$$

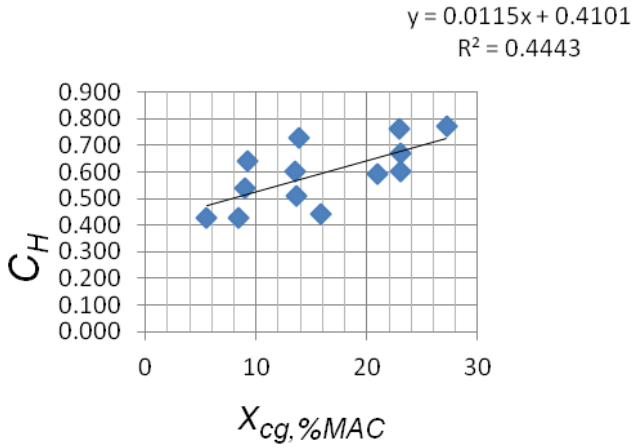

Figure 3.2 Graph of C_H vs $x_{cg,\%MAC}$ for personal aircraft

Here, the constants, 0.0115 and 0.4101 are dimensionless quantities. The relationship was tested for the other aircraft categories as well. However, the other categories did not yield high enough regression values and so are not produced here as results.

3.1.2 Vertical Tail Volume Coefficient

Table 3.2 lists the suggested values for vertical tail volume coefficient.

Table 3.2 Suggested values for tail volume coefficient of vertical tail (C_v)

Aircraft Type	Aero, Ref.	Aero, calc.	Average
Sailplane			0.0190
Civil props			
Homebuilt			0.0380
Personal	0.0612	0.0589	0.0601
GA- single engine			0.0443
GA- twin engine			0.0657
GA- Average			0.0550
Commuter		0.0707	0.0707
Regional Turboprop	0.0777	0.0764	0.0790
Jet			
Business Jets	0.0742	0.0799	0.0722
Jet transport	0.0755	0.0706	0.0793
Supersonic Cruise Airplanes			0.0635
Military			
Military Trainer			0.0620
Military Fighter	0.0726		0.0710
Military Cargo/bomber/Transport	0.0789		0.0742
Special Purpose			
Agricultural			0.0360
Flying Boat			0.0550

With respect to the columns, Table 3.2 is similar to Table 3.1 with only an additional column called, "Aero, calc." added in Table 3.1. This column includes the values of C_v calculated by our group from statistics derived from 3-view diagrams of aircraft.

Most of the values in column, "Aero, calc." are quite close to the corresponding values in the rightmost column with exception to the value corresponding to jet transport category. This can be explained as many new aircraft included in this study could not have been included by older publications because of unavailability of their data at that time. Many of these new aircraft have low values of C_v thus bringing down the average. Also, as mentioned earlier, emphasis is on non-military aircraft and so no 3-views of military aircraft were considered during this study. Once again, as the suggested values are averaged over a number of previous authors (see Table 2.4) along with "Aero, Ref." and "Aero, calc.", the averages tend to be better.

It was discussed in Chapter 2.5.1 how different authors assume different definitions for the vertical tail area. Also, in cases of aircraft having dorsal fins, it is unclear from previously published material whether the dorsal fin area should be considered as a part of the vertical tail area for calculation of C_v. As this study dealt with so many different authors, it was difficult to determine the best definition of the vertical tail area especially in case of aircraft having a dorsal fin. Thus, with this aim, statistics were carried out, the results of which are shown in Table 3.3. For this, 3-view diagrams were obtained from the internet and the various parameters influencing C_v were measured and C_v was thus calculated. Two calculations of C_v

were made, one considering the dorsal fin area, S_{df} as part of the vertical tail area ($C_{v,calc,df}$), S_v and one excluding S_{df} ($C_{v,calc,wo/df}$). All the aircraft were divided into the various categories defined in Table 2.2 and averages were taken. These average values are shown in Table 3.3.

Table 3.3 Determining the area used by various authors to calculate C_v

Aircraft Type	$C_{v,ref}$	$C_{v,calc,wo/df}$	$\Delta C_{v,calc,wo/df}$	$C_{v,calc,df}$	$\Delta C_{v,calc,df}$
Personal	0.0592	0.0589	2.6677	0.0698	6.7118
Commuter	0.0707	0.0707	2.7500	0.0797	3.5595
Business Jet	0.0702	0.0799	3.4815	0.0886	8.6428
Regional Turboprop	0.0756	0.0764	4.0524	0.0907	12.9282
Jet Transport (R.E. DF)[a]	0.0753	0.0797	2.2623	0.0862	4.3293
Jet Transport	0.0809	0.0637	1.6639	0.0658	2.3412

[a] stands for jet transport with round edge dorsal fin

The columns titled, "$\Delta C_{v,calc,wo/df}$" and "$\Delta C_{v,calc,df}$" show the average deviation of "$C_{v,calc,wo/df}$" and "$C_{v,calc,df}$" respectively from "$C_{v,ref}$", the value given in reference material. In many cases, C_v could not be found in any publication for a given aircraft. Thus, the deviation columns represent the average of, only the deviation in case of aircraft that were both, calculated from 3-view diagrams as well as obtained from some published material. As "$\Delta C_{v,calc,wo/df}$" column shows consistently lower values than "$\Delta C_{v,calc,df}$" in every aircraft category studied, it can be said that the "$C_{v,ref}$" column matches better with "$C_{v,calc,wo/df}$". Thus, it can be concluded that most of the authors whose publications have been used for study during this report exclude the dorsal fin from the tail area when sizing is done by the tail volume coefficient method. It is therefore unclear what the area of a dorsal fin should be if the tail volume coefficient method is used (see Equation 2.5) and whether there is a trend between the vertical tail area, S_v and the dorsal fin area, S_{df}.

Table 3.4 and Figure 3.3 venture into an unexplored statistic. This aims to find a trend between the value of C_v, when dorsal fin is included in its calculation and when it is excluded. For this purpose, only aircraft having dorsal fins were examined. In case of the jet transport category however, aircraft having round edge dorsal fin were also included.

Table 3.4 shows the results of this particular study. The last column shows the deviation (in percentage) between calculation with dorsal fin and that without dorsal fin included. It is calculated as in Equation 3.3.

$$Deviation(\%) = \frac{C_{v,df} - C_{v,wo/df}}{C_{v,wo/df}} \% \tag{3.3}$$

$C_{v,df}$ C_v calculated with inclusion of dorsal fin

$C_{v,wo/df}$ C_v calculated with exclusion of dorsal fin

Table 3.4 Comparison of C_v with and without dorsal fin in different aircraft categories

Aircraft Type	Aero, calc.	Deviation in %
Personal with DF	0.0698	
Personal without DF	0.0589	18%
Commuter with DF	0.0797	
Commuter without DF	0.0707	13%
Business Jets with DF	0.0886	
Business Jets without DF	0.0799	11%
Jet Transport with round edge DF[#]	0.0658	
Jet Transport without round edge DF[#]	0.0637	3%
Jet transport with DF	0.0862	
Jet transport without DF	0.0797	8%
Regional Turboprop with DF	0.0907	
Regional Turboprop without DF	0.0764	19%
Average, Civil aircraft		14%

[#] jet transport with and without round edge dorsal fin has not been considered in the average
DF stands for dorsal fin

It can be observed that as structurally, the round edge dorsal fin lies in between the "dorsal fin" and "no dorsal fin", the statistic too corroborates this. This can be seen as the deviation in C_v, in case of jet transport with round edge dorsal fin is lower than that in case of jet transport with (conventional) dorsal fin. The final average given by, "Average, Civil aircraft" is calculated averaging all the values of the last column except the deviation corresponding to the jet transport with and without round edge dorsal fin. These results can be used conversely to size the dorsal fin. Thus, given that $C_{v,wo/df}$ is known, $C_{v,df}$ can be calculated, and if area of dorsal fin ($S_{v,df}$) is the only unknown parameter in Equation of $C_{v,df}$ (see Equation 2.6) then it can be found out once $C_{v,df}$ is estimated.

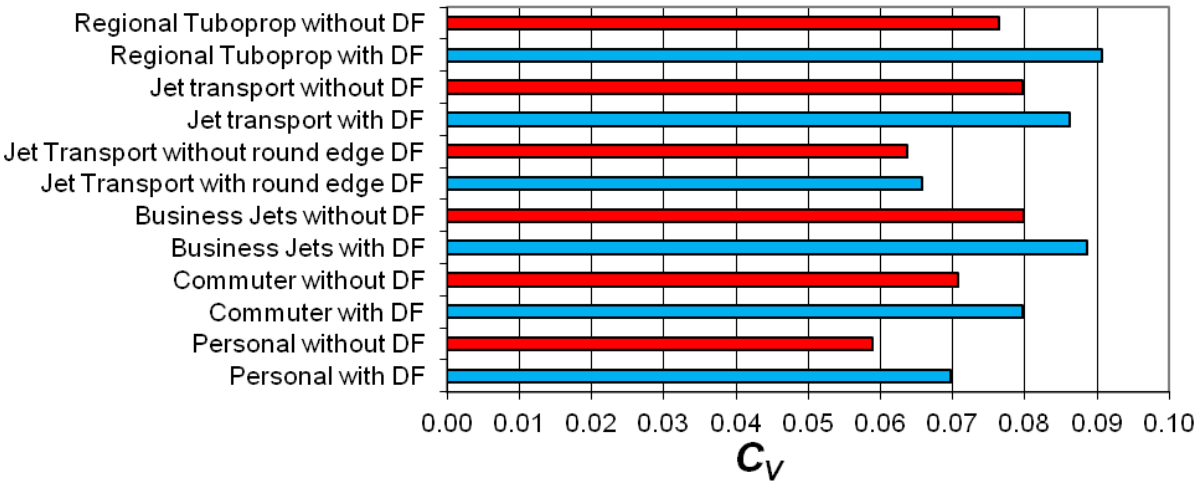

Figure 3.3 Bar diagram showing comparison of C_v calculated with and without Dorsal fin

Figure 3.3 shows a bar diagram depicting the same result given by Table 3.4. Values of $C_{v,df}$ are marked in red while the bars marked in blue indicate values of $C_{v,wo/df}$. The result already described in the above paragraph can be more clearly seen in this bar diagram.

This was compared with statistics conducted independently on different aircraft having dorsal fins in Chapter 4. A striking resemblance between the averages proves that there is a trend being followed in the difference of C_v calculated with and without the dorsal fin. The comparison between the two independent studies is given in Table 3.5. Please note that "Study 1" uses statistics collected in Chapter 3, while "Study 2" refers to those collected exclusively for dorsal fin sizing in Chapter 4.

Table 3.5 Comparison of $\Delta C_v/C_{v,wo/df}$ ratio on 2 independent studies

Aircraft Type	Study 1	Study 2
	$\Delta C_v/C_{v,wo/df}$	$\Delta C_v/C_{v,wo/df}$
Jet with DF	0.082	0.094
Jet with round edge DF	0.033	0.029
Regional Turboprops	0.187	0.186

ΔC_v stands for the difference in C_v (see Equation 3.4)

$$\Delta C_v = C_{v,df} - C_{v,wo/df} \tag{3.4}$$

$C_{v,df}$ vertical tail volume coefficient calculated including dorsal fin area
$C_{v,wo/df}$ vertical tail volume coefficient calculated excluding dorsal fin area

Table 3.5 shows the similarity in the averages calculated on the two different sets of aircraft. Thus, these values can be used for determining the increment in tail volume coefficient if a dorsal fin is added. Alternatively, it can be used to estimate a good initial value for the dorsal fin area as well.

Figures 3.4 and 3.5 show C_v plotted against a factor called Engine out ratio. Engine out ratio is defined differently for jet and propeller aircraft owing to the difference in propulsion. This ratio is defined by Equation 3.5 for jets and Equation 3.6 for props.

$$E_T = \frac{T_{TO} y_{E,o}}{n_e S_W b_W} \tag{3.5}$$

T_{TO} take off thrust total
$y_{E,o}$ Engine lever arm (Engine out distance)
n_e number of engines
S_W wing area
b_W wing span

$$E_P = \frac{P_{TO} y_{E,o}}{n_e S_W b_W} \tag{3.6}$$

P_{TO} take off power total

Here, E_T has the units of kN/m^2 while E_P has the units of kW/m^2. Like seen in case of the horizontal tail, the relationship shown when all aircraft are considered does not yield a high enough correlation. Also, in this case, jet engines produce thrust in kN while propeller engines produce power in kW. Due to these reasons, the aircraft are sorted out into the various categories as discussed earlier, and then the relationship is re-analyzed. In case of propeller driven aircraft, instead of take off thrust, take off power is used. Sorting once again produces better results and in case of two categories, regional turboprop and jet transport, good trends are observed (see Figures 3.4 and 3.5).

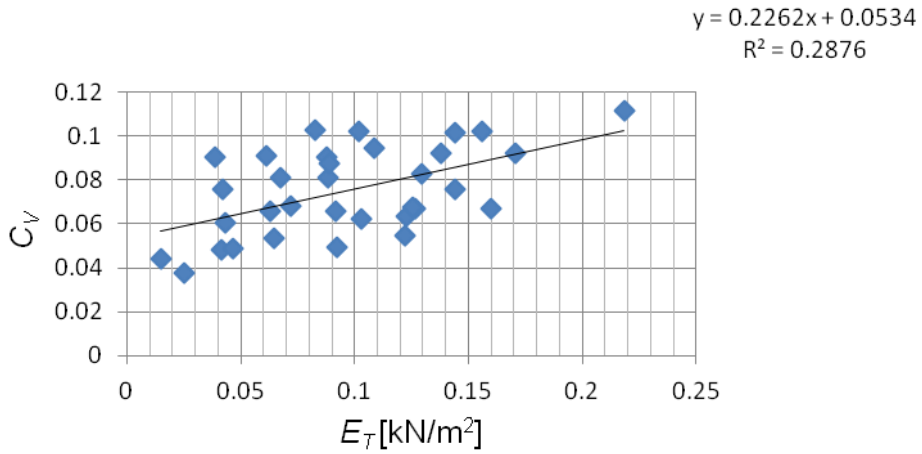

Figure 3.4 Graph of C_v vs E_T for jet transport aircraft

A certain trend is observed in Figures 3.4 and 3.5 although the regression values are still not too high. However, as the aim of this study includes exploration of all kinds of new relationships being exhibited by the parameters in consideration, we shall retain these figures as results.

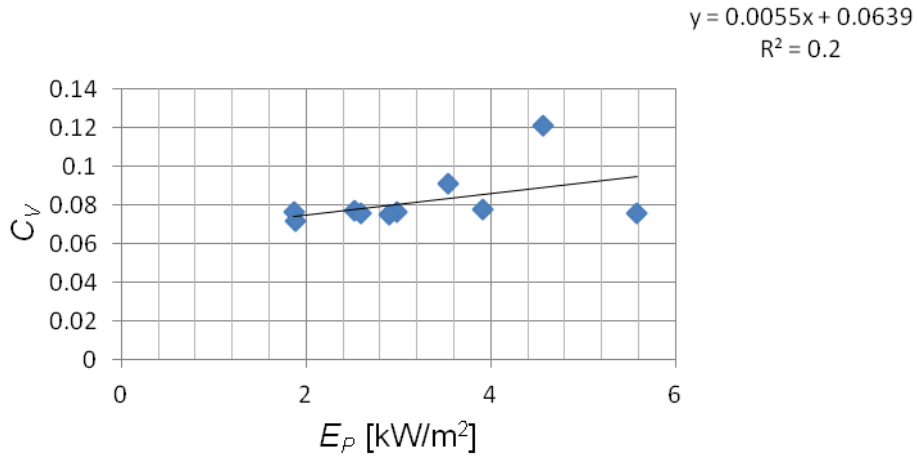

Figure 3.5 Graph of C_v vs E_R for regional turboprop aircraft

Thus, for jet transport aircraft, Equation 3.7 is applicable.

$$C_v = 0.2262 \frac{m^2}{kN} E_T + 0.0534 \tag{3.7}$$

And for regional turboprop aircraft, Equation 3.8 is applicable.

$$C_v = 0.0055 \frac{\mathrm{m}^2}{\mathrm{kW}} E_P + 0.0639 \tag{3.8}$$

In Equations 3.7 and 3.8, the constants 0.2262 and 0.0055 have the units of m^2/kN and m^2/kW respectively, while the constants 0.0534 and 0.0639 are dimensionless. Since all results discussed in this report are for the usage in the conceptual design phase, only approximations are desired. Thus, the user can use Equations 3.7 and 3.8 to improve on the approximate values given in Tables 3.1 to 3.4.

3.2 Tail Geometry

In this section, some parameters crucial in defining an aircraft's tail geometry have been discussed. It has to be noted that only parameters for which statistics have been carried out have been discussed here.

3.2.1 Horizontal Tail Geometry

Aspect ratio

Table 3.6 lists the suggested values for aspect ratio of horizontal tail. In this table, the columns, "Aero Average" and "Aero Range" are new in comparison to previous tables in this chapter. The last two columns of Table 3.6 give the final average and range values that are suggested to an aircraft designer for initial sizing during conceptual design phase.

As discussed earlier, we have carried out statistics usually on the most common, non-military aircraft categories. It can be seen that there are values suggested for Military transport (propellers) but not for jet. This is because there was data available only for a limited number of military transport (jet) aircraft. The column, "Aero Average" thus, gives us the average of all aircraft aspect ratio values in that particular category. "Aero Range", unlike the ranges suggested by authors in tables of Chapter 2, denotes not the maximum and minimum values of aspect ratio found in statistics but rather the limits of 1 standard deviation on either side of the average. This therefore gives us the range of majority of the aircraft aspect ratio values inspected. While conducting statistics, an attempt was made to include as many aircraft as possible. Due to these reasons, these two columns were assigned higher weights when averaging

with the values suggested by other authors (see Table 2.5) so that the final averages and ranges are more influenced by these two columns.

Table 3.6 Suggested values for aspect ratio of horizontal tail (A_H)

Aircraft type	Aero Average	Aero Range	Average	Range
Sail Plane			8.00	6.00 ... 10.00
Civil props				
Homebuilts			3.15	1.80 … 4.50
Personal	6.00	5.07 … 6.93	5.61	4.66 … 6.57
GA - single engine			5.15	4.00 … 6.30
GA- Twin Engine			5.70	3.70 … 7.70
Commuters	4.88	3.99 … 5.76	4.74	3.78 … 5.69
Regional Turboprop	5.27	4.60 … 5.94	5.12	4.10 … 6.14
Jet				
Business jets	4.40	3.74 … 5.05	4.56	3.64 … 5.49
Jet Transports	4.44	3.53 … 5.34	4.36	3.38 … 5.34
Supersonic Cruise airplanes			2.20	1.80 … 2.60
Military				
Military Trainers			4.05	3.00 … 5.10
Military Fighter			3.68	2.77 … 4.60
Military transport (Propeller)	5.41	4.62 … 6.19	5.41	4.43 … 6.39
Military transport			4.10	1.30 … 6.90
Special Purpose				
Agricultural			4.05	2.70 … 5.40
Flying Boats, Amphibian And Float Airplanes			3.65	2.20 … 5.10

For this purpose, the suggested values given by various authors in Chapter 2 are first averaged. This average is further averaged with the values calculated by our statistics. Thus, the "Aero" columns have a weight of 1 out of 2. The average of all the values suggested by the other authors together constitutes the remaining weight of 1. The rest of the tables in this Chapter also follow the same calculation style. Table 3.7 illustrates this more clearly.

Table 3.7 Weighting method used in this study

Author 1	Author 2	Author 3	Average	Aero	Final average
x1	x2	x3	X=(x1+x2+x3)/3	Y	Z=(X+Y)/2

Taper ratio

Table 3.8 gives the suggested values for horizontal tail taper ratios that can be used during conceptual designing phase.

Table 3.8 Suggested values for taper ratio of horizontal tail (λ_H)

Aircraft type	Aero average	Aero Range	Average	Range
Sail Plane			0.40	0.30 … 0.50
Civil props				
Homebuilts			0.65	0.29 … 1.00
Personal	0.58	0.37 … 0.80	0.65	0.41 … 0.90
GA - single engine			0.73	0.45 … 1.00
GA - single engine			0.74	0.48 … 1.00
Commuters	0.65	0.37 … 0.92	0.67	0.38 … 0.96
Regional Turboprop	0.51	0.32 … 0.70	0.59	0.36 … 0.82
Jet				
Business jets	0.47	0.38 … 0.57	0.46	0.35 … 0.57
Jet Transports	0.37	0.28 … 0.46	0.39	0.27 … 0.51
Supersonic Cruise airplanes			0.27	0.14 … 0.39
Military				
Military Trainers			0.68	0.36 … 1.00
Military Fighter			0.40	0.20 … 0.60
Military transport (Prop)	0.50	0.32 … 0.67	0.51	0.30 … 0.73
Military transport			0.56	0.31 … 0.80
Special Purpose				
Agricultural			0.80	0.59 … 1.00
Flying Boats, Amphibian And Float Airplanes			0.67	0.33 … 1.00

Quarter-chord sweep

Figure 3.6 and Figure 3.7 show plots between $\Delta\varphi_{25,H}$ and $\varphi_{25,W}$. Here $\Delta\varphi_{25,H}$ is defined by Equation 3.9.

$$\Delta\varphi_{25,\mathrm{H}} = \varphi_{25,H} - \varphi_{25,W} \tag{3.9}$$

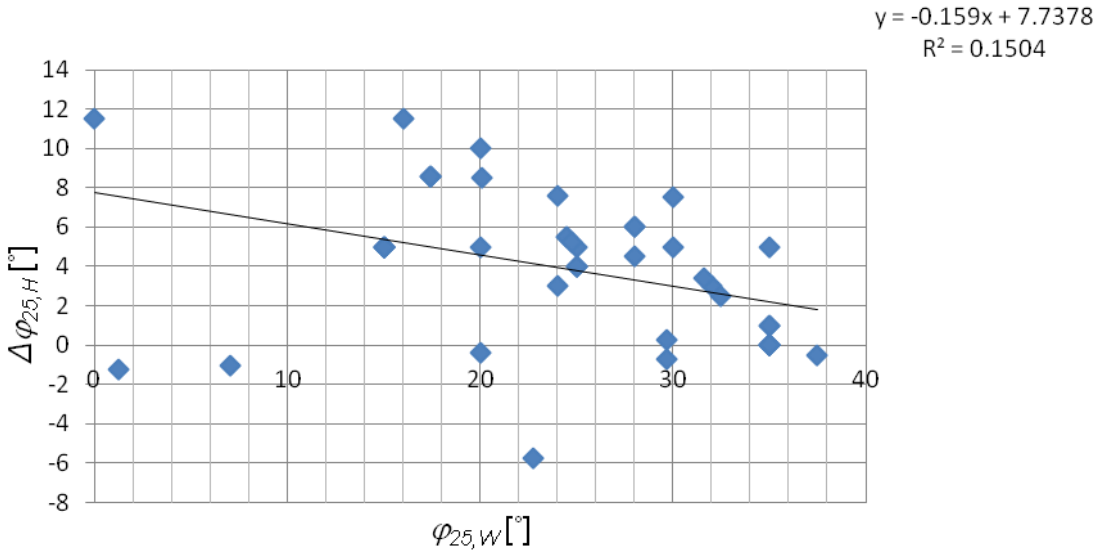

Figure 3.6 Graph of $\Delta\varphi_{25,H}$ vs $\varphi_{25,W}$

Table 3.9 gives the suggested average and range values for horizontal tail quarter chord sweep angles.

Table 3.9 Suggested values for quarter chord sweep of horizontal tail ($\varphi_{25,H}$) in degrees

Aircraft type	Aero average	Aero Range	Average	Range
Civil props				
Homebuilts			10.0	0 … 20
GA - single engine			5.0	0 … 10
GA - single engine			8.5	0 … 17
Regional Turboprop			16.5	0 … 33
Jet				
Business jets	26.7	22 … 32	24.5	16 … 33
Jet Transports	31.1	26 … 36	28.8	22 … 36
Supersonic Cruise airplanes			46.0	32 … 60
Military				
Military Trainers			15.0	0 … 30
Military Fighter			27.5	0 … 55
Military transport			20.0	5 … 35
Special Purpose				
Agricultural			5.0	0 … 10
Flying Boats, Amphibian And Float Airplanes			8.5	0 … 17

As can be seen in Figure 3.6, there is a very low correlation shown between the two parameters. Once again, we attempted to improve this correlation by sorting the aircraft based on their category.

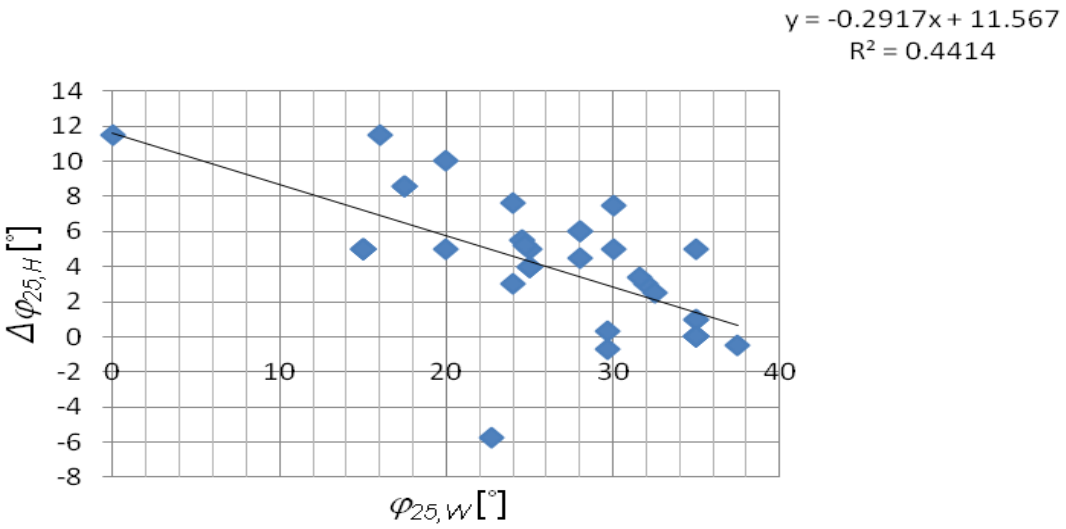

Figure 3.7 Graph of $\Delta\varphi_{25,H}$ vs $\varphi_{25,W}$ for jet transport aircraft

Figure 3.7 shows the same relation being considered in the case when only jet transport are analyzed. This graph shows quite a good regression value of 0.4414. Hence, it can be used as a guideline during conceptual design phase of jet transport. Equation 3.10 gives this result.

$$\Delta\varphi_{25,H} = -0.2917\varphi_{25,W} + 11.567° \tag{3.10}$$

Here, the constant -0.2917 is dimensionless while the constant 11.567 is defined in degrees. Thus, given the wing quarter chord sweep, the increment or decrement needed to be applied to the wing sweep to obtain the horizontal tail sweep can be known.

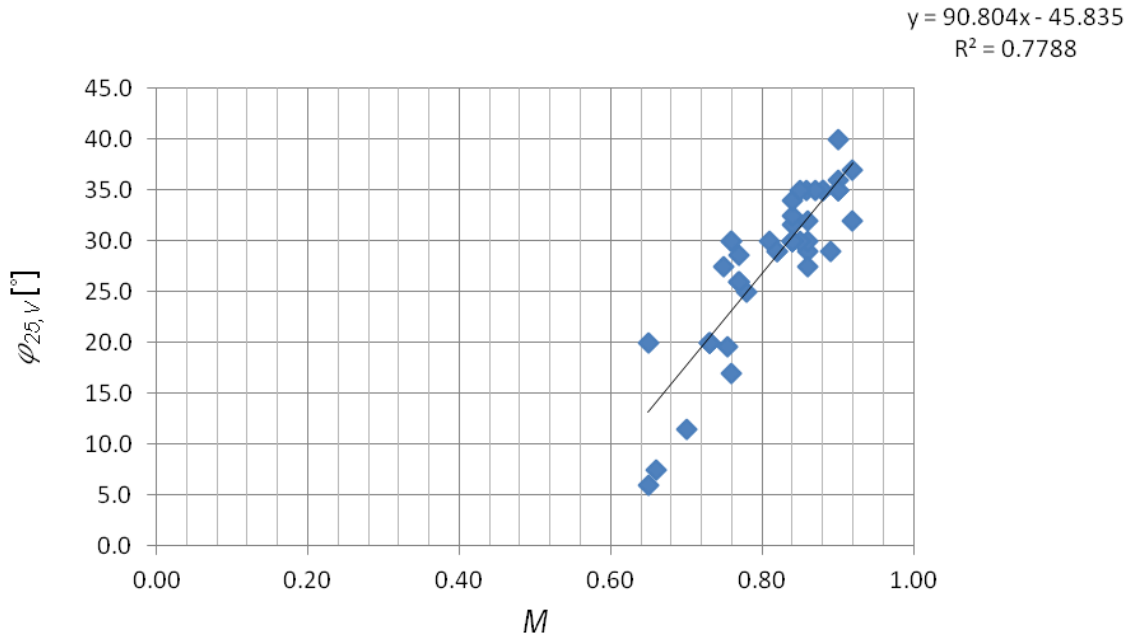

Figure 3.8 Graph of $\varphi_{25,H}$ vs Mach number, M for jet transport aircraft

Raymer 1992 contains a graph plotting wing sweep against Mach number, M. As the horizontal tail is similar to the wing in many ways, we decided to develop a statistic for the same relationship in case of horizontal tail. Figure 3.8 shows the results of this statistic. As can be seen, the two parameters, horizontal tail quarter chord sweep, $\varphi_{25,H}$ and Mach number, M share a very high correlation with each other. Thus, Equation 3.11 can be used in determining the value of $\varphi_{25,H}$, once the mach number of the aircraft is known.

For $M > 0.505$,

$$\varphi_{25,H} = 90.804°M - 45.835° \tag{3.11}$$

For $M \leq 0.505$, $\varphi_{25,H}$ can be estimated to 0.
Here the constants 90.804 and -45.835 have the units of degrees. It must be noted that this relation can be used only for jet transport aircraft as the other categories of aircraft do not show the same relation and show lower correlation values.

Relative thickness ratio

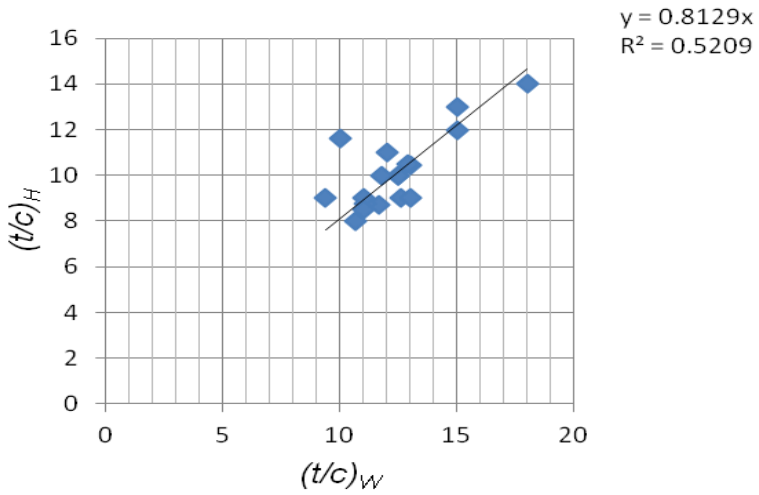

Figure 3.9 Graph of $(t/c)_H$ vs $(t/c)_W$

In Section 2.5.6, a quote from **Raymer 1992** has been taken that states that in case of "high speed aircraft, the horizontal tail is usually about 10% thinner than the wing". Figure 3.9 compares the relative thickness ratio of the horizontal tail against that of the wing for all types of aircraft. The figure indicates quite a good correlation between the two parameters (regression value of 0.5209). It can also be seen to have a very similar result to the one prescribed by **Raymer 1992**. Equation 3.12 gives this result.

$$(t/c)_H = 0.8129(t/c)_W \tag{3.12}$$

Here, the constant 0.8129 is a dimensionless quantity.

3.2.2 Vertical Tail Geometry

All the parameters considered in the previous section are considered in this section for the vertical tail.

Aspect ratio

Table 3.10 Suggested values for aspect ratio of vertical tail (A_v)

Aircraft type	Aero average	Aero Range	Average	Range
Sail Plane			1.75	1.50 … 2.00
Civil props				
Homebuilts			0.90	0.40 … 1.40
Personal	1.44	1.21 … 1.67	1.45	1.18 … 1.72
GA - single engine			1.55	0.90 … 2.20
GA - single engine			1.25	0.70 … 1.80
Commuters	1.49	1.25 … 1.72	1.50	1.21 … 1.78
Regional Turboprop	1.65	1.41 … 1.88	1.59	1.29 … 1.89
Jet				
Business jets	1.24	0.94 … 1.54	1.25	0.89 … 1.61
Jet Transports	1.50	1.10 … 1.89	1.45	0.95 … 1.94
Supersonic Cruise airplanes			1.80	1.20 … 2.40
Military				
Military Trainers			1.95	1.00 … 2.90
Military Fighter			1.20	0.73 … 1.67
Military transport (Prop)	1.66	1.42 … 1.90	1.62	1.35 … 1.90
Military transport			1.40	0.90 … 1.90
Special Purpose				
Agricultural			1.00	0.60 … 1.40
Flying Boats, Amphibian And Float Airplanes			1.20	0.73 … 1.67

Table 3.10 lists the suggested average and range values for vertical tail aspect ratio.

Taper ratio

Table 3.11 Suggested values for taper ratio of vertical tail (λ_v)

Aircraft type	Aero average	Aero Range	Average	Range
Sail Plane			0.50	0.40 … 0.60
Civil props				
Homebuilts			0.49	0.26 … 0.71
Personal	0.37	0.27 … 0.47	0.39	0.28 … 0.50
GA - single engine			0.45	0.32 … 0.58
GA - single engine			0.54	0.33 … 0.74
Commuters	0.41	0.28 … 0.53	0.44	0.27 … 0.62
Regional Turboprop	0.39	0.28 … 0.50	0.46	0.29 … 0.63
Jet				
Business jets	0.41	0.25 … 0.56	0.46	0.27 … 0.66
Jet Transports	0.46	0.28 … 0.63	0.48	0.28 … 0.69
Supersonic Cruise airplanes			0.32	0.20 … 0.43
Military				
Military Trainers			0.53	0.32 … 0.74
Military Fighter			0.34	0.21 … 0.46
Military transport (Prop)	0.40	0.29 … 0.51	0.40	0.26 … 0.55
Military transport			0.64	0.28 … 1.00
Special Purpose				
Agricultural			0.59	0.43 … 0.74
Flying Boats, Amphibian And Float Airplanes			0.69	0.37 … 1.00

Table 3.11 lists the suggested average and range values for vertical tail taper ratio.

Quarter-chord sweep

Table 3.12 Suggested values for quarter chord sweep of vertical tail ($\varphi_{25,v}$)

Aircraft type	Aero average	Aero Range	Average	Range
Civil props				
Homebuilts			23.5	0 ... 47
Personal	27.2	24 … 30	27.1	24 … 30
GA - single engine			27.0	12 ... 42
GA - single engine			31.5	18 ... 45
Commuters	29.3	25 … 33	29.2	24 … 35
Regional Turboprop	23.6	18 … 29	23.1	13 … 33
Jet				
Business jets	42.5	36 … 49	42.8	33 … 52
Jet Transports	38.7	35 … 43	40.1	33 … 47
Supersonic Cruise airplanes			51.0	37 ... 65
Military				
Military Trainers			22.5	0 ... 45
Military Fighters			34.5	9 ... 60
Military transport (Prop)	15.8	10 … 22	16.2	10 … 22
Military transport			17.2	0 ... 37
Special Purpose				
Agricultural			16.0	0 ... 32
Flying Boats, Amphibian And Float Airplanes			16.0	0 ... 32

Table 3.12 lists the suggested average and range values for quarter chord sweep angle of the vertical tail. Figure 3.10 meanwhile is a result of a statistic studied between vertical tail sweep and wing sweep. It was seen in Section 2.5.5 from **Raymer 1992**, that the vertical tail quarter chord sweep angle lays between 35° ... 55° for aircraft with "high airspeeds". We investigated this wisdom by comparing the wing and vertical tail quarter chord sweep angles of aircraft of different categories. Figure 3.10 shows the results of this investigation.

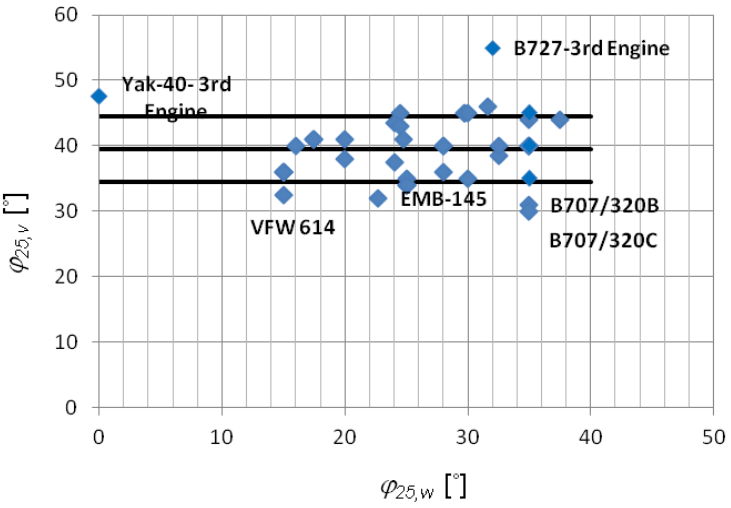

Figure 3.10 Graph of $\varphi_{25,v}$ vs $\varphi_{25,W}$ for jet transport aircraft

Out of all the jet transport aircraft that we considered in our investigation, most of the aircraft lay in a window region of 35° ... 45° (within 1 standard deviation on either side of the mean value). The aircraft that lie outside this window are labeled in the Figure 3.10. As the vertical tail sweep can be dependent on an array of factors other than the wing sweep, it is difficult to single out a single reason why these aircraft show anomalous behavior from the rest. This can be a topic of future research. The 3 black lines indicate the mean value and mean ± 1 standard deviation on either side.

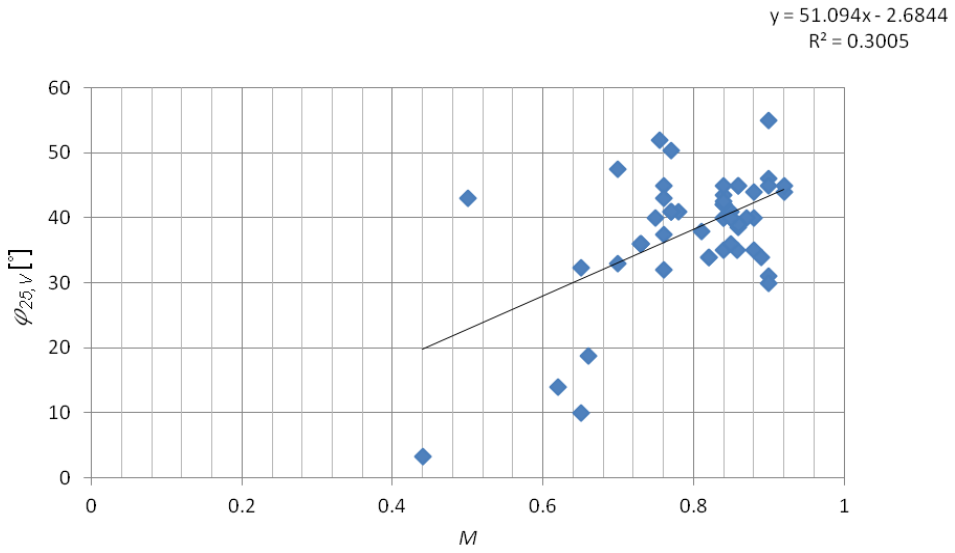

Figure 3.11 Graph of $\varphi_{25,v}$ vs M

In Section 3.2.1, $\varphi_{25,H}$ was observed to show a very good correlation with the aircraft Mach number, M. Unfortunately, Figure 3.11 indicates that the same does not hold true in case of vertical tail as the regression value is comparably much smaller. In case of vertical tail therefore, the user is suggested to use values given in Table 3.12 based on the aircraft category to decide on an initial sweep angle.

Relative thickness ratio

Figure 3.12 displays a fair correlation between $(t/c)_v$ and $(t/c)_W$. Thus, a relation can be developed based on this figure. Equation 3.13 gives this relation.

$$(t/c)_v = 0.924(t/c)_W \tag{3.13}$$

Here the constant 0.924 is a dimensionless quantity. This relation can be used to estimate the relative thickness ratio of the vertical tail, given the relative thickness ratio of the wing.

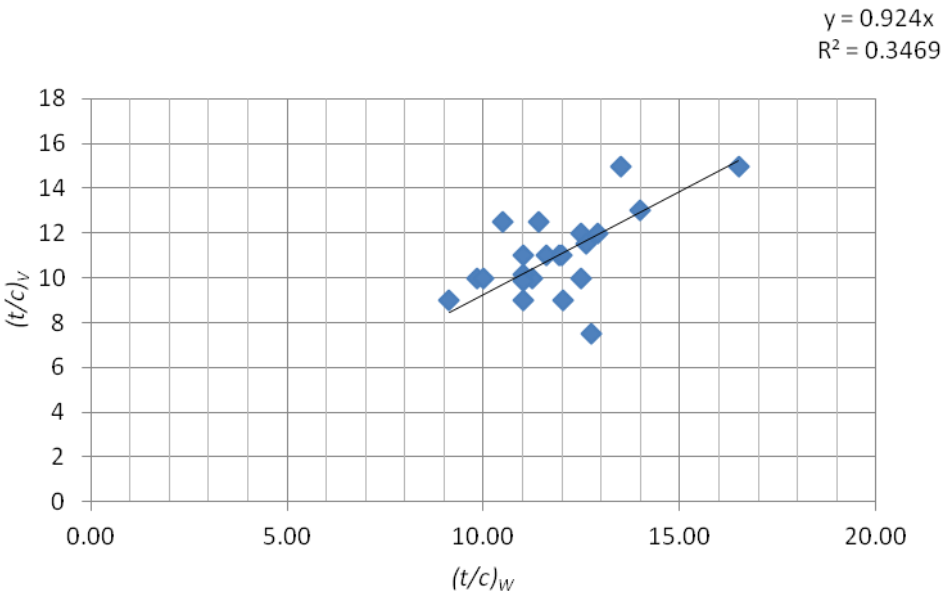

Figure 3.12 Graph of $(t/c)_v$ vs $(t/c)_W$

3.2.3 Control Surfaces Geometry

Section 2.5.7 deals in detail with sizing of chord lengths of the control surfaces. The results were finally produced as a function of the corresponding tail chord lengths. Similarly, in this section too, two parameters shall be discussed. Here, the results shall be given as functions of the tail spans.

Table 3.13 gives the average and standard deviation values for the ratios $y_{t,E} : b_H/2$ and $y_{r,E} : b_H/2$ (as defined in Figure 2.38).

Table 3.13 Statistics results for $y_{t,E} : b_H/2$ and $y_{r,E} : b_H/2$

Tail Type	$y_{t,E}:b_H/2$		$y_{r,E}:b_H/2$	
	Average	Std. Dev.	Average	Std. Dev.
Conventional tail	0.932	0.094	0.016	0.029
T-tail	0.950	0.073	0.009	0.019
Cruciform tail	0.948	0.062	0.012	0.034

It was observed that the results showed lower standard deviation values when the aircraft were divided on the basis of tail type. Even though **Raymer 1992** does not give different suggestions for aircraft having different tail types, its estimations for general aircraft given in Chapter 2 are more or less reiterated by these results and can be used during the conceptual design phase.

Table 3.14 Statistics results for $y_{t,R}:b_v$ and $y_{r,R}:b_v$

Tail Type	$y_{t,R}:b_v$		$y_{r,R}:b_v$	
	Average	Std. Dev.	Average	Std. Dev.
Conventional tail	0.981	0.042	0.070	0.133
T-tail	0.810	0.068	0.034	0.067
Cruciform tail	0.841	0.182	0.063	0.134

Table 3.14 gives the average and standard deviation values for the ratios $y_{t,R} : b_v$ and $y_{r,R} : b_v$ (as defined in Figure 2.39). It was observed that the results showed lower standard deviation values when the aircraft were divided on the basis of tail type. Table 3.14 too corroborates suggestion values given by **Raymer 1992** for general aircraft. Values for horizontal and vertical tail control surfaces given in Table 3.13 and Table 3.14 can be thus considered as an improvement over suggestions given in previous publications (see Chapter 2).

4 Dorsal Fin and Round Edge Dorsal Fin Sizing

4.1 Introduction to Sizing Methods

This chapter presents the sizing method developed to design a dorsal fin or round edge on a vertical tail of an aircraft. Both methods could be used in principle for all categories of aircraft. However they have only been applied to data of commercial aircraft. Figures 4.1 and 4.2 present a side view of a conventional tail with a dorsal fin.
Figure **4.3** shows the side view of a round edge dorsal fin on a conventional tail. All the parameters are labeled in the figures. These are the parameters that were used in the sizing methods. The dorsal fin parameters (Figures 4.1 and 4.2) have been investigated for commercial jet and propeller aircraft, whereas the parameters of round edge dorsal fins (
Figure **4.3**) have been investigated only for commercial jet transports.

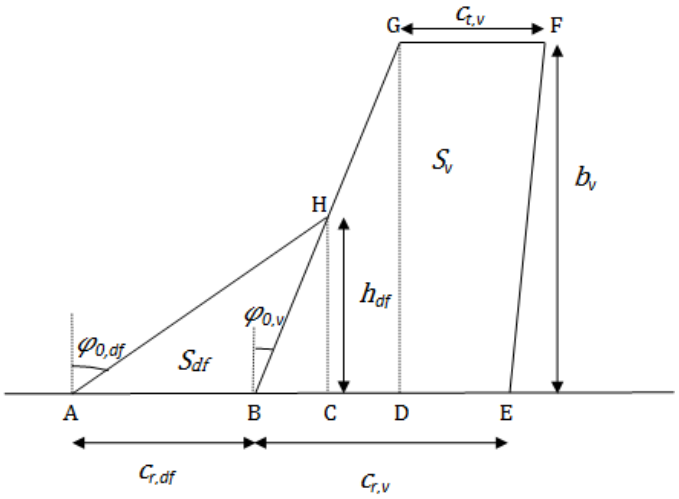

Figure 4.1 Dorsal fin attached to a conventional tail (a)

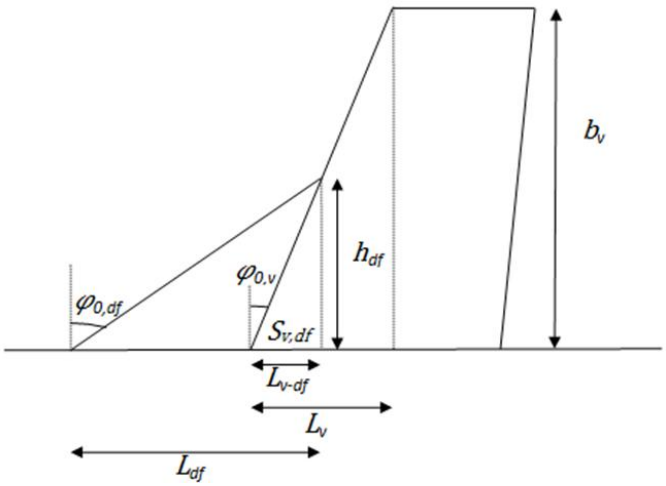

Figure 4.2 Dorsal Fin attached to a conventional tail (b)

24 commercial jet aircraft with a dorsal fin were selected for investigation. All the aircraft are transport category aircraft. The commercial jet aircraft and the reference for the data (3-views) used for evaluation of each of the aircraft are:

- Boeing 737-300 (**B737 2011**)
- Boeing 737-400 (**B737 2011**)
- Boeing 737-500 (**B737 2011**)
- Boeing 737-600 (**B737 2011**)
- Boeing 737-700 (**B737 2011**)
- Boeing 737-800 (**B737 2011**)
- Boeing 737-900 (**B737 2011**)
- Embraer 135 (**ERJ135 2008**)
- Embraer 170 (**EMB170 2003**)
- Embraer 175 (**EMB175 2012**)
- Embraer 190 (**EMB190 2012**)
- Embraer 195 (**EMB195 2012**)
- Embraer ERJ 140 (**EMB140 2005**)
- Embraer ERJ 145 (**EMB145 2007**)
- Fokker 28 (**Blueprints 2013**)
- Fokker 70 (**Blueprints 2013**)
- Fokker 100 (**Blueprints 2013**)
- Ilyushin Il-62 (**Blueprints 2013**)
- Tupolev Tu-104 (**Blueprints 2013**)
- Tupolev Tu-110 (**Blueprints 2013**)
- Tupolev Tu-124 (**Blueprints 2013**)
- Tupolev Tu-134 (**Blueprints 2013**)
- Vickers VC 10 (**Blueprints 2013**)
- Vickers Super VC 10 (**Blueprints 2013**)

22 propeller transport aircraft with a dorsal fin were selected for investigation. These commercial propeller aircraft are:

- Aerospatiale N 262 (**Blueprints 2013**)
- Antonov An- 140 (**Blueprints 2013**)
- ATR 42 (**Blueprints 2013**)
- ATR 72 (**Blueprints 2013**)
- Beriev 32k (**Blueprints 2013**)
- Bombardier Dash 8 Q- 400 (**Blueprints 2013**)
- Bombardier Dash 8 Q- 300 (**Blueprints 2013**)
- British Aerospace Avro 748 (**Blueprints 2013**)
- British Aerospace Jetstream 41 (**Blueprints 2013**)

- De Havilland Canada Dash 7 (**Blueprints 2013**)
- Embraer 110 (**Blueprints 2013**)
- Embraer 120 (**Blueprints 2013**)
- Fairchild Swearingen Metroliner iii/ Fairchild Aerospace Metro iii (**Blueprints 2013**)
- Fokker F- 27 (**Blueprints 2013**)
- Fokker F-27- 500 Friendship (**Blueprints 2013**)
- Grumman G 159 (**Blueprints 2013**)
- Ilyushin Il- 18 (**Blueprints 2013**)
- Ilyushin Il- 114 (**Blueprints 2013**)
- NAMC YS- 11 (**Jane's 2003**)
- Saab 340 (**Blueprints 2013**)
- Saab 2000 (**Blueprints 2013**)
- Vickers Vanguard (**Blueprints 2013**)

In order to investigate the dorsal fin geometry, these parameters were measured from the side view of the aircraft (3-views) listed under commercial jet aircraft and commercial propeller aircraft above:

- h_{df}
- $c_{r,v}$
- $c_{r,df}$
- $c_{t,v}$
- b_v
- L_v
- L_{df}
- $L_{v\text{-}df}$

Based on these parameters other parameters could be calculated:

- S_v
- S_{df}
- S_{df+}
- $\varphi_{o,v}$
- $\varphi_{o,df}$
- $\Delta\varphi$

S_{df+} is the combined area of dorsal fin, S_{df} and the portion of vertical tail area, $S_{v\text{-}df}$.

$$S_{df+} = S_{df} + S_{v-df} \tag{4.1}$$

$\Delta\varphi$ represents the positive difference between leading edge dorsal fin sweep angle, $\varphi_{o,df}$ and leading edge vertical tail sweep angle, $\varphi_{o,v}$.

$$\Delta\varphi = \varphi_{o,df} - \varphi_{o,v} \tag{4.2}$$

Other parameters obtained from the geometric relations are:

$$\varphi_{o,df} = 90° - \arctan\frac{h_{df}}{L_{df}} \tag{4.3}$$

$$\varphi_{o,v} = 90° - \arctan\frac{b_v}{L_v} \tag{4.4}$$

$$S_{v-df} = \frac{1}{2} L_{v-df}\, h_{df} \tag{4.5}$$

$$S_{df} = \left(\frac{1}{2} h_{df}\, L_{df}\right) - S_{v-df} \tag{4.6}$$

$$S_v = \frac{1}{2}\left(c_{t,v} + c_{r,v}\right) b_v \tag{4.7}$$

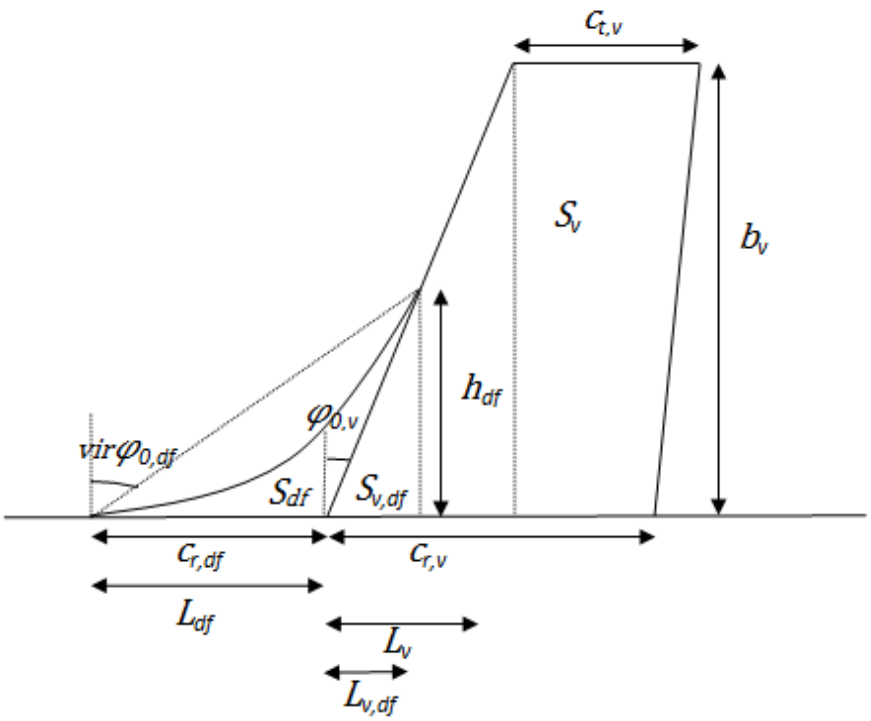

Figure 4.3 Round edge dorsal fin with a conventional tail

Similarly, all the parameters mentioned above were also measured and calculated for round edge dorsal fin aircraft also. It should be noted that round edge dorsal fin do not have a constant sweep angle of the leading edge like dorsal fins as it can be seen from

Figure **4.3**. Therefore, a virtual straight line is drawn from the top of h_{df} to the end of $c_{r,df}$ producing a virtual leading edge dorsal fin sweep angle, $\varphi_{df,vir}$. 3-views were used to measure the parameters. Aircraft investigated for round edge dorsal fin are listed below.

For round edge dorsal fin sizing method 44 commercial jet aircraft were selected. These aircraft are:

- Airbus 300-600 (**A300-600 2002**)
- Airbus 300F4-600 (**A300-F4 2002**)
- Airbus 318 (**A318 2005**)
- Airbus 319 (**A319 2005**)
- Airbus 320-200 (**A320 2005**)
- Airbus 321 (**A321 2005**)
- Airbus 330-200 (**A330 2005**)
- Airbus 330-300 (**A330 2005**)
- Airbus 340-200 (**A340-200/300 2005**)
- Airbus 340-300 (**A340-200/300 2005**)
- Airbus 340-500 (**A340-500/600 2005**)
- Airbus 340-600 (**A340-500/600 2005**)
- Airbus 350-900 (**A350-900 2005**)
- Airbus 380 (**A380 2005**)
- Boeing 707-120B (**B707 2011**)
- Boeing 707-320 (**B707 2011**)
- Boeing 707-320B (**B707 2011**)
- Boeing 717-200 (**B717 2011**)
- Boeing 720, 720B (**B720 2011**)
- Boeing 747-8F (**B747-8 2012**)
- Boeing 747-8 (**B747-8 2012**)
- Boeing 757-200 (**B757 2011**)
- Boeing 757-300 (**B757 2011**)
- Boeing 767-200 (**B767 2011**)
- Boeing 767-300 (**B767 2011**)
- Boeing 767-300F (**B767 2011**)
- Boeing 767-400ER (**B767 2011**)
- Boeing 777-200 (**B777 2011**)
- Boeing 777-300 (**B777 2011**)
- Boeing 777F (**B777 2011**)
- Boeing 787-8 (**B787 2011**)
- Bombardier Aerospace CS 100 (**Blueprints 2013**)
- Bombardier Aerospace CS 300 (**Blueprints 2013**)
- Comac ARJ21 Xiangfeng (**Blueprints 2013**)

- Convair CV-880 (**Blueprints 2013**)
- Dassault Mercure 3v (**Blueprints 2013**)
- Emivest SJ30 (**Blueprints 2013**)
- Ilyushin Il-86 (**Blueprints 2013**)
- Ilyushin Il-76 (**Blueprints 2013**)
- McDonnell Douglas MD-80 (**Blueprints 2013**)
- McDonnell Douglas MD-90 (**Blueprints 2013**)
- McDonnell Douglas DC-9 (**Blueprints 2013**)
- Mitsubishi Regional Jet 70 (**Jane's 2003**)
- Mitsubishi Regional Jet 90 (**Jane's 2003**)

4.2 Systematic Approach of Dorsal Fin Sizing Methods

4.2.1 Overview of the Systematic Approach

To size a dorsal fin it is necessary to know the values of parameters that define the geometry of a dorsal fin. $c_{r,df}$, h_{df}, $\varphi_{o,df}$ and S_{df} are the basic parameters that defines a dorsal fin (Figure 4.4).

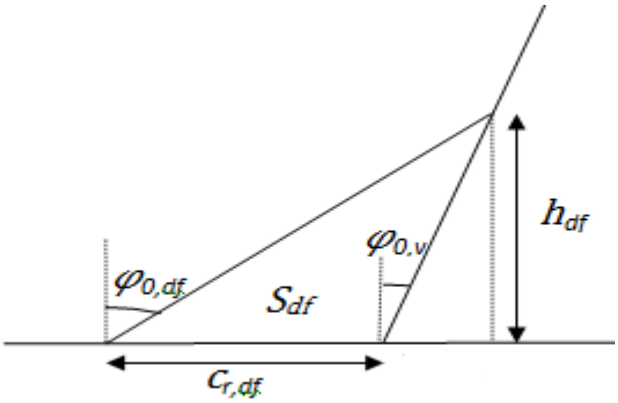

Figure 4.4 Basic parameters of an aircraft dorsal fin

Firstly, our statistical approach measures all the parameters of the dorsal fin and vertical tail from 3-views (parameters mentioned in Chapter 4.1). Since the dorsal fin is a part of the vertical tail, it is conceived that there will be a set of correlations between the dorsal fin parameters and the vertical tail parameters of an aircraft. Analysis of statistical data reveals useful correlations between vertical tail parameters and dorsal fin parameters. Such rational relationships are used to synthesize dorsal fin sizing methods. Methods developed from statistical analysis finally could be used to size an aircraft dorsal fin, provided vertical tail parameters for that aircraft are known. Sizing methods decide the basic parameters of the dorsal fin. Vertical tail parameters are considered as the known parameters since these parameters are fixed

during the design phase. Vertical tail parameters are: b_v, $c_{r,v}$, $c_{t,v}$, S_v and $\varphi_{o,v}$ (see Figure 4.1). For existing aircraft, vertical tail parameters are usually mentioned as part of aircraft specifications or aircraft dimensions, when searched on the Internet. Vertical tail parameters can also be determined as presented in Chapter 3.

For this report, mentioned vertical tail parameters are also measured from 3-views to maintain consistency throughout. All the measurements from 3-views are converted to scale. Measured vertical tail parameters may differ slightly from the ones given in airport planning manuals or mentioned on the Internet. Measurements from 3-views for this report considered the exposed area and the exposed lengths of the vertical tail. It is not explicitly mentioned in the airport planning manual or in the Internet whether the given parameter values are calculated from the exposed area or from the area which includes the portion within the fuselage.

To investigate further, variations in dorsal fin parameters are introduced. Variations of dorsal fin parameters are S_{df+} for S_{df} (Equation 4.1), $\Delta\varphi$ for $\varphi_{o,df}$ (Equation 4.2), L_{df} for $c_{r,df}$ (Figure 4.2). Such parameters are analyzed to determine new possibilities and relationships with vertical tail parameters.

4.2.2 Statistics on Dorsal Fin Parameters

Possible relationships between the dorsal fin and its corresponding vertical tail parameters:

$$S_{df} = f(S_V) \tag{4.8}$$

$$S_{df+} = f(S_V) \tag{4.9}$$

$$\varphi_{o,df} = f(\varphi_{o,v}) \tag{4.10}$$

$$\Delta\varphi = f(\varphi_{0,v}) \tag{4.11}$$

$$c_{r,df} = f(c_{r,v}) \tag{4.12}$$

$$L_{df} = f(c_{r,df}) \tag{4.13}$$

$$h_{df} = f(b_v) \tag{4.14}$$

Figures 4.5 to 4.11 show the plots for the considered relationships. Plots are generated from the data collected for jet and propeller aircraft listed in Chapter 4.1. Equations and regression values for each plot are presented in Table 4.1 and Table 4.2. Trendlines of all the plots pass through the origin except for that of $\Delta\varphi$ vs. $\varphi_{o,df}$. For e.g. if $y = mx + c$ is followed for Figure 4.5, the constant c indicates a residual value of S_{df} even when S_v equals zero. This implies a presence of the dorsal fin even in the absence of a vertical tail, which is not practically feasible. Same applies for Figure 4.6, 4.9 and 4.10.

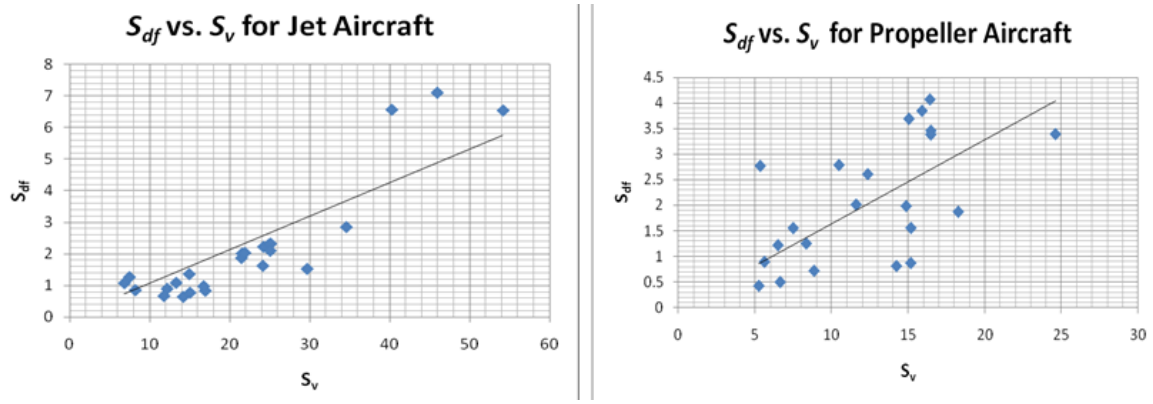

Figure 4.5 Plots of S_{df} vs. S_v for jet and propeller aircraft

As it could be seen from Figure 4.5, in case of jet aircraft S_{df} shows a good linear correlation with S_v. There are however 3 aircraft at the top of the plot which deviate from expected behavior. In case of propeller aircraft the scatter is more dispersed than jet aircraft but linear relationship still exists between the parameters.

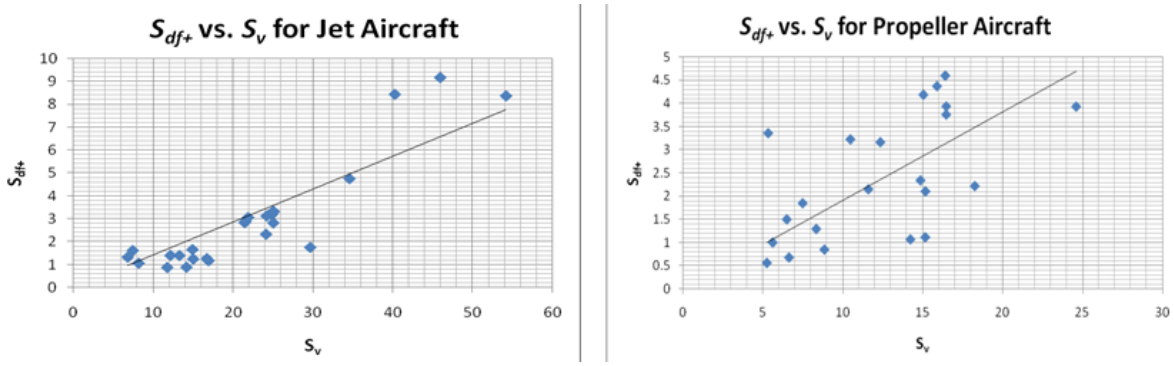

Figure 4.6 Plots for S_{df+} vs. S_v for jet and propeller aircraft

S_{df+} vs. S_v exhibits similar trends like Figure 4.5. Since S_{df+} (4.1) includes a small sectional area from the vertical tail with S_{df}, it is almost similar to S_{df}.

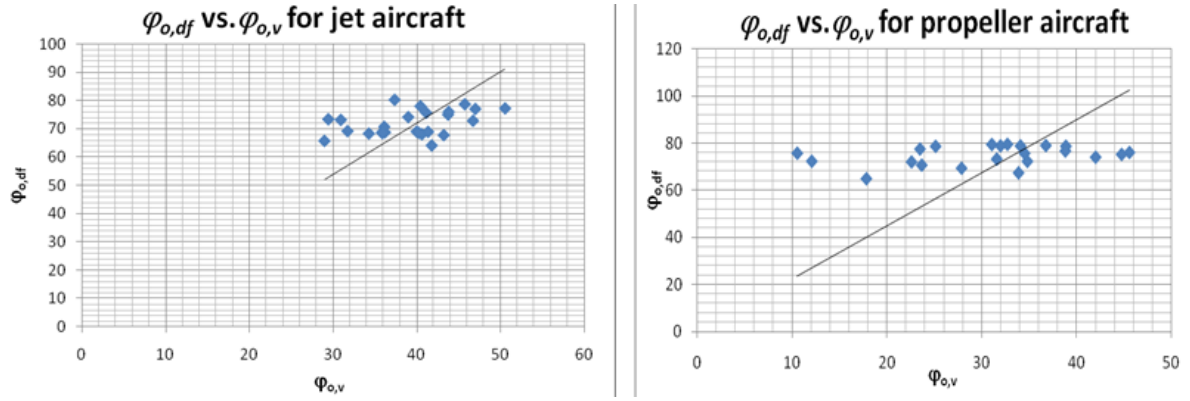

Figure 4.7 Plots of $\varphi_{o,df}$ vs. $\varphi_{o,v}$ for jet and propeller aircraft

For both jet and propeller aircraft $\varphi_{o,df}$ is almost constant with increase of $\varphi_{o,v}$. There exists no linear relationship between $\varphi_{o,df}$ and $\varphi_{o,v}$ as it could be observed from the scatter plots and the trendlines. All the points in the scatter plots lie within a range of $\varphi_{o,df}$ and the points are not widely dispersed. Average value for $\varphi_{o,df}$ are:

- Jet, average $\varphi_{o,df}$: 72°
- Prop, average $\varphi_{o,df}$: 74°

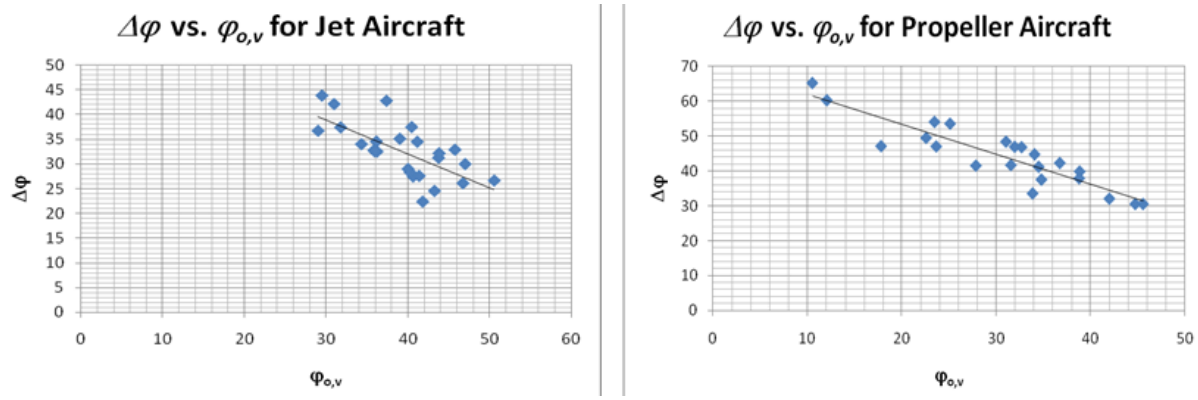

Figure 4.8 Plots of $\Delta\varphi$ vs. $\varphi_{o,v}$ for jet and propeller aircraft

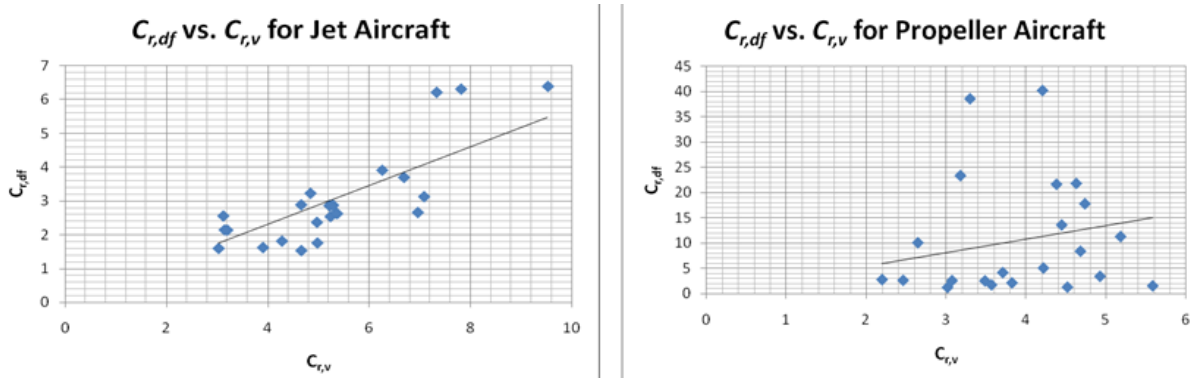

Figure 4.9 Plots of $c_{r,df}$ vs.$c_{r,v}$ for jet and propeller aircraft

In case of both jet and propeller aircraft (see Figure 4.8), $\Delta\varphi$ decreases gradually as $\varphi_{o,v}$ increases. The scatters in both the graphs are close to the trendlines. This indicates there is a good relationship between the two parameters and $\varphi_{o,df}$ depends on $\varphi_{o,v}$ (4.2). It is also evident

from the explanation given in Chapter 2.3, where it is mentioned how leading edge sweep angle of the vertical tail affects the leading edge sweep angle of a dorsal fin.

For jet aircraft (see Figure 4.9), $c_{r,df}$ increases with the increase of $c_{r,v}$. However, three aircraft at the top of the plot display different behavior than expected. These three aircraft are not the same aircraft as pointed out for jet aircraft in Figure 4.6. In propeller aircraft (Figure 4.8) even though the scatter plots indicate no relationship between $c_{r,df}$ and $c_{r,v}$ ($R^2 = 0$), the relation is considered further. It remains to be seen later (Chapter 4.1.3), how well the sizing method as a whole will do based on this relation in comparison with sizing methods based on other parameters The sizing methods developed are applicable to both jet and propeller aircraft. So, instead of taking a simple average of the $c_{r,df}$ values the trendline is still considered in case of propeller aircraft to maintain uniformity within the method for jet aircraft.

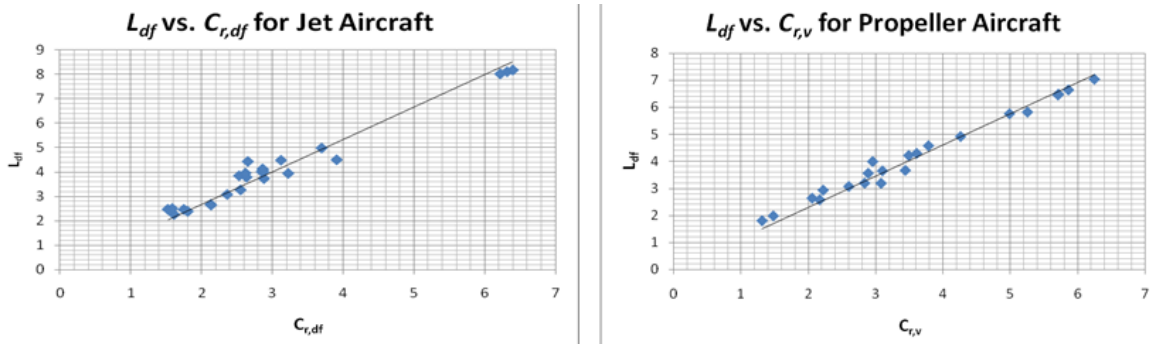

Figure 4.10 Plots of L_{df} vs. $c_{r,df}$ for jet and propeller aircraft

L_{df} vs. $c_{r,df}$ (see Figure 4.10) show very good correlation between the parameters for both jet and propeller aircraft. Most of the scatter points in case of both jet and propeller aircraft passes through the trendline.

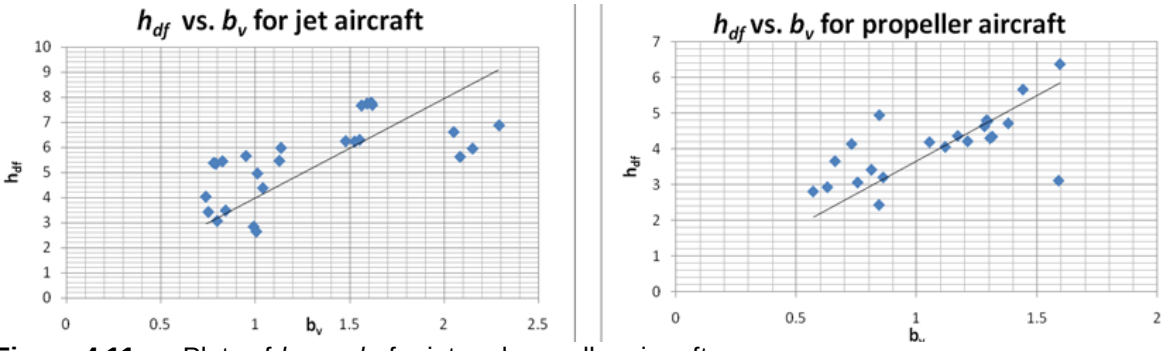

Figure 4.11 Plots of h_{df} vs. b_v for jet and propeller aircraft

Trendlines for both jet and propeller aircraft indicates there is a linear relationship between h_{df} and b_v. But the scatter plots indicate points are dispersed and not close to the trendlines. This exhibit poor correlation between h_{df} and b_v for both jet and propeller aircraft.

Tables 4.1 and 4.2 displays the respective equations and its regression value for the plots of jet and propeller aircraft from Figures 4.5 to 4.11.

Table 4.1 Equations and regression values of the plots for jet aircraft (Figures 4.5 to 4.11)

Relationship	Figure no.	Equation for jet aircraft	R^2 value for jet aircraft
$S_{df} = f(S_v)$	4.5	$S_{df} = 0.106 S_v$	0.751
$S_{df+} = f(S_v)$	4.6	$S_{df+} = 0.143 S_v$	0.782
$\varphi_{o,df} = f(\varphi_{o,v})$	4.7	$\varphi_{o,df} = 1.799 \varphi_{o,v}$	-3.48
$\Delta\varphi = f(\varphi_{o,v})$	4.8	$\Delta\varphi = 59.42° - 0.684 \varphi_{o,v}$	0.475
$c_{r,df} = f(c_{r,v})$	4.9	$c_{r,df} = 0.575 c_{r,v}$	0.644
$L_{df} = f(c_{r,df})$	4.10	$L_{df} = 1.330 c_{r,df}$	0.956
$h_{df} = f(b_v)$	4.11	$h_{df} = 3.972 b_v$	0.046

Table 4.2 Equations and regression values of the plots for propeller aircraft (Figures 4.5 to 4.11)

Relationship	Figure no.	Equation for propeller aircraft	R^2 value for propeller aircraft
$S_{df} = f(S_v)$	4.5	$S_{df} = 0.164 S_v$	0.332
$S_{df+} = f(S_v)$	4.6	$S_{df+} = 0.190 S_v$	0.333
$\varphi_{o,df} = f(\varphi_{o,v})$	4.7	$\varphi_{o,df} = 2.244 \varphi_{o,v}$	-25.3
$\Delta\varphi = f(\varphi_{o,v})$	4.8	$\Delta\varphi = 70.49° - 0.859 \varphi_{o,v}$	0.812
$c_{r,df} = f(c_{r,v})$	4.9	$c_{r,df} = 2.699 c_{r,v}$	0.000
$L_{df} = f(c_{r,df})$	4.10	$L_{df} = 1.156 c_{r,df}$	0.975
$h_{df} = f(b_v)$	4.11	$h_{df} = 3.664 b_v$	0.111

Evaluation of the listed relationships from Tables 4.1 and 4.2 concludes:

- $\varphi_{o,df}$ versus $\varphi_{o,v}$ results in a negative regression value for both jet and propeller aircraft. Regression value confirms there is no linear relationship between the parameters. Thus, this relationship, $\varphi_{o,df} = f(\varphi_{o,v})$, is not considered for sizing methods.
- However, $\Delta\varphi$ show linear relationship with $\varphi_{o,v}$ when plotted. Good regression value is noted in case of propeller aircraft (Table 4.2). Regression value for jet aircraft also indicates linear relationship between the parameters up to an extent.
- h_{df} against vertical tail height, b_v, for both jet and propeller aircraft exhibits the regression value of almost 0. Therefore it is considered that h_{df} is independent of the relevant vertical tail parameters, b_v.

Summing up, the relationships considered for analysis of dorsal fins are:

- $S_{df} = f(S_v)$
- $S_{df+} = f(S_v)$
- $\Delta\varphi = f(\varphi_{o,v})$
- $c_{r,df} = f(c_{r,v})$
- $L_{df} = f(c_{r,df})$

4.2.3 Synthesis of Dorsal Fin Sizing Methods

This chapter explains how the sizing methods have been derived from considered relationships in Chapter 4.2.2.

In Chapter 4.2.2 it is explained why statistics of h_{df} have not been considered. Since h_{df} can't be obtained from the statistics, it is considered to be obtained from the methods developed to design the dorsal fin. Methods developed opt to find the value of basic parameters of dorsal fin using rational combinations of relationships and its respective equations obtained from the plots (Tables 4.1 and 4.2). It is necessary to consider at least 2 relationships and its respective equations from statistics to start calculating the basic parameters of the dorsal fin like h_{df} (line segment, CH from Figure 4.13 or 4.14). Points ABCH (Figure 4.13 or 4.14) outlines the dorsal fin.

Combinations are checked as shown in
Figure **4.12**. The parameters are connected in triangles. Method numbers on the triangle sides, connecting the parameters, indicate the combination considered for that particular method. For e.g. Method 1 connects 2 relationships indicating these 2 relationships and their respective equations from statistics have been used in Method 1 to size a dorsal fin. This way all the possible combinations based on selected parameters are checked.

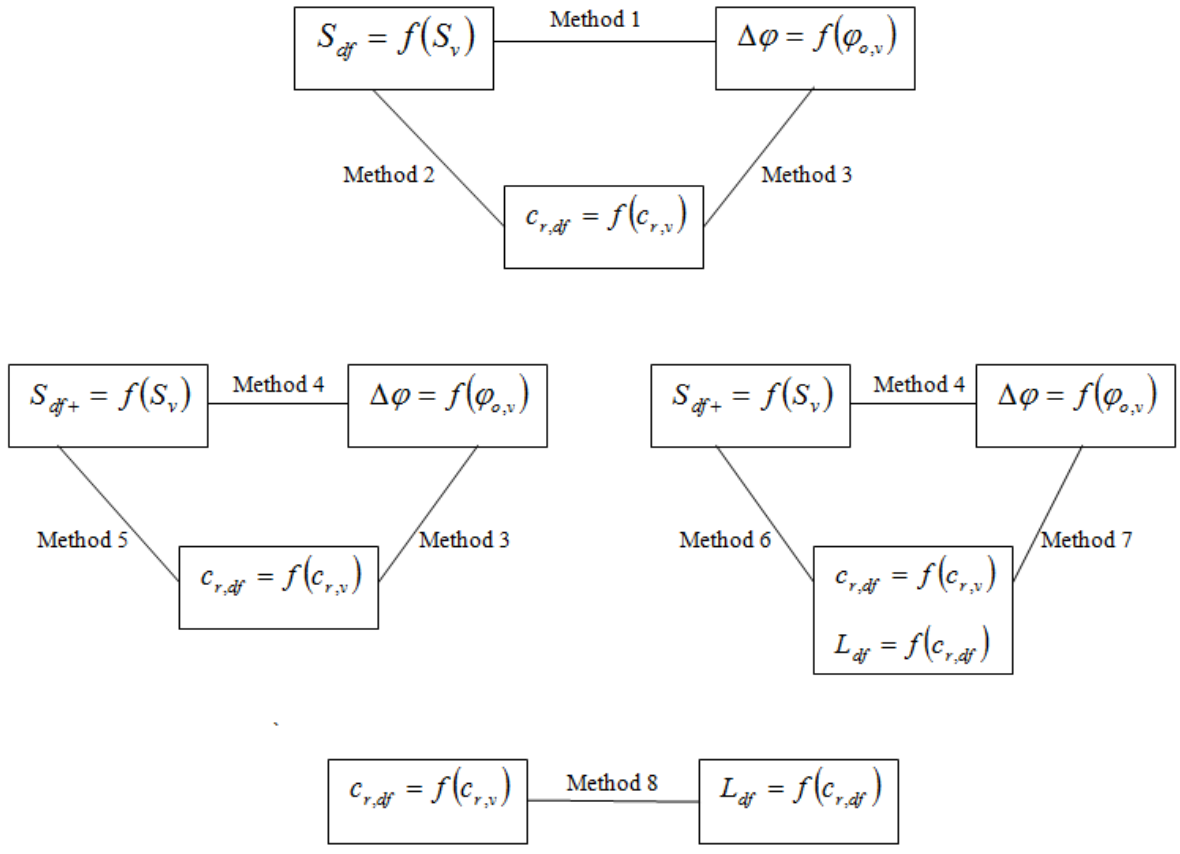

Figure 4.12 All possible combinations of relationships and the respective method associated.

Methods 1 to 8 show the derivation of sizing methods. For Method 1 to 8 refer to Figures 4.13 and 4.14.

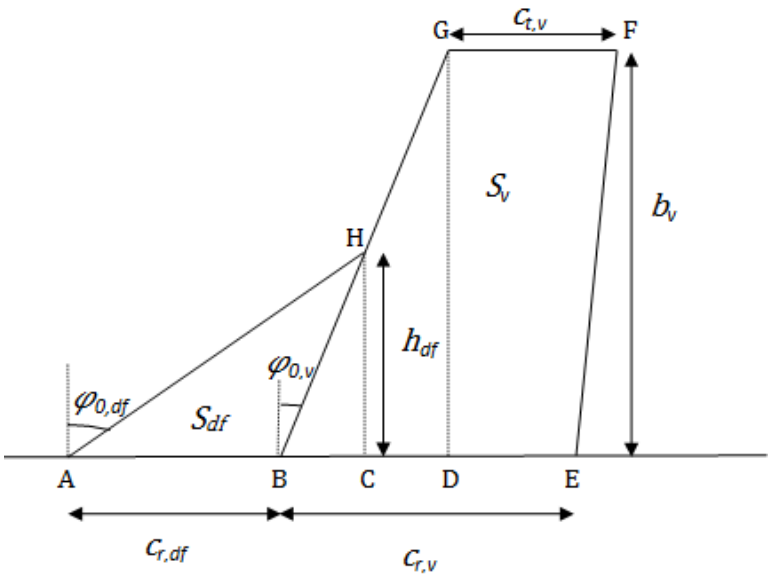

Figure 4.13 The vertical tail with a dorsal fin (a)

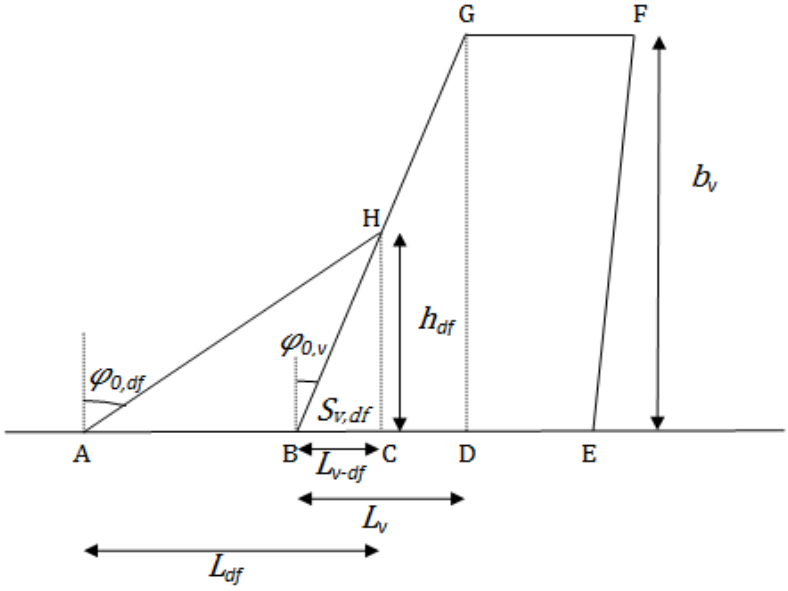

Figure 4.14 The vertical tail with a dorsal fin (b)

Method 1

Given $S_{df} = f(S_v)$ and $\Delta\varphi = f(\varphi_{o,v})$

Idea of the method

With h_{df} calculated from (4.25) or (4.29) for jet or propeller, respectively, points C and H on the fin can be found (Figure 4.13 or 4.14). In addition using $\varphi_{o,df}$ from (4.23) or (4.27) the

leading edge of the dorsal fin can be draw from point H down to the fuselage and point A is located. Points A and C are connected to form the base of the dorsal fin. Thus, the dorsal fin for an aircraft (jet and propeller) can be sized by the method proposed.

From ΔBHC (Figure 4.14),

$$\tan\varphi_{o,v} = \frac{L_{v-df}}{h_{df}}$$

$$L_{v-df} = h_{df}\tan\varphi_{o,v} \tag{4.15}$$

From the area of the triangle,

$$S_{v-df} = \frac{1}{2} L_{v-df}\, h_{df} \tag{4.16}$$

Substituting the value of $L_{v\text{-}df}$ from (4.15) into (4.16) we get,

$$S_{v-df} = \frac{1}{2} h_{df}{}^{2} \tan\varphi_{o,v} \tag{4.17}$$

From ΔAHC (Figure 4.14),

$$\tan\varphi_{o,df} = \frac{L_{df}}{h_{df}}$$

$$L_{df} = h_{df}\tan\varphi_{o,df} \tag{4.18}$$

From the area of the triangle,

$$S_{df+} = \frac{1}{2} L_{df}\, h_{df}$$

Substituting (4.17) into (4.18) we get,

$$S_{df+} = \frac{1}{2} h_{df}{}^{2} \tan\varphi_{o,df} \tag{4.19}$$

Equation 4.1 repeated

$$S_{df+} = S_{df} + S_{v-df} \tag{4.20}$$

Substituting (4.17) and (4.19) into (4.20) we get,

$$\frac{1}{2} h_{df}{}^{2} \tan\varphi_{o,df} = S_{df} + \frac{1}{2} h_{df}{}^{2} \tan\varphi_{o,df}$$

$$S_{df} = \frac{1}{2} h_{df}^{\ 2} \tan\varphi_{o,df} - \frac{1}{2} h_{df}^{\ 2} \tan\varphi_{o,v}$$

$$S_{df} = \frac{1}{2} h_{df}^{\ 2} \left(\tan\varphi_{o,df} - \tan\varphi_{o,v}\right)$$

$$h_{df}^{\ 2} = \frac{2S_{df}}{\tan\varphi_{o,df} - \tan\varphi_{o,v}}$$

$$h_{df} = \sqrt{\frac{2S_{df}}{\tan\varphi_{o,df} - \tan\varphi_{o,v}}} \tag{4.21}$$

For jet aircraft

From Table 4.1,

$$\Delta\varphi = 59.42° - 0.684\varphi_{o,v} \tag{4.22}$$

From Equation 4.2,

$$\Delta\varphi = \varphi_{o,df} - \varphi_{o,v}$$

Substituting (4.21) into (4.2) we get,

$$59.42° - 0.684\varphi_{o,v} = \varphi_{o,df} - \varphi_{o,v}$$

$$\varphi_{o,df} = 59.42° + 0.316\varphi_{o,v} \tag{4.23}$$

From Table 4.1,

$$S_{df} = 0.106 S_v \tag{4.24}$$

Substituting (4.23) and (4.24) into (4.21) gives,

$$h_{df} = \sqrt{\frac{2 \cdot 0.106 S_v}{\tan\left(59.42° + 0.316\varphi_{o,v}\right) - \tan\varphi_{o,v}}} \tag{4.25}$$

For propeller aircraft

From Table 4.2,

$$\Delta\varphi = 70.49° - 0.859\varphi_{o,v} \tag{4.26}$$

Substituting (4.26) into (4.2) we get,

$$70.49° - 0.859\varphi_{o,v} = \varphi_{o,df} - \varphi_{o,v}$$

$$\varphi_{o,df} = 70.49° + 0.141\varphi_{o,v} \quad (4.27)$$

From Table 4.2,

$$S_{df} = 0.164\, S_v \quad (4.28)$$

Substituting (4.27) and (4.28) into (4.21) gives,

$$h_{df} = \sqrt{\frac{2 \cdot 0.164 S_v}{\tan\left(70.49° + 0.141\varphi_{o,v}\right) - \tan\varphi_{o,v}}} \quad (4.29)$$

Method 2

Given $c_{r,df} = f\left(c_{r,v}\right)$ and $S_{df} = f\left(S_v\right)$

Idea of the method

With h_{df} calculated from (4.32) or (4.34) for jet or propeller, respectively, points C and H on the fin can be found (Figure 4.13 or 4.14). The length of the dorsal fin, $c_{r,df}$, calculated from (4.31) or (4.33) is drawn from point B and point A can be located. Therefore, points A and H are joined producing the leading edge of the dorsal fin. Thus, a dorsal fin for jet or propeller aircraft can be sized using Method 2 as proposed.

From the area of the triangle,

$$S_{df} = \frac{1}{2} c_{r,df}\, h_{df}$$

$$h_{df} = \frac{2 \cdot S_{df}}{c_{r,df}} \quad (4.30)$$

For jet aircraft

From Table 4.1,

$$S_{df} = 0.106\, S_v \quad (4.24)$$

$$c_{r,df} = 0.575 c_{r,v} \tag{4.31}$$

Substituting (4.24) and (4.31) into (4.30) we get,

$$h_{df} = \frac{2 \cdot 0.106 S_v}{0.575 c_{r,v}} \tag{4.32}$$

For propeller aircraft

From Table 4.2

$$S_{df} = 0.164 S_v \tag{4.28}$$

$$c_{r,df} = 2.699 c_{r,v} \tag{4.33}$$

Substituting (4.28) and (4.33) into (4.30) we get,

$$h_{df} = \frac{2 \cdot 0.164 S_v}{2.699 c_{r,v}} \tag{4.34}$$

Method 3

Given $\Delta\varphi = f(\varphi_{o,v})$ and $c_{r,df} = f(c_{r,v})$

Idea of the method

With h_{df} calculated from (4.39) or (4.40) for jet or propeller, respectively, points C and H can be found (Figure 4.13 or 4.14). The length of the dorsal fin $c_{r,df}$ from (4.31) or (4.33) can be drawn from point B and meets the leading edge of the dorsal fin at point A. Now the leading edge sweep of the dorsal fin can be drawn from A to H. The resulting angel $\varphi_{o,df}$ can be measured and can be compared with the calculated $\varphi_{o,df}$ from (4.23) and (4.27). Thus, using Method 3, the dorsal fin for a jet or propeller aircraft can be designed including even one check.

Equation 4.15 repeated,

$$L_{v-df} = \tan\varphi_{o,v} \, h_{df}$$

From Figure 4.13 and 4.14,

$$L_{df} = c_{r,df} + L_{v-df} \tag{4.35}$$

Substituting (4.15) into (4.35) we get,

$$L_{df} = c_{r,df} + \tan\varphi_{o,v}\, h_{df} \tag{4.36}$$

From ΔAHC,

$$\tan\varphi_{o,df} = \frac{L_{df}}{h_{df}} \tag{4.37}$$

Substituting (4.36) into (4.37) we get,

$$\tan\varphi_{o,df} = \frac{c_{r,df} + \tan\varphi_{o,v}\, h_{df}}{h_{df}}$$

$$\tan\varphi_{o,df}\, h_{df} = c_{r,df} + \tan\varphi_{o,v}\, h_{df}$$

$$c_{r,df} = \tan\varphi_{o,df}\, h_{df} - \tan\varphi_{o,v}\, h_{df}$$

$$c_{r,df} = h_{df}\left(\tan\varphi_{o,df} - \tan\varphi_{o,v}\right)$$

$$h_{df} = \frac{c_{r,df}}{\tan\varphi_{o,df} - \tan\varphi_{o,v}} \tag{4.38}$$

<u>For jet aircraft</u>

Equations 4.23 and 4.31 are repeated,

$$\varphi_{o,df} = 59.42° + 0.316\varphi_{o,v} \tag{4.23}$$

$$c_{r,df} = 0.575\, c_{r,v} \tag{4.31}$$

Substituting (4.23) and (4.31) into (4.38) we get,

$$h_{df} = \frac{0.575\, c_{r,v}}{\tan\left(59.42° + 0.361\varphi_{o,v}\right) - \tan\varphi_{o,v}} \tag{4.39}$$

For propeller aircraft

Equations 4.27 and 4.33 is repeated,

$$\varphi_{o,df} = 70.49° + 0.141\varphi_{o,v} \tag{4.27}$$

$$c_{r,df} = 2.699\, c_{r,v} \tag{4.33}$$

Substituting (4.33) and (4.27) into (4.38) we get,

$$h_{df} = \frac{2.699 c_{r,v}}{\tan\left(70.49° + 0.141\varphi_{o,v}\right) - \tan\varphi_{o,v}} \tag{4.40}$$

Method 4

Given $\Delta\varphi = f\left(\varphi_{o,v}\right)$ and $S_{df+} = f\left(S_v\right)$

Idea of the method

With h_{df} calculated from (4.44) or (4.46) for jet or propeller, respectively, points C and H can be located (Figure 4.13 or 4.14). L_{df} for jet aircraft can be calculated from (4.18) using parameters calculated from (4.44) and (4.23) and point A can be found, drawn from point C. Similarly L_{df} for propeller aircraft can be calculated from (4.18) using parameters calculated from (4.46) and (4.27) locating point C. Now the leading edge sweep of the dorsal fin can be drawn from A to H. The resulting angel $\varphi_{o,df}$ for jet or propeller can be measured and can be compared with the calculated $\varphi_{o,df}$ from (4.23) and (4.27). Thus, using Method 4, the dorsal fin for a jet or propeller aircraft can be designed including even one check.

From the area of the triangle,

$$S_{df+} = \frac{1}{2} L_{df}\, h_{df} \tag{4.41}$$

Equation 4.18 repeated

$$L_{df} = h_{df} \tan\varphi_{o,df}$$

Substituting (4.18) into (4.41) we get,

$$S_{df+} = \frac{1}{2} {h_{df}}^2 \tan\varphi_{o,df}$$

$$h_{df}{}^{2} = \frac{2\,S_{df+}}{\tan\varphi_{o,df}}$$

$$h_{df} = \sqrt{\frac{2\,S_{df+}}{\tan\varphi_{o,df}}} \tag{4.42}$$

For jet aircraft

Equation 4.23 is repeated,

$$\varphi_{o,df} = 59.42° + 0.316\varphi_{o,v} \tag{4.23}$$

From Table 4.1

$$S_{df+} = 0.143\,S_v \tag{4.43}$$

Substituting (4.23) and (4.43) into (4.42) we get,

$$h_{df} = \sqrt{\frac{2\cdot 0.143 S_v}{\tan\left(59.42° + 0.316\varphi_{o,v}\right)}} \tag{4.44}$$

For propeller aircraft

Equation 4.27 is repeated,

$$\varphi_{o,df} = 70.49° + 0.141\varphi_{o,v} \tag{4.27}$$

From Table 4.2

$$S_{df+} = 0.190\,S_v \tag{4.45}$$

Substituting (4.23) and (4.43) into (4.42) we get,

$$h_{df} = \sqrt{\frac{2\cdot 0.190\,S_v}{\tan\left(70.49° + 0.141\varphi_{o,v}\right)}} \tag{4.46}$$

Method 5

Given $c_{r,df} = f\left(c_{r,v}\right)$ and $S_{df+} = f\left(S_v\right)$

Idea of the method

With h_{df} calculated from (4.49) or (4.50) for jet or propeller aircraft, respectively, points C and H can be found. The length of the dorsal fin, $c_{r,df}$, calculated from (4.31) or (4.33) is drawn from point B and point A can be located. Therefore, points A and H are joined producing the leading edge sweep of the dorsal fin. Thus, using method 5 a dorsal fin for jet or propeller aircraft can be designed.

Equation 4.35 and 4.41 is repeated,

$$L_{df} = c_{r,df} + L_{v-df} \tag{4.35}$$

$$S_{df+} = \frac{1}{2} L_{df}\, h_{df} \tag{4.41}$$

Substituting (4.35) into (4.41) we get,

$$S_{df+} = \frac{1}{2}\left(c_{r,df} + L_{v-df}\right) h_{df} \tag{4.47}$$

Equation 4.15 repeated,

$$L_{v-df} = \tan\varphi_{o,v}\, h_{df}$$

Substituting (4.15) into (4.47) we get,

$$S_{df+} = \frac{1}{2}\left(c_{r,df} + \tan\varphi_{o,v}\, h_{df}\right) h_{df}$$

$$2S_{df+} = c_{r,df} h_{df} + \tan\varphi_{o,v} {h_{df}}^2$$

Rearranging,

$${h_{df}}^2 \tan\varphi_{o,v} + h_{df} c_{r,df} - 2S_{df+} = 0$$

Since this is a quadratic equation, roots of the quadratic equation are:

$$h_{df} = \frac{-c_{r,df} \pm \sqrt{{c_{r,df}}^2 + 4\tan\varphi_{o,v}\, S_{df+}}}{2\tan\varphi_{o,v}}$$

In this case only positive root is considered since negative value for h_{df} does not have any physical meaning.

$$h_{df} = \frac{-c_{r,df} + \sqrt{{c_{r,df}}^2 + 4\tan\varphi_{o,v}\, S_{df+}}}{2\tan\varphi_{o,v}} \tag{4.48}$$

For jet aircraft

Equation 4.31 and 4.43 is repeated,

$$c_{r,df} = 0.575\, c_{r,v} \tag{4.31}$$

$$S_{df+} = 0.143\, S_v \tag{4.43}$$

Substituting (4.31) and (4.43) into (4.48) we get,

$$h_{df} = \frac{-0.575\, c_{r,v} + \sqrt{\left(0.575\, c_{r,v}\right)^2 + 4\left(0.143\, S_v\right)\left(\tan\varphi_{o,v}\right)}}{2\tan\varphi_{o,v}} \tag{4.49}$$

For propeller aircraft

Equation 4.33 and 4.45 is repeated,

$$c_{r,df} = 2.699\, c_{r,v} \tag{4.33}$$

$$S_{df+} = 0.190\, S_v \tag{4.45}$$

Substituting (4.33) and (4.45) into (4.48) we get,

$$h_{df} = \frac{-2.699\, c_{r,v} + \sqrt{\left(2.699\, c_{r,v}\right)^2 + 4\left(0.190\, S_v\right)\left(\tan\varphi_{o,v}\right)}}{2\tan\varphi_{o,v}} \tag{4.50}$$

Method 6

Given $S_{df+} = f\left(S_v\right)$, $c_{r,df} = f\left(c_{r,v}\right)$ and $L_{df} = f\left(c_{r,df}\right)$

Idea of the method

$c_{r,df}$ calculated from (4.31) or (4.33) for jet or propeller, respectively, can be drawn from point B and point A can be located (Figure 4.13 and 4.14). From point A, L_{df} calculated from (4.53)

or (4.56) is drawn and point C is found. Moving perpendicular up, point H is found. Points A and H are connected to form the leading edge sweep of the dorsal fin. h_{df} can be measured and compared with calculated h_{df} (4.54) and (4.57). Thus, using Method 6, the dorsal fin for jet or propeller aircraft can be designed including even one check. The advantage of this method is also that points C and H are not found from fitting h_{df} (with some trial and error) into the fin, but from straight forward considerations.

Equation 4.41 repeated,

$$S_{df+} = \frac{1}{2} L_{df}\, h_{df}$$

$$h_{df} = \frac{2 S_{df+}}{L_{df}} \tag{4.51}$$

For jet aircraft

Equation 4.31 is repeated,

$$c_{r,df} = 0.575 c_{r,v} \tag{4.31}$$

From Table 4.1,

$$L_{df} = 1.330 c_{r,df} \tag{4.52}$$

Substituting (4.31) into (4.52) we get,

$$L_{df} = 0.76475 c_{r,v} \tag{4.53}$$

Equation 4.45 is repeated,

$$S_{df+} = 0.190 S_v \tag{4.45}$$

Substituting (4.45) and (4.52) into (4.51) we get,

$$h_{df} = \frac{2 \cdot 0.190 S_v}{0.76475 c_{r,v}} \tag{4.54}$$

For propeller aircraft

Equation 4.33 is repeated,

$$c_{r,df} = 2.699\, c_{r,v} \tag{4.33}$$

From Table 4.2,

$$L_{df} = 1.156\, c_{r,df} \tag{4.55}$$

Substituting (4.33) into (4.55) we get,

$$L_{df} = 3.120044\, c_{r,v} \tag{4.56}$$

Equation 4.45 is repeated,

$$S_{df+} = 0.190\, S_v \tag{4.45}$$

Substituting (4.45) and (4.55) into (4.51) we get,

$$h_{df} = \frac{2 \cdot 0.190\, S_v}{3.120044\, c_{r,v}} \tag{4.57}$$

Method 7

Given $c_{r,df} = f(c_{r,v})$, $L_{df} = f(c_{r,df})$ and $\Delta\varphi = f(\varphi_{o,v})$

Idea of the method

$c_{r,df}$ calculated from (4.31) or (4.33) for jet or propeller aircraft, respectively, can be drawn from point B and point A can be located (Figure 4.13 and 4.14). From point A, L_{df} calculated from (4.53) or (4.56) is drawn and point C is found. Moving perpendicular up, point H is found. Points A and H are connected to form the leading edge sweep of the dorsal fin. h_{df} can be measured and compared with calculated h_{df} from (4.59) and (4.60). The resulting angle $\varphi_{o,df}$ can be measured and can be compared with the calculated $\varphi_{o,df}$ from (4.23) and (4.27). Thus, using Method 7, the dorsal fin for an aircraft can be designed including even two checks. The advantage of this method is (as with method 6) also that points C and H are not found from fitting h_{df} (with some trial and error) into the fin, but from straight forward considerations.

Equation 4.37 is repeated,

$$\tan\varphi_{o,df} = \frac{L_{df}}{h_{df}}$$

$$h_{df} = \frac{L_{df}}{\tan\varphi_{o,df}} \tag{4.58}$$

For jet aircraft

Equation 4.23, 4.31 and 4.53 is repeated,

$$\varphi_{o,df} = 59.42° + 0.316\varphi_{o,v} \tag{4.23}$$

$$c_{r,df} = 0.575 c_{r,v} \tag{4.31}$$

$$L_{df} = 0.76475 c_{r,v} \tag{4.53}$$

Substituting (4.23) and (4.53) into (4.58) we get,

$$h_{df} = \frac{0.76475 c_{r,v}}{\tan\left(59.42° + 0.361\varphi_{o,v}\right)} \tag{4.59}$$

For propeller aircraft

Equation 4.27, 4.33 and 4.56 is repeated,

$$\varphi_{o,df} = 70.49° + 0.141\varphi_{o,v} \tag{4.27}$$

$$c_{r,df} = 2.699 c_{r,v} \tag{4.33}$$

$$L_{df} = 3.120044 c_{r,v} \tag{4.56}$$

Substituting (4.27) and (4.56) into (4.58) we get,

$$h_{df} = \frac{3.120044 c_{r,v}}{\tan\left(70.49° + 0.141\varphi_{o,v}\right)} \tag{4.60}$$

Method 8

Given $c_{r,df} = f(c_{r,v})$ and $L_{df} = f(c_{r,df})$,

Idea of the method

From method 6 and 7 we learned that knowledge of $c_{r,df} = f(c_{r,v})$ and $L_{df} = f(c_{r,df})$ are already sufficient to draw the dorsal fin. The idea is the same as for Method 6:
$c_{r,df}$ calculated from (4.31) or (4.33) for jet or propeller, respectively, can be drawn from point B and point A can be located (Figure 4.13 and 4.14). From point A, L_{df} calculated from (4.51) or (4.55) is drawn and point C is found. Moving perpendicular up, point H is found. Points A and H are connected to form the leading edge of the dorsal fin. h_{df} can be measured and compared with calculated h_{df} (4.63) and (4.64). Thus, using Method 8, the dorsal fin for an aircraft can be designed including even one check. The advantage of this method is also that points C and H are not found from fitting h_{df} (with some trial and error) into the fin, but from straight forward considerations.

From ΔBHC (Figure 4.13),

$$\tan\varphi_{o,v} = \frac{L_{v-df}}{h_{df}}$$

$$h_{df} = \frac{L_{v-df}}{\tan\varphi_{o,v}} \tag{4.61}$$

From Figure 4.14,

$$L_{v-df} = L_{df} - c_{r,df} \tag{4.62}$$

Substituting (4.62) into (4.61) we get,

$$h_{df} = \frac{L_{df} - c_{r,df}}{\tan\varphi_{o,v}} \tag{4.63}$$

For jet aircraft

Equations 4.31 and 4.53 are repeated,

$$c_{r,df} = 0.575 c_{r,v} \tag{4.31}$$

$$L_{df} = 0.76475 c_{r,v} \tag{4.53}$$

Substituting (4.31) and (4.53) into (4.63) we get,

$$h_{df} = \frac{0.76475 c_{r,v} - 0.575 c_{r,v}}{\tan \varphi_{o,v}} \tag{4.64}$$

For propeller aircraft

Equation 4.33 and 4.56 is repeated,

$$c_{r,df} = 2.699 c_{r,v} \tag{4.33}$$

$$L_{df} = 3.120044 c_{r,v} \tag{4.56}$$

Substituting (4.33) and (4.56) into (4.63) we get,

$$h_{df} = \frac{2.699 c_{r,v} - 3.120044 c_{r,v}}{\tan \varphi_{o,v}} \tag{4.65}$$

4.2.4 Evaluation, Selection and Application of Dorsal Fin Sizing Methods

Pre-Selection of Methods with Averaged Correlation Coefficients
Considering all the possible combinations of parameters, 8 sizing methods for dorsal fin are derived. Out of 8 sizing methods, 2 methods have been shortlisted and selected to size an aircraft dorsal fin for jet or propeller aircraft. The method systematic and process of method selection is explained in this chapter.

Although it is possible to use all the methods to design a dorsal fin for jet and propeller aircraft, all the methods have to be evaluated to find which gives the minimum error.

Table 4.3 lists the regression values of relationships associated with the methods for both jet and propeller aircraft.

Table 4.3 Regression analysis of the methods

	R^2	R^2	R^2	R^2	Rank
Method 1	$S_{df} = f(S_v)$	$\Delta\varphi = f(\varphi_{o,v})$		Average	
Jet	0.751	0.475		0.613	7
Propeller	0.332	0.812		0.572	3
Average of Jet and Propeller				**0.593**	5
Method 2	$S_{df} = f(S_v)$	$c_{r,df} = f(c_{r,v})$		Average	
Jet	0.751	0.575		0.633	5
Propeller	0.332	0.000		0.166	8
Average of Jet and Propeller				**0.415**	8
Method 3	$\Delta\varphi = f(\varphi_{o,v})$	$c_{r,df} = f(c_{r,v})$		Average	
Jet	0.475	0.575		0.525	8
Propeller	0.812	0.000		0.406	6
Average of Jet and Propeller				**0.466**	6
Method 4	$S_{df+} = f(S_v)$	$\Delta\varphi = f(\varphi_{o,v})$		Average	
Jet	0.782	0.475		0.629	6
Propeller	0.333	0.812		0.573	2
Average of Jet and Propeller				**0.601**	4
Method 5	$c_{r,df} = f(c_{r,v})$	$S_{df+} = f(S_v)$		Average	
Jet	0.575	0.782		0.679	3
Propeller	0.000	0.333		0.167	7
Average of Jet and Propeller				**0.423**	7
Method 6	$c_{r,df} = f(c_{r,v})$	$S_{df+} = f(S_v)$	$L_{df} = f(c_{r,df})$	Average	
Jet	0.575	0.782	0.956	0.771	1
Propeller	0.000	0.333	0.975	0.436	5
Average of Jet and Propeller				**0.604**	3
Method 7	$\Delta\varphi = f(\varphi_{o,v})$	$c_{r,df} = f(c_{r,v})$	$L_{df} = f(c_{r,df})$	Average	
Jet	0.475	0.575	0.956	0.669	4
Propeller	0.812	0.000	0.975	0.596	1
Average of Jet and Propeller				**0.632**	1
Method 8	$c_{r,df} = f(c_{r,v})$	$L_{df} = f(c_{r,df})$		Average	
Jet	0.575	0.956		0.766	2
Propeller	0.000	0.975		0.488	4
Average of Jet and Propeller				**0.627**	2

In Table 4.3 regression values in bold face are the average of jet and propeller average regression values for the respective method. This average regression value of jet and propeller for each method (one marked in bold) indicates the accuracy of the method. Higher regression value denotes good correlation between the parameters in consideration. From Table 4.3 Method 7 shows the highest regression value, followed by Method 8, and signifies it to be the best method to be considered. Method 6 has the 3rd highest regression value. As per the outcome of regression values, methods are ranked in Table 4.3. Methods, according to their re-

gression values, are ranked separately for jet, propeller and for the average of jet and propeller.

It can be observed from Table 4.3 that regression value for the relationship $L_{df} = f(c_{r,df})$, in case of both jet and propeller aircraft, are quite high compared to the other regression values. This affects the average regression value of the method greatly. We have to keep in mind that length L_{df} comprises mostly of $c_{r,df}$ (Figures 4.13 and 4.14) and it is almost equal to $c_{r,df}$. Therefore, when L_{df} is plotted against $c_{r,df}$ a high correlation results. It is therefore rational to disregard the regression value of this relationship from method 6, 7 and 8 and analyze the methods.

Table 4.4 Regression analysis of the methods excluding $L_{df} = f(c_{r,df})$

	R^2	R^2	R^2	R^2	Rank
Method 1	$S_{df} = f(S_v)$	$\Delta\varphi = f(\varphi_{o,v})$		Average	
Jet	0.751	0.475		0.613	4
Propeller	0.332	0.812		0.572	2
Average of Jet and Propeller				**0.593**	**2**
Method 2	$S_{df} = f(S_v)$	$c_{r,df} = f(c_{r,v})$		Average	
Jet	0.751	0.575		0.633	2
Propeller	0.332	0.000		0.166	5
Average of Jet and Propeller				**0.451**	**4**
Method 3	$\Delta\varphi = f(\varphi_{o,v})$	$c_{r,df} = f(c_{r,v})$		Average	
Jet	0.475	0.575		0.525	5
Propeller	0.812	0.000		0.406	3
Average of Jet and Propeller				**0.466**	**3**
Method 4	$S_{df+} = f(S_v)$	$\Delta\varphi = f(\varphi_{o,v})$		Average	
Jet	0.782	0.475		0.629	3
Propeller	0.333	0.812		0.573	1
Average of Jet and Propeller				**0.601**	**1**
Method 5	$c_{r,df} = f(c_{r,v})$	$S_{df+} = f(S_v)$		Average	
Jet	0.575	0.782		0.679	1
Propeller	0.000	0.333		0.167	4
Average of Jet and Propeller				**0.423**	**5**
Method 6	$c_{r,df} = f(c_{r,v})$	$S_{df+} = f(S_v)$	$L_{df} = f(c_{r,df})$	Average	
Jet	0.575	0.782		0.679	1
Propeller	0.000	0.333		0.167	4
Average of Jet and Propeller				**0.423**	**5**
Method 7	$\Delta\varphi = f(\varphi_{o,v})$	$c_{r,df} = f(c_{r,v})$	$L_{df} = f(c_{r,df})$	Average	
Jet	0.475	0.575		0.525	5
Propeller	0.812	0.000		0.406	3
Average of Jet and Propeller				**0.466**	**3**

Table 4.4 presents regression value for the method without considering the values for $L_{df} = f(c_{r,df})$. In that case method 8 is omitted since $L_{df} = f(c_{r,df})$is one of the two relationships and just with one relationship analysis cannot be performed. For methods 6 and 7 the favorable value for $L_{df} = f(c_{r,df})$ is omitted.

As seen in Table 4.4, the average regression values and its respective ranks are marked in bold. From the average of jet and propeller it can be noted that Method 4 shows the highest regression value followed by Method 1. This indicates good correlation and that the parameters are dependent on each other. Since, the method is applicable to both jet and propeller aircraft it is therefore important to evaluate the average of regression values of jet and propeller aircraft combined (marked in bold).

Hence, Method 1 and 4 are pre-selected to design the dorsal fin in jet or propeller aircraft. Two methods are considered since S_{df+} (of Method 4) is the variation of S_{df} only. Reader can decide between any of the two methods for use to size the dorsal fin.

Check of Methods on Aircraft Data

With the pre-selection of two methods after evaluation it is required to implement the method with aircraft data so that it can be verified how well the method work out. As outlined in the "Idea of the Method" (Chapter 4.2.3), Method 1 and 4 calculate the height of the dorsal fin h_{df} as the start of the design. Checking the accuracy of the method here, h_{df} calculated from the methods are compared with the h_{df} measured from the 3 views of jet and propeller aircraft listed in Chapter 4.1. Difference between the calculated h_{df} and measured h_{df} (from 3-views) reflects the accuracy of the methods. Table 4.5 and Table 4.6 (from Excel) display result for the difference between h_{df} calculated and h_{df} measured for jet and propeller aircraft. All the values are measured to 2 decimal places. Though it is measured to 2 decimal places, Excel takes into account the complete value (which is more than 2 decimal places) rather than the value with 2 decimal places for calculation. Thus calculation results in a slightly different value than that obtained for a value with 2 decimal places. For e.g, in Table 4.6, the h_{df} calculated and h_{df} theoretical for Q-300 are equal, 1.31m. But the difference calculated is 1%, which is due to the values taken into account after 2 decimal places, even though it is not displayed for Q-300.

Table 4.5 Application of method 1 and 4 on jet aircraft data

		For jet aircraft														
	Method1	S_v	S_{df}	$\varphi_{a,v}$	$\varphi_{a,df}$	*hdf* calculated	*hdf* theoretical	difference	Method 4	S_v	S_{df}	$\varphi_{a,v}$	$\varphi_{a,df}$	*hdf* calculated	*hdf* theoretical	difference
		m	m	m	m	m	m			m	m	m	m	m	m	
B737- 300		21.45	2.27	39.99	72.06	1.42	1.48	4%		21.45	3.07	39.99	72.06	1.41	1.48	5%
B 737- 400		21.53	2.28	40.62	72.26	1.42	1.53	7%		21.53	3.08	40.62	72.26	1.40	1.53	8%
EMB 170		14.16	1.50	36.13	70.84	1.18	0.79	49%		14.16	2.03	36.13	70.84	1.19	0.79	50%
EMB 175		16.92	1.79	41.36	72.49	1.25	0.95	32%		16.92	2.42	41.36	72.49	1.24	0.95	30%
EMB 190		15.00	1.59	43.22	73.08	1.16	1.01	15%		15.00	2.15	43.22	73.08	1.14	1.01	13%
EMB 195		12.15	1.29	29.01	68.59	1.14	1.13	1%		12.15	1.74	29.01	68.59	1.17	1.13	3%
B 737- 500		21.87	2.32	40.25	72.14	1.43	1.55	8%		21.87	3.13	40.25	72.14	1.42	1.55	9%
B 737- 600		24.83	2.63	34.31	70.26	1.58	1.59	1%		24.83	3.55	34.31	70.26	1.60	1.59	0%
B 737- 700		24.20	2.57	36.21	70.86	1.54	1.56	1%		24.20	3.46	36.21	70.86	1.55	1.56	1%
B 737- 800		24.98	2.65	35.85	70.75	1.57	1.61	2%		24.98	3.57	35.85	70.75	1.58	1.61	2%
B 737- 900		25.09	2.66	35.91	70.77	1.58	1.62	3%		25.09	3.59	35.91	70.77	1.58	1.62	2%
VC 10		40.24	4.27	41.13	72.42	1.93	2.08	7%		40.24	5.75	41.13	72.42	1.91	2.08	8%
Super VC 10		45.92	4.87	38.99	71.74	2.09	2.29	9%		45.92	6.57	38.99	71.74	2.08	2.29	9%
Tu 104		25.03	2.65	50.53	75.39	1.42	1.14	25%		25.03	3.58	50.53	75.39	1.37	1.14	20%
Tu 110		16.71	1.77	43.73	73.24	1.22	0.83	48%		16.71	2.39	43.73	73.24	1.20	0.83	45%
Tu 124		11.75	1.25	46.70	74.18	1.00	0.74	36%		11.75	1.68	46.70	74.18	0.98	0.74	32%
Tu 134		24.12	2.56	46.97	74.26	1.44	1.04	38%		24.12	3.45	46.97	74.26	1.39	1.04	34%
il 62		34.56	3.66	41.78	72.62	1.78	2.15	17%		34.56	4.94	41.78	72.62	1.76	2.15	18%
EMB 135		7.44	0.79	30.96	69.20	0.88	0.99	11%		7.44	1.06	30.96	69.20	0.90	0.99	9%
ERJ 140		8.17	0.87	29.48	68.73	0.93	0.80	16%		8.17	1.17	29.48	68.73	0.95	0.80	19%
ERJ 145		6.81	0.72	31.76	69.46	0.84	1.01	17%		6.81	0.97	31.76	69.46	0.85	1.01	15%
Fokker 100		13.28	1.41	45.72	73.87	1.08	0.75	43%		13.28	1.90	45.72	73.87	1.05	0.75	39%
Fokker 70		54.16	5.74	43.79	73.26	2.20	2.05	7%		54.16	7.75	43.79	73.26	2.16	2.05	5%
Fokker 28		14.91	1.58	40.44	72.20	1.18	0.84	40%		14.91	2.13	40.44	72.20	1.17	0.84	39%
Average								**18%**								**17%**
Standard Deviation								**16%**								**15%**

Table 4.6 Application of methods 1 and 4 on propeller aircraft data

		For propeller aircraft														
	Method1	S_v	S_{df}	$\varphi_{a,v}$	$\varphi_{a,df}$	*hdf* calculated	*hdf* theoretical	difference	Method 4	S_v	S_{df}	$\varphi_{a,v}$	$\varphi_{a,df}$	*hdf* calculated	*hdf* theoretical	difference
		m	m	m	m	m	m			m	m	m	m	m	m	
Saab 340		7.50	1.23	38.90	75.97	0.88	0.86	2%		7.50	1.42	38.90	75.97	0.84	0.86	2%
Saab 2000		10.48	1.72	36.79	75.68	1.04	1.12	7%		10.48	1.99	36.79	75.68	1.01	1.12	10%
Q- 400		16.48	2.70	31.09	74.87	1.32	1.21	9%		16.48	3.13	31.09	74.87	1.30	1.21	7%
Q- 300		16.42	2.69	32.74	75.11	1.31	1.31	1%		16.42	3.12	32.74	75.11	1.29	1.31	1%
EMB 120		6.50	1.07	38.85	75.97	0.82	0.84	3%		6.50	1.24	38.85	75.97	0.79	0.84	7%
EMB 110/111		5.62	0.92	32.01	75.00	0.77	0.63	22%		5.62	1.07	32.01	75.00	0.76	0.63	20%
il 114		15.17	2.49	34.84	75.40	1.26	0.85	49%		15.17	2.88	34.84	75.40	1.23	0.85	45%
il 18		18.27	3.00	17.85	73.01	1.43	1.44	1%		18.27	3.47	17.85	73.01	1.46	1.44	1%
F- 27		16.48	2.70	23.51	73.81	1.34	1.29	4%		16.48	3.13	23.51	73.81	1.35	1.29	5%
An- 140		12.36	2.03	31.61	74.95	1.14	1.38	17%		12.36	2.35	31.61	74.95	1.12	1.38	19%
Bae 748		11.61	1.90	12.09	72.20	1.15	1.17	2%		11.61	2.21	12.09	72.20	1.19	1.17	2%
Beriev 32K		5.25	0.86	42.04	76.42	0.73	0.57	28%		5.25	1.00	42.04	76.42	0.69	0.57	22%
de havilland dash 7		15.90	2.61	34.11	75.30	1.29	1.31	2%		15.90	3.02	34.11	75.30	1.26	1.31	4%
Aerospatiale N262		8.35	1.37	10.56	71.98	0.97	0.81	20%		8.35	1.59	10.56	71.98	1.02	0.81	25%
Fokker F- 27- 500		15.05	2.47	25.16	74.04	1.28	1.30	1%		15.05	2.86	25.16	74.04	1.28	1.30	1%
Bae jetstream 41		6.64	1.09	33.91	75.27	0.83	0.75	10%		6.64	1.26	33.91	75.27	0.81	0.75	8%
Fairchild metro iii		5.34	0.88	27.90	74.42	0.76	1.59	52%		5.34	1.01	27.90	74.42	0.75	1.59	53%
Grumman G- 159		8.86	1.45	34.55	75.36	0.96	0.66	45%		8.86	1.68	34.55	75.36	0.94	0.66	42%
ATR 42		14.24	2.33	45.61	76.92	1.19	0.73	63%		14.24	2.71	45.61	76.92	1.12	0.73	54%
ATR 72		15.18	2.49	44.79	76.80	1.23	1.05	17%		15.18	2.88	44.79	76.80	1.16	1.05	10%
Vickers Vanguard		24.62	4.04	22.62	73.68	1.64	1.60	3%		24.62	4.68	22.62	73.68	1.65	1.60	4%
NAMC YS- 11		14.87	2.44	23.69	73.83	1.27	1.28	1%		14.87	2.83	23.69	73.83	1.28	1.28	0%
Average								**16%**								**16%**
Standard Deviation								**19%**								**17%**

In Table 4.5 and Table 4.6, the average of difference between the calculated h_{df} and theoretical h_{df} (3-views), and the standard deviation are marked in bold. The average difference for jet

aircraft (Figure 4.15) with Method 1 is 18% and with Method 2 is 17%. Both the averages are almost similar. Standard deviation is also measured for both the methods since it indicates the extent of data deviation from the average value (**Wikipedia 2013h**). The lower the value of standard deviation, the less is the deviation from the average and vice versa. The standard deviation for Method 1 and Method 4 are 16% and 15%, respectively.

For propeller aircraft (Table 4.6) the average and standard deviation compared to jet aircraft is almost similar. For Method 1 and Method 4 the average difference is equal, i.e., 16%. Though the standard deviations are different; for Method 1 and Method 4 standard deviations are 19% and 17%, respectively.

Physical significance of average difference and standard deviation

The average of difference calculated in Table 4.5 and Table 4.6 for jet and propeller aircraft signifies the average error in the calculated h_{df} from the theoretical h_{df}. Therefore, lower average value indicates lower error and hence indicates that the method is successful. In case of both jet and propeller aircraft (Table 4.5 and Table 4.6) the error lies in the range 16% … 18%. Standard deviation is calculated to verify how much the error deviates from the average error. If the standard deviation is zero, the average error can be fixed. Such a constant error can be added or subtracted from the calculated h_{df} to obtain accurate values. Table 4.7 summarizes the average error and standard deviation of Method 1 and 4 for jet and propeller aircraft.

Table 4.7 Summary of average error and standard deviation

		Method 1	Method 4
Jet	Average error	18%	17%
	Standard deviation	16%	15%
Propeller	Average error	16%	16%
	Standard deviation	19%	17%

For handbook calculation the average error range to size the height of the dorsal fin, h_{df}, is acceptable. If the error was large (like 50% or more) the method would fail to calculate a fair value of the parameter. Other parameters to design a dorsal fin can be calculated as explained in the "Idea of the Method" and thus, a dorsal fin for jet or propeller aircraft can be designed (Chapter 4.2.3). Since the difference between the errors (Table 4.7) is quite low, user may choose any of the method to design a dorsal fin for jet or propeller aircraft.

4.3 Systematic Approach of Round Edge Dorsal Fin Sizing Methods

Unlike a dorsal fin, a round edge dorsal fin does not have a sharp leading edge. Therefore, the approach used for round edge dorsal fin sizing is different than that for dorsal fin. The basic parameters necessary to size a round edge dorsal fin are h_{df}, L_{df} and $c_{r,df}$. From dorsal fin method selection, existence of a relationship between dorsal fin leading edge sweep angle and vertical tail leading edge sweep angle was quite convincing. It is therefore investigated in case of round edge dorsal fin also to check for any correlation between vertical tail leading edge sweep angle, $\varphi_{o,v}$ and virtual leading edge round edge dorsal fin, $\varphi_{df,vir}$ (Chapter 4.1) So, a virtual dorsal fin leading edge sweep angle is introduced as $\varphi_{df,vir}$. Figure 4.15 presents a round edge dorsal fin and the basic parameters necessary to size a round edge dorsal fin. For round edge dorsal fin $\Delta\varphi$ is the difference between $\varphi_{df,vir}$ and $\varphi_{o,v}$.

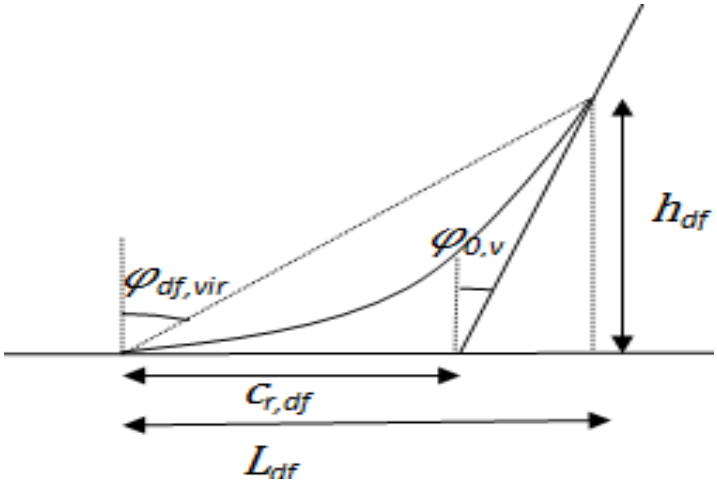

Figure 4.15 Basic parameters of an aircraft round edge dorsal fin

Relationships selected for investigation for round edge dorsal fin are:

- $\varphi_{df,vir} = f(\varphi_{o,df})$
- $c_{r,df} = f(c_{r,v})$
- $L_{df} = f(c_{r,v})$
- $h_{df} = f(b_v)$

Figures 4.16 to 4.19 show statistical plots of the considered relationships for jet aircraft.

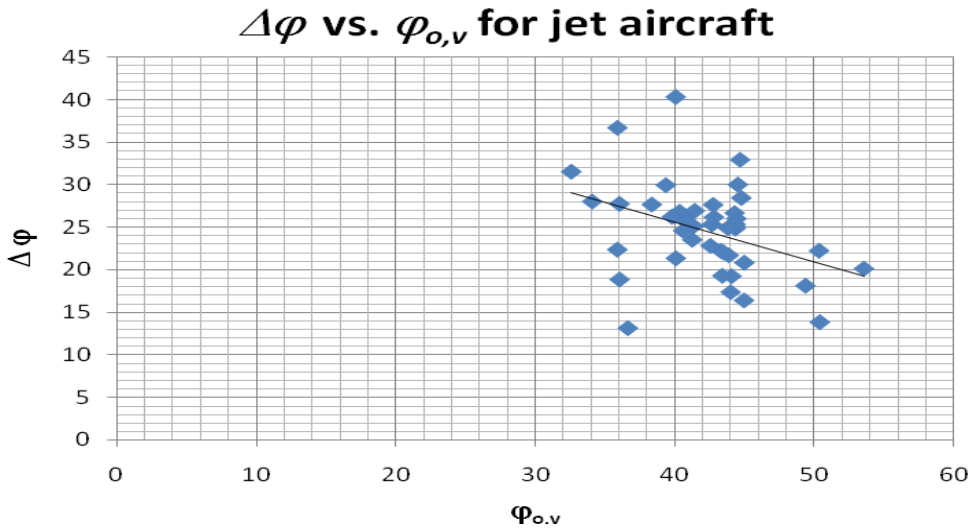

Figure 4.16 Plots of $\Delta\varphi$ vs. $\varphi_{o,v}$ for jet aircraft.

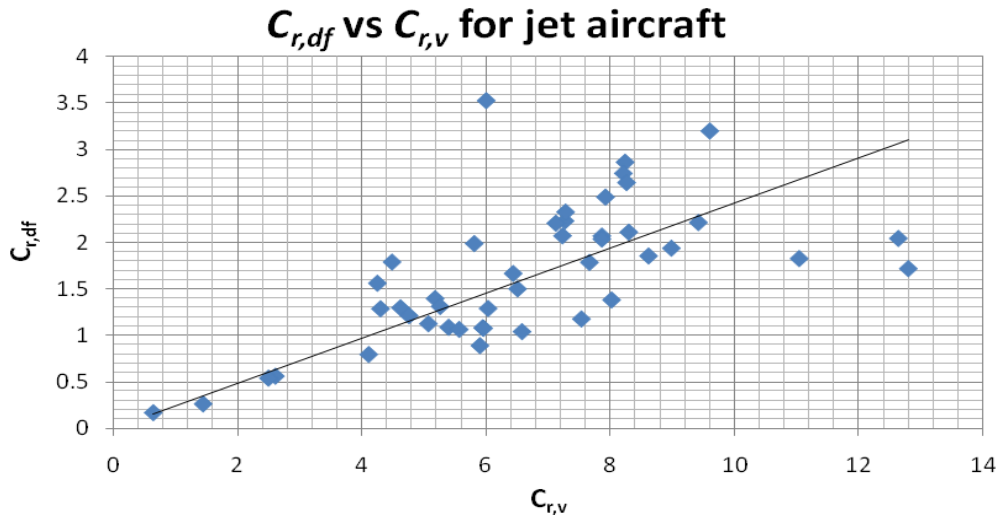

Figure 4.17 Plots of $c_{r,df}$ vs. $c_{r,v}$ for jet aircraft

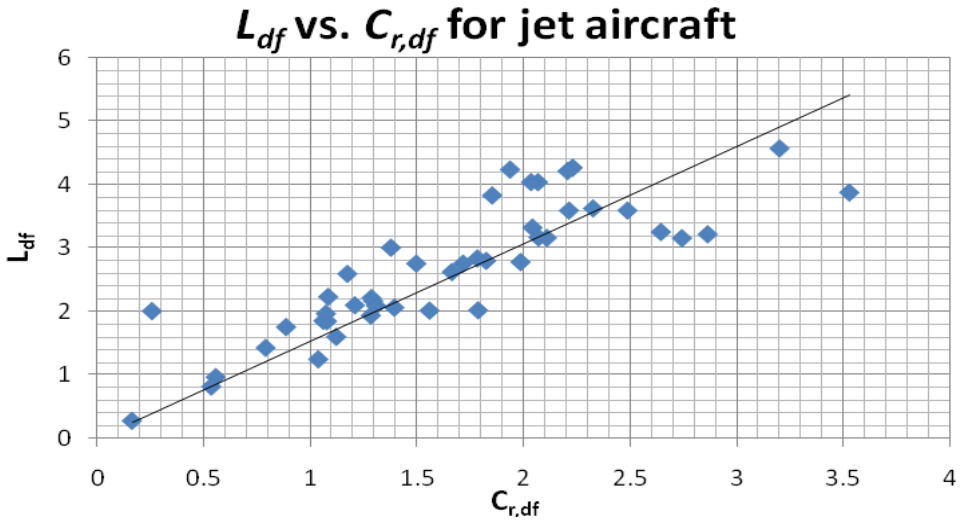

Figure 4.18 Plots of $c_{r,df}$ vs. L_{df} for jet aircraft

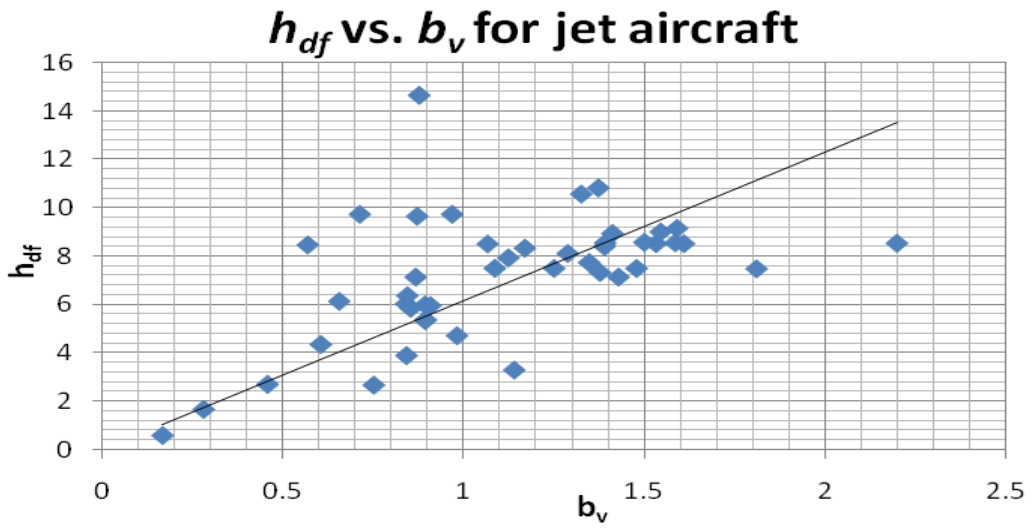

Figure 4.19 Plots of h_{df} vs. b_v

Table 4.8 presents the regression values and remarks for the considered relationships for round edge dorsal fin.

Table 4.8 Equations, regression values and remarks of the plots for considered relationships

Relationship	Figure no.	Equation	R^2 value	Remarks
$\Delta\varphi = f(\varphi_{o,v})$	4.18	$\Delta\varphi = 44.26° - 0.465\varphi_{o,v}$	0.138	low R^2; almost no correlation
$c_{r,df} = f(c_{r,v})$	4.19	$c_{r,df} = 0.243 c_{r,v}$	0.373	shows fair link; considered
$L_{df} = f(c_{r,df})$	4.20	$L_{df} = 1.534 c_{r,df}$	0.619	highest R^2; considered
$h_{df} = f(b_v)$	4.21	$h_{df} = 6.141 b_v$	0.082	very low R^2; no correlation

Unlike dorsal fin, round edge dorsal fin does not exhibit any connection between parameters $\Delta\varphi$ and $\varphi_{o,v}$. Also, h_{df} vs. b_v shows very low regression value, which means there is no correlation between the parameters. However, $c_{r,df}$ vs. $c_{r,v}$ and L_{df} vs. $c_{r,df}$ demonstrate interdependence upto a degree. Given these two considered relationships, Method 8 developed in Chapter 4.2.3 is the best suited method to size a round edge dorsal fin. Table 4.9 presents the average regression value for the selected method.

Table 4.9 Average regression

Method 8	$c_{r,df} = f(c_{r,v})$	$L_{df} = f(c_{r,df})$	Average
Jet	0.373	0.619	0.496

Table 4.9 represents the average error and standard deviation of the error with application of Method 8 on jet aircraft listed for investigation (Chapter 4.1) of round edge dorsal fin sizing. Average error is marked in bold and its value is 26%. Standard deviation is also marked in bold and is 23%. This error of 26% percentage is accepted for handbook calculation. The physical significance of average error and standard deviation is explained in Chapter 4.2.4. As

explained in the "Idea of the Method" (Chapter 4.2.3) of Method 8, other parameters to size a round edge dorsal fin can be calculated.

Table 4.10 Application of method 8 on jet aircraft data

			For jet aircraft					
	Method 8	$C_{r,v}$	$C_{r,df}$	L_{df}	$\varphi_{0,v}$	h_{df} calculated	h_{df} theoretical	difference
		m	m	m	m	m		
SJ 30		8.29	2.02	3.09	44.10	1.11	1.59	30%
A 300F4- 600		7.66	1.86	2.85	43.33	1.05	1.29	18%
A 320- 200		5.39	1.31	2.01	39.37	0.85	0.84	1%
A 330- 200		7.92	1.92	2.95	45.02	1.03	1.61	36%
A 330- 300		8.02	1.95	2.99	44.45	1.06	1.07	1%
A 340- 200		7.86	1.91	2.93	44.37	1.04	1.53	32%
A 340- 300		7.86	1.91	2.93	44.32	1.04	1.39	25%
A 340- 500		8.61	2.09	3.21	42.69	1.21	1.55	22%
A 340- 600		8.98	2.18	3.35	44.41	1.19	1.59	25%
A 318		5.94	1.44	2.21	41.27	0.88	0.87	1%
A 319		5.56	1.35	2.07	40.62	0.84	0.85	1%
A 321		4.10	1.00	1.53	40.74	0.62	0.60	2%
A 350- 900		6.57	1.60	2.45	42.58	0.93	0.57	63%
A 380		11.04	2.68	4.12	35.89	1.98	0.88	126%
B 707- 120B		5.95	1.45	2.22	36.04	1.06	1.38	23%
B 707- 320		6.02	1.46	2.25	36.04	1.07	1.09	1%
B 707- 320B		5.89	1.43	2.20	36.64	1.03	1.48	30%
B 717- 200		4.61	1.12	1.72	43.90	0.62	0.98	37%
B 720, 720B		5.80	1.41	2.16	32.57	1.18	1.35	13%
B 747- 8F		12.64	3.07	4.71	49.42	1.40	1.37	2%
B 747-8		12.80	3.11	4.77	50.44	1.37	1.33	4%
B 757- 200		6.50	1.58	2.42	43.53	0.89	1.25	29%
B 757- 300		6.43	1.56	2.40	44.03	0.86	1.43	40%
B 767- 200		7.27	1.77	2.71	43.43	1.00	2.20	55%
B 767- 300		7.12	1.73	2.65	42.77	1.00	1.50	33%
B 767- 300F		7.23	1.76	2.69	44.39	0.96	1.17	18%
B 767- 400ER		7.27	1.77	2.71	42.83	1.02	1.39	27%
B 777- 200		8.23	2.00	3.07	44.80	1.08	0.97	11%
B 777- 300		8.21	1.99	3.06	44.54	1.08	0.87	24%
B 777F		8.26	2.01	3.08	44.71	1.08	0.71	52%
B 787-8		7.53	1.83	2.81	45.00	0.98	1.41	31%
MD 80		4.75	1.15	1.77	40.09	0.73	1.14	36%
MD 90		1.43	0.35	0.53	40.36	0.22	0.84	74%
DC 9		0.63	0.15	0.23	35.88	0.11	0.17	32%
il 86		9.41	2.29	3.51	50.39	1.01	1.12	10%
il 76		9.60	2.33	3.58	41.45	1.41	1.81	22%
MRJ 70		4.24	1.03	1.58	38.37	0.69	0.89	22%
MRJ 90		4.48	1.09	1.67	39.81	0.70	0.90	22%
ARJ 21		4.29	1.04	1.60	43.83	0.58	0.75	23%
CS 100		5.17	1.26	1.93	40.76	0.78	0.89	13%
CS 300		5.25	1.28	1.96	41.37	0.77	0.91	15%
SJ 30		2.60	0.63	0.97	53.62	0.25	0.28	11%
Dassault mercure3v		5.06	1.23	1.89	34.08	0.97	0.84	15%
Convair cv-880		5.99	1.46	2.23	40.08	0.92	0.65	41%
Average								**26%**
Standard Deviation								**23%**

However, in dorsal fin there is a sharp leading edge sweep but in round edge dorsal fin it is an arc (see Figure **4.17**). With points A and H located (4.13 or 4.14), these two points can be considered as the tangents and an ellipse can be fitted in to produce the arc of the round edge dorsal fin. If the lengths BA and BH (4.13 or 4.14) are equal, lines perpendicular from the tangents (from points A and H) can be drawn until both the lines coincide into a point. This

point is the centre and a circle can be drawn from the point, with radius length from centre point till the tangent, to produce the arc of the round edge dorsal fin. Thus, using Method 8 a round edge dorsal fin can be designed for jet aircraft.

5 Summary

The purpose of this report was to provide more assistance to a user during conceptual design phase of the aircraft tail and dorsal fin. Many authors in the past have done work on tail sizing and so the aim was to either refine the values suggested by other authors or to explore new relationships that can aid a user in estimating a particular tail parameter size. In case of dorsal fin sizing however, very little resources were available prior to this report. This report aimed therefore to be a precedent for future research work in this direction.

The scope of this report extends to the conceptual design phase of the aircraft tail and dorsal fin. This report is not meant to be used as a guideline to fix final values of parameter sizes but rather only to estimate well during the 1st phase of design.

This report mainly uses statistical analyses to arrive at its results. It relies on the philosophy that aircraft of similar type show similarity in their parameter sizes. This has been illustrated by previous authors in the past too. This report simply aimed to take it one step further. Where data was not available, parameters were measured from the 3-view drawings of aircraft.

This report gives prospective users suggestions to estimate various tail and dorsal fin parameter sizes for usage during the conceptual design phase. Moreover, it draws attention to the trends followed by various unknown parameters with respect to change in other known parameters.

Using this report, a user can therefore estimate various tail and dorsal fin parameter sizes having only basic information like the category in which the aircraft being designed lies.

This report has categorized aircraft on the basis of number of passengers, engine type, etc. Further categorizing aircraft may lead to better results. Also, this report's findings come from a single method i.e. statistical analysis. Including more practical data like wind-tunnel testing, simulations, advanced software, etc may also improve the approximations given in this report. These can be taken up as future work.

References

A300 2002 AIRBUS, Customer Services: *A300 Airplane Characteristics for Airport Planning*. Blagnac ; Airbus, 2002 (A.AC E 00A). – Airbus S.A.S., 31707 Blagnac Cedex, France, Customer Services, Technical Data Support and Services, URL : http://www.airbus.com/support/maintenance-engineering/technical-data/aircraft-characteristics/ and http://www.airbus.com/fileadmin/media_gallery/files/tech_data/AC/AC_A300_20091201.pdf (2013-01-24)

A300-600 2002 AIRBUS, Customer Services: *A300- 600 Airplane Characteristics for Airport Planning.* Blagnac ; Airbus, 2002 (C. AC). – Airbus S.A.S., 31707 Blagnac Cedex, France, Customer Services, Technical Data Support and Services, URL : http://www.airbus.com/support/maintenance-engineering/technical-data/aircraft-characteristics/ and http://www.airbus.com/fileadmin/media_gallery/files/tech_data/AC/AC_A300-600_20091201.pdf (2013-01-24)

A300-F4/600 2002 AIRBUS, Customer Services: *A300-F4/- 600 Airplane Characteristics for Airport Planning.* Blagnac ; Airbus, 2002 (C. AC). – Airbus S.A.S., 31707 Blagnac Cedex, France, Customer Services, Technical Data Support and Services, URL : http://www.airbus.com/support/maintenance-engineering/technical-data/aircraft-characteristics/ and http://www.airbus.com/fileadmin/media_gallery/files/tech_data/AC/AC_A300F4-600_20091201.pdf (2013-01-24)

A310 2002 AIRBUS, Customer Services: *A310 Airplane Characteristics for Airport Planning.* Blagnac ; Airbus, 2002 (B. AC). – Airbus S.A.S., 31707 Blagnac Cedex, France, Customer Services, Technical Data Support and Services, URL : http://www.airbus.com/support/maintenance-engineering/technical-data/aircraft-characteristics/ and http://www.airbus.com/fileadmin/media_gallery/files/tech_data/AC/AC_A310_20091201.pdf (2013-01-24)

A318 2005 AIRBUS, Customer Services: *A318 Aircraft Characteristics Airport and Maintenance Planning.* Blagnac ; Airbus, 2005. – Airbus S.A.S., Customer Services, Technical Data Support and Services, 31707 Blagnac Cedex, France, URL : http://www.airbus.com/support/maintenance-engineering/technical-

data/aircraft-characteristics/ and http://www.airbus.com/fileadmin/media_gallery/files/tech_data/AC/Airbus-AC-A318-Jun2012.pdf (2013-01-24)

A319 2005 AIRBUS, Customer Services: *A319 Aircraft Characteristics Airport and Maintenance Planning*. Blagnac ; Airbus, 2005. – Airbus S.A.S., Customer Services, Technical Data Support and Services, 31707 Blagnac Cedex, France, URL : http://www.airbus.com/support/maintenance-engineering/technical-data/aircraft-characteristics/ and http://www.airbus.com/fileadmin/media_gallery/files/tech_data/AC/Airbus-AC-A319-Jun2012.pdf (2013-01-24)

A320 2005 AIRBUS, Customer Services: *A320 Aircraft Characteristics Airport and Maintenance Planning*. Blagnac ; Airbus, 2005. – Airbus S.A.S., Customer Services, Technical Data Support and Services, 31707 Blagnac Cedex, France, URL : http://www.airbus.com/support/maintenance-engineering/technical-data/aircraft-characteristics/ and http://www.airbus.com/fileadmin/media_gallery/files/tech_data/AC/Airbus-AC-A320-Jun2012.pdf (2013-01-24)

A321 2005 AIRBUS, Customer Services: *A321 Aircraft Characteristics Airport and Maintenance Planning*. Blagnac ; Airbus, 2005. – Airbus S.A.S., Customer Services, Technical Data Support and Services, 31707 Blagnac Cedex, France, URL : http://www.airbus.com/support/maintenance-engineering/technical-data/aircraft-characteristics/ and http://www.airbus.com/fileadmin/media_gallery/files/tech_data/AC/Airbus-AC-A321-Jun2012.pdf (2013-01-24)

A330 2005 AIRBUS, Customer Services: *A330 Airplane Characteristics for Airport Planning*. Blagnac ; Airbus, 2005. – Airbus S.A.S., Customer Services, Technical Data Support and Services, 31707 Blagnac Cedex, France, URL : http://www.airbus.com/support/maintenance-engineering/technical-data/aircraft-characteristics/ and http://www.airbus.com/fileadmin/media_gallery/files/tech_data/AC/Airbus-AC_A330_Dec11.pdf (2013-01-24)

A340-200/300 2005 AIRBUS, Customer Services: *A340-200/-300 Airplane Characteristics for Airport Planning*. Blagnac ; Airbus, 2005. – Airbus S.A.S., Customer Services, Technical Data Support and Services, 31707 Blagnac Cedex, France, URL : http://www.airbus.com/support/maintenance-engineering/technical-data/aircraft-characteristics/ and

http://www.airbus.com/fileadmin/media_gallery/files/tech_data/AC/Airbus-AC_A340-200_300_Dec11.pdf (2013-01-24)

A340-500/600 2005 AIRBUS, Customer Services: *A340-500/-600 Airplane Characteristics for Airport Planning.* Blagnac ; Airbus, 2005. – Airbus S.A.S., Customer Services, Technical Data Support and Services, 31707 Blagnac Cedex, France, URL : http://www.airbus.com/support/maintenance-engineering/technical-data/aircraft-characteristics/ and http://www.airbus.com/fileadmin/media_gallery/files/tech_data/AC/Airbus-AC_A340-500_600_Dec11.pdf (2013-01-24)

A350-900 2005 AIRBUS, Customer Services: *A350-900 Preliminary Data : Airplane Characteristics for Airport Planning.* Blagnac ; Airbus, 2005. – Airbus S.A.S., Customer Services, Technical Data Support and Services, 31707 Blagnac Cedex, France, URL : http://www.airbus.com/support/maintenance-engineering/technical-data/aircraft-characteristics/ and http://www.airbus.com/fileadmin/media_gallery/files/tech_data/AC/Airbus-AC-A350-July11.pdf (2013-01-24)

A380 2005 AIRBUS, Customer Services: *A380 Airplane Characteristics Airport and Maintenance Manual.* Blagnac ; Airbus, 2005. – Airbus S.A.S., Customer Services, Technical Data Support and Services, 31707 Blagnac Cedex, France, URL : http://www.airbus.com/support/maintenance-engineering/technical-data/aircraft-characteristics/ and http://www.airbus.com/fileadmin/media_gallery/files/tech_data/AC/Airbus-AC_A380_20121101.pdf (2013-01-24)

Abbott 1959 ABBOTT, Ira H.: *Theory of Wing Sections* : *Including a Summary of Airfoil Data.* New York, 1959 : Dover Publications, Inc, 1959.

Aero 2013 *Aero Favourite 7.* URL : http://aerofavourites.nl/fok100-04.htm (2013-01-21)

Aerofiles 2013 *Aerofiles.com.* URL : http://www.aerofiles.com/glossary.html (2013-02-13)

Aerospace 2013 *Aeospace-technology.* URL : http://www.aerospace-technology.com/projects/dash8/dash81.html (2013-01-21)

Aerospaceweb 2013 *Aerospaceweb.* URL : http://www.aerospaceweb.org/aircraft/jetliner/a320/ (2013-01-21)

Patent US 2356139 Patent US 2356139 (1944-08-22). ALLEN, Edmund T.; SCHAIRER George S. Application (1940-08-03). – *Aircraft Empennage*. Seattle ; Boeing Aircraft Company, United States Patent Office, A corporation of Washington. Serial no: 350572. URL : http://www.google.de/patents/US2356139?pg=PA4&dq=dorsal+fin+in+aircraft&hl=en&sa=X&ei=hfNjUdqTBcWrtAbDqoD4BQ&sqi=2&pjf=1&ved=0CDsQ6AEwAg#v=onepage&q=dorsal%20fin%20in%20aircraft&f=false (2012-10-15)

Audries 2013 *Audries Aircraft Analysis.* URL : http://www.audriesaircraftanalysis.com/2012/01/19/ventral-stakes-and-fins/ (2013-01-21)

Automobile 2013 *Automobile Large State.* URL : http://automobilelargestate.blogspot.de/2011/08/citation-cj3.html (2013-01-21)

Aviastar 2013a *Aviastar.* URL : http://www.aviastar.org/air/england/bae_rj-100.php (2013-01-21)

Aviastar 2013b *Aviastar.* URL : http://www.aviastar.org/air/usa/cessna_citation2.php (2013-01-21)

Aviastar 2013c *Aviastar.* URL : http://www.aviastar.org/air/canada/bombardier_dash-8-400.php (2013-01-21)

B707 2011 BOEING, Airport Technology: *707 Airplane Characteristics for Airport Planning.* Seattle : Boeing, 2011 (D6-58322). – Boeing Commercial Airplanes, P.O. Box 3707, Seattle, WA 98124-2207, USA, Attention: Manager, Airport Technology,
Mail Code: 20-93, AirportTechnology@boeing.com, URL : http://www.boeing.com/commercial/airports/707.htm and http://www.boeing.com/commercial/airports/acaps/707.pdf (2013-01-23)

B717 2011 BOEING, Airport Technology: *717-200 Airplane Characteristics for Airport Planning.* Seattle : Boeing, 2011 (D6-58330). – Boeing Commercial Airplanes, P.O. Box 3707, Seattle, WA 98124-2207, USA, Attention: Manager, Airport Technology,
Mail Code: 20-93, AirportTechnology@boeing.com, URL : http://www.boeing.com/commercial/airports/717.htm and

http://www.boeing.com/commercial/airports/acaps/717.pdf (2013-01-24)

B720 2011 BOEING, Airport Technology: *720 Airplane Characteristics for Airport Planning*. Seattle : Boeing, 2011 (D6-58323). – Boeing Commercial Airplanes, P.O. Box 3707, Seattle, WA 98124-2207, USA, Attention: Manager, Airport Technology,
Mail Code: 20-93, AirportTechnology@boeing.com, URL : http://www.boeing.com/commercial/airports/720.htm and http://www.boeing.com/commercial/airports/acaps/720.pdf (2013-01-24)

B727 2011 BOEING, Airport Technology: *727 Airplane Characteristics for Airport Planning*. Seattle : Boeing, 2011 (D6-58324). – Boeing Commercial Airplanes, P.O. Box 3707, Seattle, WA 98124-2207, USA, Attention: Manager, Airport Technology,
Mail Code: 20-93, AirportTechnology@boeing.com, URL : http://www.boeing.com/commercial/airports/727.htm and http://www.boeing.com/commercial/airports/acaps/727.pdf (2013-01-24)

B737 2011 BOEING, Airport Technology: *737 Airplane Characteristics for Airport Planning*. Seattle : Boeing, 2011 (D6-58325-6). – Boeing Commercial Airplanes, P.O. Box 3707, Seattle, WA 98124-2207, USA, Attention: Manager, Airport Technology,
Mail Code: 20-93, AirportTechnology@boeing.com, URL : http://www.boeing.com/commercial/airports/737.htm and http://www.boeing.com/commercial/airports/acaps/737.pdf (2013-01-24)

B747-8 2012 BOEING, Airport Technology: *747-8 Airplane Characteristics for Airport Planning*. Seattle : Boeing, 2012 (D6-58326-3). – Boeing Commercial Airplanes, P.O. Box 3707, Seattle, WA 98124-2207, USA, Attention: Manager, Airport Technology,
Mail Code: 20-93, AirportTechnology@boeing.com, URL : http://www.boeing.com/commercial/airports/747.htm and http://www.boeing.com/commercial/airports/acaps/747_8.pdf (2013-01-24)

B757 2011 BOEING, Airport Technology: *757-200/-300 Airplane Characteristics for Airport Planning*. Seattle : Boeing, 2011 (D6-58327). – Boeing Commercial Airplanes, P.O. Box 3707, Seattle, WA 98124-2207, USA, Attention: Manager, Airport Technology,

Mail Code: 20-93, AirportTechnology@boeing.com, URL : http://www.boeing.com/commercial/airports/757.htm and http://www.boeing.com/commercial/airports/acaps/757_23.pdf (2013-01-24)

B767 2011 BOEING, Airport Technology: *767 Airplane Characteristics for Airport Planning*. Seattle : Boeing, 2011 (D6-58328). – Boeing Commercial Airplanes, P.O. Box 3707, Seattle, WA 98124-2207, USA, Attention: Manager, Airport Technology,
Mail Code: 20-93, AirportTechnology@boeing.com, URL : http://www.boeing.com/commercial/airports/767.htm and http://www.boeing.com/commercial/airports/acaps/767.pdf (2013-01-24)

B777 2011 BOEING, Airport Technology: *777-200LR/-300ER/-Freighter Airplane Characteristics for Airport Planning*. Seattle : Boeing, 2011 (D6-58329-2). – Boeing Commercial Airplanes, P.O. Box 3707, Seattle, WA 98124-2207, USA, Attention: Manager, Airport Technology,
Mail Code: 20-93, AirportTechnology@boeing.com, URL : http://www.boeing.com/commercial/airports/777.htm and http://www.boeing.com/commercial/airports/acaps/777_2lr3er.pdf (2013-01-24)

B787 2011 BOEING, Airport Technology: *787 Airplane Characteristics for Airport Planning*. Seattle : Boeing, 2011 (D6-58333). – Boeing Commercial Airplanes, P.O. Box 3707, Seattle, WA 98124-2207, USA, Attention: Manager, Airport Technology,
Mail Code: 20-93, AirportTechnology@boeing.com, URL : http://www.boeing.com/commercial/airports/787.html and http://www.boeing.com/commercial/airports/acaps/787.pdf (2013-01-24)

Blueprints 2013 *The-Blueprints.com*. URL: http://www.the-blueprints.com (2013-01-10)

Crane 2012 CRANE, Dale: Dictionary of Aeronautical Terms. Aviation Supplies & Academic : 2012. – ISBN 1560278641. Also online: **DATWiki 2013**

Crawford 2009 Crawford, Bill: Unusual Attitudes and the Aerodynamics of Maneuvering Flight. Flight Emergency & Advanced Maneuvers Training, Inc., 2009. – URL: http://www.flightlab.net/Flightlab.net/Download_Course_Notes_files/FLNotebookpdfs.pdf (2013-01-10)

DATCOM 1978 FINCK, R. D.: *USAF Stability and Control Datcom*. Long Beach (CA) : McDonnell Douglas Corporation, Douglas Aircraft Division, 1978. – Report prepared under contract F33615-76-C-3061 on behalf of the Air Force Wright Aeronautical Laboratories, Flight Dynamics Laboratory, Wright-Patterson AFB (OH)

DATWiki 2013 Crane, Dale: DATWiki (Online Dictionary). URL : http://www.datwiki.net/search.php (2013-01-16)

EMB120 2000 EMBRAER, Technical Publication: *EMB120 Brasilia : Airport Planning Manual*. São Paulo : Embraer, 2000 (A.P. – 120/731). – Empresa Brasileira de Aeronáutica S.A, Av. Brigadeiro Faria Lima 2170, Caixa Postal 8050, CEP 12227-901, São José dos Campos, São Paulo, Brazil, Attention: Technical Publications; distrib@embraer.com.br; URL: http://www.embraercommercialjets.com/#/en/apm and http://www.embraercommercialjets.com/img/apm/12.pdf (2013-01-24)

EMB170 2003 EMBRAER, Technical Publications: *Embraer 170 Airport Planning Manual*. São Paulo : Embraer, 2003 (APM-1346). – Embraer S.A, P.O. BOX 8050, CEP 12227-901, Sao Jose Dos Campos, SaoPaulo, Brazil, Attention: Technical Publication; distrib@embraer.com.br; URL : http://www.embraercommercialjets.com/#/en/apm and http://www.embraercommercialjets.com/img/apm/8.pdf (2013-01-24)

EMB175 2012 EMBRAER, Technical Publications: *Embraer 175 Airport Planning Manual*. São Paulo : Embraer, 2012 (APM-2259). – Embraer S.A, P.O. BOX 8050, CEP 12227-901, Sao Jose Dos Campos, Sao Paulo, Brazil, Attention: Technical Publication; distrib@embraer.com.br; URL : http://www.embraercommercialjets.com/#/en/apm and http://www.embraercommercialjets.com/img/apm/9.pdf (2013-01-24)

EMB190 2012 EMBRAER, Technical Publications: *Embraer 190 Airport Planning Manual*. São Paulo : Embraer, 2012 (APM-1901). – Embraer S.A, P.O. BOX 8050, CEP 12227-901, Sao Jose Dos Campos, Sao Paulo, Brazil, Attention: Technical Publication; distrib@embraer.com.br; URL : http://www.embraercommercialjets.com/#/en/apm and http://www.embraercommercialjets.com/img/apm/10.pdf (2013-01-24)

EMB195 2012 EMBRAER, Technical Publications : *Embraer 195 Airport Planning Manual*. São Paulo : Embraer, 2012 (APM-1997). – Embraer S.A,

P.O. BOX 8050, CEP 12227-901, Sao Jose Dos Campos, Sao Paulo, Brazil, Attention: Technical Publication; distrib@embraer.com.br; URL : http://www.embraercommercialjets.com/#/en/apm and http://www.embraercommercialjets.com/img/apm/11.pdf (2013-01-24)

ERJ135 2008 EMBRAER, Technical Publications: *EMB 135 Airport Planning Manual*. São Paulo : Embraer, 2008 (APM- 145/1238). – Embraer S.A, P.O. BOX 8050, CEP 12227-901, Sao Jose Dos Campos, Sao Paulo, Brazil, Attention: Technical Publication; distrib@embraer.com.br; URL : http://www.embraercommercialjets.com/#/en/apm and http://www.embraercommercialjets.com/img/apm/1.pdf (2013-01-24)

ERJ140 2005 EMBRAER, Technical Publications Airport Planning Manual: *ERJ 140 Airport Planning Manual*. São Paulo : Embraer, 2005 (APM-145/1521). – Embraer S.A, P.O. BOX 8050, CEP 12227-901, Sao Jose Dos Campos , Sao Paulo, Brazil, Attention: Technical Publication; distrib@embraer.com.br; URL : http://www.embraercommercialjets.com/#/en/apm and http://www.embraercommercialjets.com/img/apm/2.pdf (2013-01-24)

ERJ145 2007 EMBRAER, Technical Publications: *EMB 140 Airport Planning Manual*. São Paulo : Embraer, 2007 (APM- 145/1100). – Embraer S.A, P.O. BOX 8050, CEP 12227-901, Sao Jose Dos Campos, Sao Paulo, Brazil, Attention. Technical Publication; distrib@embraer.com.br; URL : http://www.embraercommercialjets.com/#/en/apm and http://www.embraercommercialjets.com/img/apm/3.pdf (2013-01-24)

FlightGlobal 2013 *FlightGlobal*. URL : http://www.flightglobal.com/airspace/media/civilaviation1949-2006cutaways/default.aspx?Sort=Subject&PageIndex=5 (2013-01-10)

Fly Fokker 2013 *Fly Fokker*. URL : http://www.flyfokker.com/Fokker-100-Basics (2013-01-23)

FreeDictionary 2013 *TheFreeDictionary*. URL : http://www.thefreedictionary.com/ (2013-02-13)

Howe 2000 HOWE, Denis: *Aircraft Conceptual Design Synthesis*. London and Bury St Edmunds, UK : Professional Engineering Publishing Limited, 2000. – ISBN 1-86058-301-6.

Huenecke 1987 HUENECKE, Klaus: *Modern Combat Aircraft Design.* Annapolis, MD, USA : Naval Institute Press, 1987. – ISBN 0870214268, 978-0870214264.

Jane's 2008 JACKSON, Paul (Ed.): *Jane's All the World's Aircraft 2008-09.* Surrey, UK : Jane's Information Group Limited, 2008. – ISBN 13-978-0-7106-28374

Jenkinson 1999 JENKINSON, Lloyd R.: *Civil Jet Aircraft Design*. London, Sydney, Auckland : Arnold, A member of the Hodder Headline Group, 1999. – ISBN 0-340-74152-X

Kroo 2013 *Aircraft Design: Synthesis and Analysis.* URL : http://adg.stanford.edu/aa241/stability/taildesign.html (2013-02-13)

MAD 1980 AGARD: *Multilingual Aeronautical Dictionary.* London : Technical Editing and Reproduction, 1980. – ISBN 92-835-01666-7

Morichon 2006a MORICHON, Lucie: *Selected statistics in aircraft design*. Hamburg : Department of Automotive and Aeronautical engineering, Hamburg University of Applied Sciences, 2006. – URL: http://library.ProfScholz.de

Morichon 2006b MORICHON, Lucie: EXCEL file for: *Selected statistics in aircraft design*. Hamburg : Department of Automotive and Aeronautical engineering, Hamburg University of Applied Sciences, 2006. - URL: http://www.ProfScholz.de/arbeiten/DataMorichon.xls

Nicolai 1975 NICOLAI, Leland M.: *Fundamentals of Aircraft Design*. Ohio : METS, Inc, 1975.

Obert 2009 OBERT, Ed: *Aerodynamic Design Of Transport Aircraft*. Amsterdam : IOS Press, 2009. – ISBN 978-1-58603-970-7

Prendrel 2013 *Prendre l' Avion.* URL : http://prendrelavion.com/l%E2%80%99a320-le-best-seller-d%E2%80%99airbus/ (2013-01-21)

Raymer 1992 RAYMER, Daniel P.: *Aircraft Design : A Conceptual Approach*. Washington : AIAA, 1992. – ISBN 0-930403-51-7

Roskam 1985 ROSKAM, Jan: *Airplane Design : Part II: Preliminary Configuration Design and Integration of the Propulsion System*. Ottawa, Kansas : Roskam Aviation and Engineering Corporation, 1985.

Roux 2007 ROUX, Élodie: *Avions Civils à Réaction : Plan 3 Vues et Données Caractéristiques*. Blagnac : Éditions Élodie Roux, 2007. – ISBN 978-2-9529380-2-0

Sadraey 2013 SADRAEY, Mohammad H.: *Aircraft Design : A Systems Engineering Approach*. Chichester, UK : John Wiley & Sons, 2013. – ISBN 978-1-119-95340-1

Scholz 2009 SCHOLZ, Dieter: *Short Course Aircraft Design*. Hamburg: University of applied sciences, Hamburg, Short course, 2010.

Schaufele 2007 SCHAUFELE, Roger D.: *The Elements of Aircraft Preliminary Design*. Santa Ana, California : Aries Publication, 2007. – ISBN 0-9701986-0-4

Stajets 2013 *Stajets*. URL : http://www.stajets.com/charter-solutions/fleet/cessna-citation-bravo-2/ (2013-01-21)

Skyhigh 2013 *Skyhighhobby*. URL : http://www.skyhighhobby.com/wp-content/uploads/2009/12/wing-Aspect-Ratio.jpg (2013-02-13)

Torenbeek 1982 TORENBEEK, Egbert: *Synthesis of Subsonic Airplane Design*. Dordrecht, NL : Kluwer Academic Publishers, 1987. – ISBN 90-247-2724-3

Truckenbrodt 2001 TRUCKENBRODT, Erich; SCHLICHTING, Hermann: *Aerodynamik des Flugzeuges*. Berlin Heidelberg New York : Springer-Verlag, 2001. – ISBN 3-540-67375-X

Tutavia 2013 *Tutavia.ru* . URL : http://tutavia.ru/index/0-151 (2013-01-21)

Whitford 1987 WHITFORD, Ray: *Design for Air Combat*. London : Jane's Publishing Company, 1987. – ISBN 0-7106-0426-2

Wikipedia 2013a *Aspect Ratio*. URL: http://en.wikipedia.org/wiki/Aspect_ratio_(wing) (2013-01-17)

Wikipedia 2013b *Coefficient of Determination*. URL : http://en.wikipedia.org/wiki/R-squared (2013-01-17)

Wikipedia 2013c *Leading Edge*. URL: http://en.wikipedia.org/wiki/Leading_edge (2013-01-17)

Wikipedia 2013d *Mach Number*. URL: http://en.wikipedia.org/wiki/Mach_number (2013-01-17)

Wikipedia 2013e *Chord (Aircraft)*. URL: http://en.wikipedia.org/wiki/Mean_Aerodynamic_Chord#Mean_aerodynamic_chord (2013-01-17)

Wikipedia 2013f *Regression Analysis*. URL: http://en.wikipedia.org/wiki/Regression_analysis (2013-01-17)

Wikipedia 2013g *Trailing Edge*. URL: http://en.wikipedia.org/wiki/Trailing_edge (2013-01-17)

Wikipedia 2013h *Standard Deviation.* URL : http://en.wikipedia.org/wiki/Standard_deviation (2013-02-11)

Appendix A

List of Aircraft Used for Analysis

The following aircraft were used for analysis in different sections of this report. All 306 aircraft are listed alphabetically and against their respective aircraft categories.

Table A.1 List of Aircraft

Aircraft	Type
A300/600	Jet Transport
A300-600	Jet Transport
A310/300	Jet Transport
A310-300	Jet Transport
A319/100	Jet Transport
A319-100	Jet Transport
A320/200	Jet Transport
A320-200	Jet Transport
A321/200	Jet Transport
A321-100	Jet Transport
A330/200	Jet Transport
A340/200	Jet Transport
A340-300	Jet Transport
AC Jet Commander 1121	Business Jet
Aerital. G222	Military Transport
Aermacchi MB-339A	Military Trainers
Aermacchi MB-339K	Military Fighter
Aero Boero 260Ag	Agricultural
Aero L39C	Military Trainers
Aerospatiale corvette	Business Jet
Aerospatiale Corvette SN601	Business Jet
Aerospatiale N262	Regional Turboprop
Airbus A-300 B2	Jet Transport
Airbus a300-b1	Jet Transport
An- 140	Regional Turboprop
Antonov An-12BP	Military Transport
Antonov An-22	Military Transport
Antonov An-26	Military Transport
ATR 72	Regional Turboprop
ATR-42	Regional Turboprop
B 314A	Amphibious
B 707-120	Jet Transport
B 707-320C	Jet Transport
B 727	Jet Transport
B 737	Jet Transport

B 747	Jet Transport
B 757	Jet Transport
B 767	Jet Transport
B707/320C	Jet Transport
B717/200	Jet Transport
B727/200Adv	Jet Transport
B737/200	Jet Transport
B737-300	Jet Transport
B737-400	Jet Transport
B737-500	Jet Transport
B747-200	Jet Transport
B747-400	Jet Transport
B777/200	Jet Transport
BAC 1-11 Srs. 400	Jet Transport
BAC-111 Sr,200	Jet Transport
Bae 125 Sr. 700	Business Jet
Bae 146	Jet Transport
Bae 748 Sr. ii	Regional Turboprop
Bae RJ100	Jet Transport
Bae RJ115	Jet Transport
BAe RJ70	Jet Transport
Bae RJ85	Jet Transport
Beech C-99	Commuter
Beech Commuter 1900	Commuter
Beech Duchess	Personal
Beech Duke B60	Personal
Beech Super King Air 200	Commuter
Beechcraft B-45 mentor	Personal
Beechcraft Queen Air M 80	Personal
Bellanca Skyrocket	Personal
Beriev 32K	Commuter
Beriev M-12	Amphibious
Boeing 707/120	Jet Transport
Boeing 720/022	Jet Transport
Boeing 737/100	Jet Transport
Boeing 747/200B	Jet Transport
Boeing AST-100	Supersonic Cruise
Boeing b-47	Military Fighter
Boeing SST	Supersonic Cruise
Boeing YC-14	Military Transport
Breguet 941	Regional Turboprop
Breguet atlantic	Military Transport
Bristol 175 Brittania	Regional Turboprop
Bristol Britannia	Regional Turboprop
British Aerospace Hawk Mk1	Military Trainers
British Aerospace HS 125-700	Business jet

BV-222	Amphibious
C-160 transall	Military Transport
Canadair Challenger	Business Jet
Canadair CL 215	Amphibious
Canadair CL-215	Commuter
canadair cl-44	Regional Turboprop
Canadair CL-44 C	Military Transport
Canadair Reg.Jet100	Jet Transport
Candair Challenger CL-601	Business jet
Casa 212 SR.200	Military Transport
CASA 235	Military Transport
CASA C101	Military Trainers
Cessna 172, Normal category	Personal
Cessna 177, NC	Personal
Cessna 177, Utility Cat.	Personal
Cessna 206 Skywagon	Personal
Cessna 303	Personal
Cessna 310R	Personal
Cessna 340	Personal
Cessna 402B	Personal
Cessna 406	Commuter
Cessna 414A	Personal
Cessna A37B	Military Fighter
Cessna AG Husky	Agricultural
Cessna cardinal RG	Personal
Cessna citation 500	Business jet
Cessna Citation 501	Business jet
Cessna citation ii	Business Jet
Cessna citation iii	Business Jet
Cessna Model 337	Personal
Cessna Skylane RG	Personal
Cessna Skywagon 207	Personal
Cessna T303	Personal
Concorde Rockwell B1B	Supersonic Cruise
Convair 240	Regional Turboprop
Convair 340	Regional Turboprop
Convair B58	Supersonic Cruise
D/B Atlant. 2	Military Transport
Dassault Breguet FR A-10A	Military Fighter
Dassault Breguet Grum. A6A	Military Fighter
Dassault Breguet Grum. F14A	Military Fighter
Dassault Breguet Mir. 2000	Military Fighter
Dassault Breguet Mir. F1C	Military Fighter
Dassault Breguet Mir. IIIE	Military Fighter
Dassault Breguet North. F5E	Military Fighter
Dassault Breguet Super Et.	Military Fighter

Dassault Breguet Vht A7A	Military Fighter
Dassault Breguet/Dornier Alphajet	Military Trainers
Dassault falcon 10	Business Jet
Dassault falcon 20	Business Jet
Dassault falcon 50	Business Jet
dassault mercure	Jet Transport
Dassault Mirage IVA	Supersonic Cruise
Dassault Mystere 20F	Military Fighter
De Havilland dh-125	Business Jet
De Havilland DHC-2 Beaver	Personal
DH-121 trident	Jet Transport
DHC-4 Caribou	Military Transport
DHC-5 Buffalo	Military Transport
DHC-6 Twin Otter	Commuter
DHC-7	Regional Turboprop
Dornier 228 SR.200	Commuter
Dornier Do 24	Amphibious
Dornier Do 28-D-I	Commuter
Dornier Do Seastar	Amphibious
douglas dc-10	Jet Transport
Douglas DC-6	Military Transport
Douglas dc-8	Jet Transport
Douglas dc-9	Jet Transport
EMB 110/111	Commuter
EMB 120	Regional Turboprop
EMB-121	Personal
EMB201A	Agricultural
EMB-312	Military Trainers
Embraer Bandeirante	Commuter
Embraer EMB-145	Jet Transport
Embraer Xingu	Personal
Epsilon	Military Trainers
Fairchild metro iii	Regional Turboprop
Fiat g-222	Military Transport
Fokker F100	Jet Transport
Fokker F130	Jet Transport
Fokker f-27	Regional Turboprop
Fokker f-28	Jet Transport
Fokker F-70	Jet Transport
Fokker S-11 Instructor	Personal
Fokker VFW F-27 Mk 200	Regional Turboprop
Fokker VFW F-28 Mk 1000	Jet Transport
GAF Nomad	Commuter
Gates Learjet 24	Business jet
Gates Learjet 35A	Business jet
Gates Learjet 55	Business jet

GD F-111A	Supersonic Cruise
General Dynamics F-16	Military Fighter
General Dynamics FB-11A	Military Fighter
Grum. E2C	Military Transport
Grumman G- 159	Regional Turboprop
Grumman Gulfstream I	Commuter
Grumman J4F-1	Amphibious
Grumman JRF-6B	Amphibious
Grumman Tiger	Personal
Gulfstream ii	Business Jet
Hal HA-31	Agricultural
Handley Page (BAe) Jetstream	Commuter
Handley page herald	Regional Turboprop
HFB- 320	Business Jet
HFB Hansa	Business Jet
HS Andover C.Mk I	Military Transport
HS-125 IA/ IB	Business Jet
Hurel Dubois HD 32	Commuter
IAI westwind ii	Business Jet
IAR-822	Agricultural
Ilyushin Il-114	Regional Turboprop
Ilyushin Il-62M/MK	Jet Transport
Ilyushin Il-86	Jet Transport
Ilyushin Il-96-300	Jet Transport
Ilyushin Il-18	Regional Turboprop
Ilyushin Il-76T	Military Transport
Israel Aircraft Ind. Astra	Business jet
Israel Aircraft Ind. Westwind	Business jet
kawasaki c-1a	Military Transport
Lear Fan 2100	Personal
Lear Jet 25	Business Jet
Learjet 23	Business Jet
Learjet 55	Business Jet
Let Z-37A	Agricultural
Lockheed 1011 Tristar	Jet Transport
Lockheed 188C Electra	Commuter
Lockheed BA Nimrod 2	Military Transport
lockheed c 141	Military Transport
Lockheed C-130 E	Military Transport
Lockheed c-130 hercules	Military Transport
Lockheed C-141A	Military Transport
Lockheed C-141B	Military Transport
Lockheed C-5A	Military Transport
Lockheed Electra	Commuter
Lockheed l- 1011	Jet Transport
Lockheed L-1049 H	Regional Turboprop

Lockheed L-1649 A	Regional Turboprop
Lockheed P3C	Military Transport
Lockheed S-3A viking	Military Fighter
M PBM-3	Amphibious
McD. Douglas DC-9/10	Jet Transport
McD. Douglas DC-9/33F	Jet Transport
McDonell Douglas F-15	Military Fighter
McDonell Douglas F-4E	Military Fighter
McDonell Douglas KC-10A	Military Transport
Mcdonnell Douglas MD 11	Jet Transport
Mcdonnell Douglas MD 81	Jet Transport
Mcdonnell Douglas MD 90/30	Jet Transport
McK G21-G	Amphibious
MD DC-8/21	Jet Transport
MD-11	Jet Transport
MD-12LR	Jet Transport
MD-90/30	Jet Transport
Microturbo Microjet 200B	Military Trainers
MIG-25	Military Fighter
Mitshubishi diamond	Business Jet
NAMC YS-11	Regional Turboprop
NASA SSXjet I	Supersonic Cruise
NASA SSXjet II	Supersonic Cruise
NASA SSXjet III	Supersonic Cruise
NDN IT	Military Trainers
NDN-6	Agricultural
Neiva T25	Military Trainers
Nord 262	Regional Turboprop
Nord 262	Regional Turboprop
North am, sabreliner	Business Jet
North Am. RA-5C	Supersonic Cruise
North Am. XB-70A	Supersonic Cruise
P68B	Amphibious
Piaggio P-148 (3 seater)	Personal
Piaggio P166-DL3	Personal
Pil. PC-7	Military Trainers
Pilatus PC-6-M2 Porter	Personal
Piper Cherokee Lance	Personal
Piper Cheyenne I	Personal
Piper Cheyenne III	Personal
Piper Chieftain	Personal
Piper Navajo Chief	Personal
Piper PA 30C Twin Commanche	Personal
Piper PA-31P	Personal
Piper PA-36	Agricultural
Piper PA-44-180T	Personal

Piper Seneca	Personal
Piper Warrior	Personal
PZL TS-11	Military Trainers
PZL-104	Agricultural
PZL-106A	Agricultural
PZL-M18	Agricultural
Q- 300	Regional Turboprop
Q- 400	Regional Turboprop
Rockwell Commander	Personal
Saab 2000	Regional Turboprop
Saab 340	Regional Turboprop
Saab 91-B Safir	Personal
Schweizer Ag-Cat B	Agricultural
Scottish Aviation Bullfinch	Personal
SE-210 Caravelle	Jet Transport
SF-260M	Military Trainers
Short belfast	Military Transport
Short SD-360	Regional Turboprop
Shorts Sandr'ham	Amphibious
Shorts Shetland	Amphibious
SM S-211	Military Trainers
SM S-700	Amphibious
SM US-1	Amphibious
Su-7BMK	Military Fighter
Sud Av Caravelle 10R	Jet Transport
T-34C	Military Trainers
Trago Mills SAH-1	Personal
Tu-134	Jet Transport
Tu-154M	Jet Transport
Tu-16	Military Transport
Tu-204/200	Jet Transport
Tu-22	Supersonic Cruise
Tu-22M	Supersonic Cruise
Tu-334	Jet Transport
Tupolev Tu-144	Supersonic Cruise
Turbo Saratoga SP	Personal
VFW Fokker-614	Jet Transport
Vickers Vanguard	Regional Turboprop
Vickers Viscount	Regional Turboprop
Yak-52	Military Trainers
Yakovlev YAK-40	Jet Transport